Oil & Natural Gas Technology

DOE Award No.: DE-NT0006555

Final Scientific/Technical Report

October 1, 2008 to September 30, 2011

USE OF POLYMERS TO RECOVER VISCOUS OIL FROM UNCONVENTIONAL RESERVOIRS

Submitted by:
New Mexico Petroleum Recovery Research Center
New Mexico Tech, 801 Leroy, Socorro, NM 87801

Authored By: Randall Scott Seright (Principal Investigator)
Prepared for:
United States Department of Energy
National Energy Technology Laboratory

October 12, 2011

Office of Fossil Energy

DISCLAIMER

DEDICATION

This report is dedicated to the memory of my great friend Robert Dunn Sydansk. Bob showed extraordinary dedication toward advancing the science, engineering, and application of conformance improvement in reservoirs using polymers and gels. Bob invented the Cr(III)-carboxylate-HPAM gel conformance improvement technology. Weekly (and often daily) technical discussions with him were among the best parts of my job. I miss his insights, vision, and friendship.

ABSTRACT

This final technical progress report summarizes work performed the project, "Use of Polymers to Recover Viscous Oil from Unconventional Reservoirs." The objective of this three-year research project was to develop methods using water soluble polymers to recover viscous oil from unconventional reservoirs (i.e., on Alaska's North Slope). The project had three technical tasks. First, limits were re-examined and redefined for where polymer flooding technology can be applied with respect to unfavorable displacements. Second, we tested existing and new polymers for effective polymer flooding of viscous oil, and we tested newly proposed mechanisms for oil displacement by polymer solutions. Third, we examined novel methods of using polymer gels to improve sweep efficiency during recovery of unconventional viscous oil.

This report details work performed during the project. First, using fractional flow calculations, we examined the potential of polymer flooding for recovering viscous oils when the polymer is able to reduce the residual oil saturation to a value less than that of a waterflood. Second, we extensively investigated the rheology in porous media for a new hydrophobic associative polymer. Third, using simulation and analytical studies, we compared oil recovery efficiency for polymer flooding versus in-depth profile modification (i.e., "Bright Water") as a function of (1) permeability contrast, (2) relative zone thickness, (3) oil viscosity, (4) polymer solution viscosity, (5) polymer or blocking-agent bank size, and (5) relative costs for polymer versus blocking agent. Fourth, we experimentally established how much polymer flooding can reduce the residual oil saturation in an oil-wet core that is saturated with viscous North Slope crude. Finally, an experimental study compared mechanical degradation of an associative polymer with that of a partially hydrolyzed polyacrylamide.

Detailed results from the first two years of the project may be found in our first and second annual reports. Our latest research results, along with detailed documentation of our past work, can be found on our web site at http://baervan.nmt.edu/randy/.

As an overall summary of important findings for the project, polymer flooding has tremendous potential for enhanced recovery of viscous oil. Fear of substantial injectivity reduction was a primary hurdle that limited application of polymer flooding. However, that concern is largely mitigated by (1) use of horizontal wells and (2) judicious injection above the formation parting pressure. Field cases now exist where 200-300-cp polymer solutions are injected without significant reductions in injectivity. Concern about costs associated with injection of viscous polymer solutions was a second major hurdle. However, that concern is reduced substantially by realization that polymer viscosity increases approximately with the square of polymer concentration. Viscosity can be doubled with only a 40% increase in polymer concentration. Up to a readily definable point, increases in viscosity of the injected polymer solution are directly related to increases in sweep efficiency and oil recovery. Previously published simulation results—suggesting that shear-thinning polymer solutions were detrimental to sweep efficiency—were shown to be unfounded (both theoretically and experimentally).

TABLE OF CONTENTS

LIST OF TABLES

TABLE OF FIGURES

ACKNOWLEDGMENTS

Financial support for this work is gratefully acknowledged from the United States Department of Energy (NETL/National Petroleum Technology Office), the State of New Mexico, ConocoPhillips, CP Kelco, SNF Floerger, and Statoil. ConocoPhillips was kind in providing a North Slope oil sample and information on relevant North Slope viscous oil reservoirs. CP Kelco and SNF Floerger provided important polymer samples for use in this work. I greatly appreciate the efforts of those individuals who contributed to this project. Karthik Kamaraj was largely responsible for the work in Chapter 2, with help from Guoyin Zhang and Yi Liu. Kate Wavrik and Tianguang Fan performed the core floods and viscosity measurements associated with Chapter 3. I also appreciate useful discussions with Nicolas Gaillard and Cédrick Favéro of SNF for the work in Chapter 3. Dr. Dongmei Wang (University of North Dakota) and Guoyin Zhang provided critical contributions to Chapter 4. Olatokunbo O. Akanni performed some preliminary work for Chapter 4. Dr. Robert Lane (Texas A&M) provided useful input for Chapter 4. Yi Liu performed the work in Chapter 5. Hao Wan performed the work in Chapter 6. Guoyin Zhang wrote Appendix A. This material is based upon work supported by the Department of Energy under Award Number DE- NT0006555.

EXECUTIVE SUMMARY

This final technical progress report describes work performed for the project, "Use of Polymers to Recover Viscous Oil from Unconventional Reservoirs." The objective of this three-year research project was to develop methods using water soluble polymers to recover viscous oil from unconventional reservoirs (i.e., on Alaska's North Slope). The project had three technical tasks. First, limits were re-examined and redefined for where polymer flooding technology can be applied with respect to unfavorable displacements. Second, we tested existing and new polymers for effective polymer flooding of viscous oil, and we tested newly proposed mechanisms for oil displacement by polymer solutions. Third, we examined novel methods of using polymer gels to improve sweep efficiency during recovery of unconventional viscous oil.

Effect of Residual Oil Saturation on Recovery Efficiency during Polymer Flooding of Viscous Oils. We examined the potential of polymer flooding for recovering viscous oils when the polymer is able to reduce the residual oil saturation to a value less than that of a waterflood. If polymers can reduce the residual oil saturation, that is an important factor for polymer flooding of light and medium gravity crude oils. However, is it important when displacing viscous oils? Since the displacement efficiency is often poor when water or even polymer solutions are injected to displace viscous oils, some have questioned whether the S_{or} is relevant. We used fractional flow calculations to examine this question for conditions in North Slope reservoirs with viscous oils. Variables considered include oil viscosity, water/polymer viscosity, relative permeability characteristics, connate water and residual oil saturations, formation layering, presence/absence of crossflow, and pore volume throughput. We found that induced changes in S_{or} can make a significant difference to recovery efficiency. As expected, the impact of S_{or} reduction by a polymer flood on oil recovery is more pronounced in reservoirs where residual oil saturations are high at the start of polymer flooding. The impact of S_{or} reduction diminishes with increasing degree of heterogeneity. A polymer flood can be effective for recovery of viscous oils even if the reservoir is extensively waterflooded before application of the polymer flood. A reduction in S_{or} was beneficial for all waterflood delays that we examined.

Rheology of a New Sulfonic Associative Polymer in Porous Media. For hydrophobically associative polymers, incorporating a small fraction of hydrophobic monomer into an HPAM polymer can promote intermolecular associations and thereby enhance viscosities and resistance factors. We investigated the behavior of a new associative polymer in porous media. The tetra-polymer has low hydrophobic monomer content and a molecular weight (Mw) of 12-17 million g/mol. Total anionic content is 15-25 mol%, including a few percent of a sulfonic monomer. This polymer is compared with a conventional HPAM with 18-20 million g/mol Mw and 35-40% anionic content. Rheological properties (viscosity versus concentration and shear rate, elastic and loss moduli versus frequency) were similar for the two polymers (in a 2.52% TDS brine at 25°C). For both polymers in cores with permeabilities from 300-13,000 md, no face plugging or internal filter cake formation was observed, and resistance factors correlated well using the capillary bundle parameter. For the HPAM polymer in these cores, low-flux resistance factors were consistent with low-shear-rate viscosities. In contrast, over the same permeability range, the associative polymer provided low-flux resistance factors that were 2-3 times the values expected from viscosities. Moderate shear degradation did not eliminate this effect—nor did flow through

a few feet of porous rock. Propagation experiments in long cores (up to 157 cm) suggest that the unexpectedly high resistance factors could propagate deep into a reservoir—thereby providing enhanced displacement compared with conventional HPAM polymers. Compared with HPAM, the new polymer shows a significantly higher level of shear thinning at low fluxes and a lower degree of shear thickening at high fluxes.

A Comparison of Polymer Flooding with In-Depth Profile Modification. For stratified reservoirs with free crossflow and where fractures do not cause severe channeling, improved sweep is often needed after water breakthrough. For moderately viscous oils, polymer flooding is an option for this type of reservoir. However, in recent years, an in-depth profile modification method had been commercialized where a block is placed in the high-permeability zone(s). This sophisticated idea requires (1) the blocking agent must have a low viscosity (ideally a unit-mobility displacement) during placement, (2) the rear of the blocking-agent bank in the high-permeability zone(s) must outrun the front of the blocking-agent bank in adjacent less-permeable zones, and (3) an effective block to flow must form at the appropriate location in the high-permeability zone(s). Achieving these objectives is challenging but has been accomplished in at least one field test. This study asks: When is this in-depth profile modification process a superior choice over conventional polymer flooding?

Using simulation and analytical studies, we examined oil recovery efficiency for the two processes as a function of (1) permeability contrast, (2) relative zone thickness, (3) oil viscosity, (4) polymer solution viscosity, (5) polymer or blocking-agent bank size, and (5) relative costs for polymer versus blocking agent. The results reveal that in-depth profile modification is most appropriate for high permeability contrasts (e.g. 10:1), high thickness ratios (e.g., less-permeable zones being 9 times thicker than high-permeability zones), and relatively low oil viscosities. Because of the high cost of the blocking agent (relative to conventional polymers), economics favor small blocking-agent bank sizes (e.g. 5% of the pore volume in the high-permeability layer). Even though short-term economics may favor in-depth profile modification, ultimate recovery may be considerably less than from a traditional polymer flood.

Do HPAM Solutions Reduce S_{or} During Polymer Flooding Of Viscous Oils? Conventional wisdom is that the ultimate residual oil saturation (S_{or}) for a polymer flood is the same as that for a waterflood. Polymers have a minor effect on oil-water interfacial tension, so no reduction of S_{or} is expected, compared with waterflooding. Several previous literature reports are consistent with this view in water-wet cores. However, for more oil-wet conditions (especially at Daqing), HPAM solutions reportedly reduced S_{or} by 6 to 15 saturation percentage points, even with waterfloods and polymer floods conducted at the same constant capillary number. Researchers at the University of Texas suggested that observed reductions in S_{or} that were attributed to polymer flooding might be due to core heterogeneity.

We are interested in whether polymer flooding can reduce S_{or} when displacing a viscous North Slope crude (190 cp viscosity @ 25°C, 0.935 g/cm^3, provided by ConocoPhillips). Tracer studies demonstrated that hydrophobic porous polyethylene cores that we used were homogeneous. In one polyethylene core at residual oil saturation (with North Slope crude after waterflooding), injection of a 10-cp HPAM solution (with a fixed capillary number of 1.77×10^{-5}) reduced S_{or} by at least four saturation percentage points (from 31% to less than 27%). Subsequent injection of 100-cp HPAM at the same capillary number appeared to reduce S_{or} further. In a second polyethylene core at connate water saturation (i.e., highly saturated with

North Slope crude), injection of a 10-cp HPAM solution (with a fixed capillary number of 1.77×10^{-5}) reduced S_{or} by six saturation percentage points compared to waterflooding (i.e., 26% versus 32%). Future studies will test whether these effects will be seen in water-wet porous media.

Mechanical Degradation of an Associative Polymer versus HPAM. An experimental study was performed to investigate the effects of reservoir brine salinity and divalent cations on mechanical (shear) degradation of a new hydrophobic associative polymer, (SNF C1205). This polymer has a small fraction of hydrophobic monomer groups along the acrylamide/acrylate backbone. Degradation was induced by forcing polymer solutions through a short core plug using a wide range of rates (1 to 500 ft/d). Our studies investigated solutions with salinities from 0.252 to 12.65% total dissolved solids and with divalent cation (Ca^{2+}) concentrations from 0 to 1.15%. Effluent viscosities and screen-factors were measured to determine the degree of mechanical degradation. For comparison, a conventional polyacrylamide (HPAM) polymer with similar molecular weight (18-20 million g/mol) was submitted to the same tests. As expected, mechanical degradation of the associative polymer increased with velocity in porous media, and rheology of the associative polymer in the viscometer showed Newtonian behavior at low shear rates and shear thinning at higher shear rates. As with HPAM, calcium exerted a stronger influence than sodium in reducing solution viscosity. However, tests demonstrated that the degree of mechanical degradation of associative polymer solutions does not always increase with ionic strength. This finding differs from previous reports for HPAM. When compared with the conventional HPAM, even though the associative polymer may show more shear sensitivity under some circumstances, it still provided higher viscosity and screen factor, and presumably, better mobility control than the conventional HPAM.

1. INTRODUCTION

A tremendous resource of viscous oil exists in the United States and throughout the world. Usually, thermal methods (e.g., steam flooding) are considered first for recovering this oil. However, circumstances often exist that preclude application of thermal methods. Consequently, we are exploring where polymer flooding can be viable for recovering viscous oil. This report focuses on research performed during the third and final year of the project, "Use of Polymers to Recover Viscous Oil from Unconventional Reservoirs." Results from the first two years of the project may be found in our first and second annual reports (Seright 2009, Seright 2010b).

Project Objectives

The objective of this three-year research project was to develop methods using water soluble polymers to recover viscous oil from unconventional reservoirs (i.e., on Alaska's North Slope). The project had three technical tasks. First, limits were re-examined and redefined for where polymer flooding technology can be applied with respect to unfavorable displacements. Second, we tested existing and new polymers for effective polymer flooding of viscous oil, and we tested newly proposed mechanisms for oil displacement by polymer solutions. Third, we examined novel methods of using polymer gels to improve sweep efficiency during recovery of unconventional viscous oil.

Report Content

In Chapter 2, using fractional flow calculations, we examine the potential of polymer flooding for recovering viscous oils when the polymer is able to reduce the residual oil saturation to a value less than that of a waterflood. Chapter 3 extensively investigates the rheology in porous media for a new hydrophobic associative polymer. In Chapter 4, using simulation and analytical studies, we compare oil recovery efficiency for polymer flooding versus in-depth profile modification (i.e., "Bright Water") as a function of (1) permeability contrast, (2) relative zone thickness, (3) oil viscosity, (4) polymer solution viscosity, (5) polymer or blocking-agent bank size, and (5) relative costs for polymer versus blocking agent. (Appendix A provides additional detail for an analytical study of this topic.) In Chapter 5, we experimentally establish how much polymer flooding can reduce the residual oil saturation in an oil-wet core that is saturated with viscous North Slope crude. Chapter 6 provides an experimental study, comparing mechanical degradation of an associative polymer (SNF C1205) with that of a partially hydrolyzed polyacrylamide (SNF 3830S HPAM).

Our latest research results, along with detailed documentation of our past work, can be found on our web site at http://baervan.nmt.edu/randy/.

2. EFFECT OF RESIDUAL OIL SATURATION ON RECOVERY EFFICIENCY DURING POLYMER FLOODING OF VISCOUS OILS

The objective of this work is to examine the effect of reduction of residual oil saturation (S_{or}) by polymer flooding on viscous oil recovery. Polymers generally do not significantly alter the oil-water interfacial tension. Consequently, the S_{or} value after extensive polymer flooding is expected to be the same as after waterflooding. But recent reports indicate that polymer flooding is able to reduce the residual oil saturation at a constant capillary number. Wu et al. (2007) observed that HPAM polymers reduced the waterflood S_{or} by up to 15 saturation percentage points (i.e., a S_{or} of 36.8% with waterflooding versus 21.75% for polymer flooding) using a constant capillary number of $5x10^{-5}$. Huh and Pope (2008) observed S_{or} reductions ranging from 2 to 22 saturation percentage points using Antolini cores and a constant capillary number of $4x10^{-6}$.

Alaska's North Slope contains a very large unconventional oil resource—over 20 billion barrels of heavy/viscous oil (Stryker et al. 1995, Thomas et al. 2007). Seright (2010a) examined the potential of polymer flooding in such heavy oil reservoirs. However, his analysis assumed that polymer would not reduce S_{or}. If polymers can reduce the residual oil saturation, that is an important factor for polymer flooding of light and medium gravity crude oils. However, is it important when displacing viscous oils? Since the displacement efficiency is often poor when water or even polymer solutions are injected to displace viscous oils, some have questioned whether the S_{or} is relevant. This study uses fractional flow calculations to examine this question for conditions in North Slope reservoirs with viscous oils. A simple case of one homogeneous layer is analyzed, followed by consideration of free-crossflow and no-crossflow cases in a two-layer system. For these cases, polymer is injected after primary recovery of oil. Then the analysis is extended for a polymer flood when a waterflood was in operation prior to polymer injection.

Fractional Flow Calculations

Simulation results for a polymer flood can be misleading if the user is not familiar with complex assumptions inherent in a simulator. Seright (2010a) presented cases where the assumptions projected inappropriate results. So in this work, fractional flow calculations were used which provided more transparent recovery projections. Fractional flow analysis was used by several authors to predict the recovery from a polymer flood (Lake 1989, Sorbie 1991, Green and Willhite 1998, Seright 2010a).

For our fractional flow analyses, flow was assumed to be incompressible and the capillary pressure differences between phases were neglected. Polymer was assumed to exhibit Newtonian behavior and the properties observed were independent of permeability. Also, polymer retention was assumed to balance the inaccessible pore volume.

The relative permeability characteristics were given by Eqs. 1 and 2. Seright (2010a) presented the conditions for the Base case and North Slope case given by Eqs. 3 and 4, respectively. The North Slope case was representative of the viscous oils in certain North Slope reservoirs.

$$k_{rw}=k_{rwo}\,[(S_w-S_{wr})/(1-S_{or}-S_{wr})]^{nw} \quad (1)$$

$$k_{ro}=k_{roo}\,[(1-S_{or}-S_w)/(1-S_{or}-S_{wr})]^{no} \quad (2)$$

BASE CASE: k_{rwo}=0.1, k_{roo}=1, S_{or}=0.3, S_{wr}=0.3, nw=2, no=2 .....(3)

NORTH SLOPE CASE: k_{rwo}=0.1, k_{roo}=1, S_{or}=0.12, S_{wr}=0.12, nw=4, no=2.5 .....(4)

Each of the following figures plots original oil in place (OOIP) recovered on the y-axis for a given pore volume (PV) of polymer or water that was injected. OOIP is given by (1-S_{wr}). S_{wr} is connate or irreducible water saturation. All cases used 1-cp connate water and 1,000-cp oil. The residual oil saturation for waterflood and polymer flood was different, so waterflood residual oil saturation was denoted by S_{orw} and polymer flood by S_{orp}. For the analyses where a polymer flood reduces the residual oil saturation, we considered four cases: (1) no S_{orp} reduction (0%), (2) 20% S_{orp} reduction, (3) 60% S_{orp} reduction, and (4) 100% S_{orp} reduction. Note that in Case (1), S_{orw}=S_{orp}, and in Case (4), S_{orp}=0.

Effect of S_{orp} Reduction on Oil Recovery

One Homogeneous Layer. Reduction of residual oil saturation by a polymer flood has a significant effect on the amount of viscous oils recovered. A simple system of one homogeneous layer was considered first. Figs. 1 and 2 pertain to the Base case, whereas Figs. 3 and 4 to the North Slope case. Figs. 1 and 3 apply to an unfavorable displacement where 1,000-cp oil is displaced by 10-cp polymer. Favorable displacements are shown in Figs. 2 and 4, where 1,000-cp polymer displaces 1,000-cp oil. Polymer flooding provided a substantially increased recovery in all cases.

When a polymer flood caused a reduction in S_{orp}, the Base case had high potential for additional oil recovery, as is evident from Figs. 1 and 2. Even for an unfavorable displacement in Fig. 1, the increase in oil recovery with S_{orp} reduction was significant. For example, at 1 PV of 10-cp polymer injection, the oil recovery increased from 41% for S_{orp}=0.3 to 45% for S_{orp}=0.24 (a 20% S_{orp} reduction). For the North Slope case (Figs. 3 and 4), a reduction of S_{orp} made less difference to oil recovered, compared to the Base case. For example for the North Slope case at 1 PV of 10-cp polymer injection, the oil recovery increased only from 61% for S_{orp}=0.12 to 63% for S_{orp}=0.096 (again, a 20% S_{orp} reduction). The Base-case waterflood had a much higher residual oil saturation (S_{orw}=0.3), compared to North Slope case (S_{orw}=0.12). Naturally, reservoirs with high residual oil saturations were more sensitive (in terms of oil recovery) to S_{orp} reduction. Reductions of S_{orp} had a greater effect on oil recovery for favorable displacements in both the Base case and the North Slope case (at 1 PV, compare Fig. 2 with Fig. 1 and compare Fig. 4 with Fig. 3).

Table 1 presents the OOIP recovered at the end of 1 PV injection of 1-cp water, 10-cp, 100-cp and 1,000-cp polymer for displacing 1,000-cp oil. For the Base case with 10-cp polymer displacing 1,000-cp oil in one homogeneous layer, oil recovery was 23% OOIP higher for S_{orp}=0 than for S_{orp}=0.3. For the Base case with 1,000-cp polymer displacing 1,000-cp oil in one homogeneous layer, oil recovery was 41% OOIP higher for S_{orp}=0 than for S_{orp}=0.3. For the North Slope case with 10-cp polymer displacing 1,000-cp oil in one homogeneous layer, oil recovery was 9% OOIP higher for S_{orp}=0 than for S_{orp}=0.12. For the North Slope case with 1,000-cp polymer displacing 1,000-cp oil in one homogeneous layer, oil recovery was 13% OOIP higher for S_{orp}=0 than for S_{orp}=0.12. So, a reduction of S_{orp} had a significant effect on the %OOIP recovered for viscous oils. Close examination of Table 1 reveals that S_{orp} reductions of only 20% had a significant effect on oil recovery for both the Base and North Slope cases. As

expected, a given % reduction in S_{orp} had a much greater effect for the Base case than for the North Slope case—simply because the S_{orw} was 2.5 times greater for the Base case than for the North Slope case.

Comparing Fig. 2 versus Fig. 1 and Fig. 4 versus Fig. 3 reveals that reductions of S_{orp} had a greater effect on oil recovery for favorable displacements than for unfavorable displacements. As expected, the effect was less important for the North Slope case than for the Base case (again, simply because the Base case had a greater oil target).

For additional comparison, we calculated the incremental increase of oil recovery—i.e., the difference in oil recovery for the two extremes (0% reduction and 100% reduction) divided by the recovery for 0% S_{orp} reduction. In Table 1, the Base-case one-layer incremental increase rose from 54% for 1-cp polymer to 72% for 1,000-cp polymer. In contrast, the incremental increase remained about the same (~15%) for the North Slope case. As mentioned earlier, reductions in S_{or} were less important if the waterflood residual oil saturation was low (as in North Slope case).

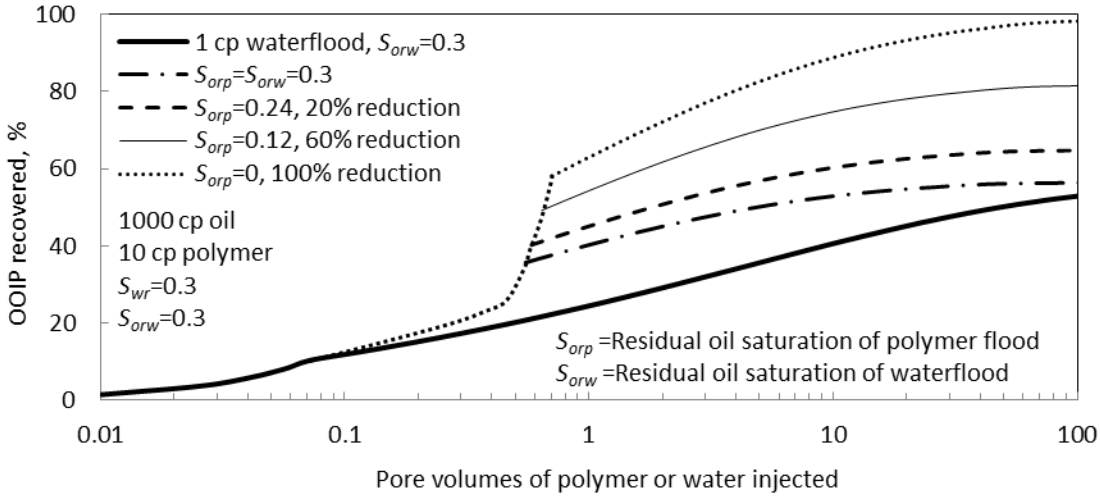

Fig. 1—10-cp polymer flood results for S_{orp} reduction, one layer. Base case.

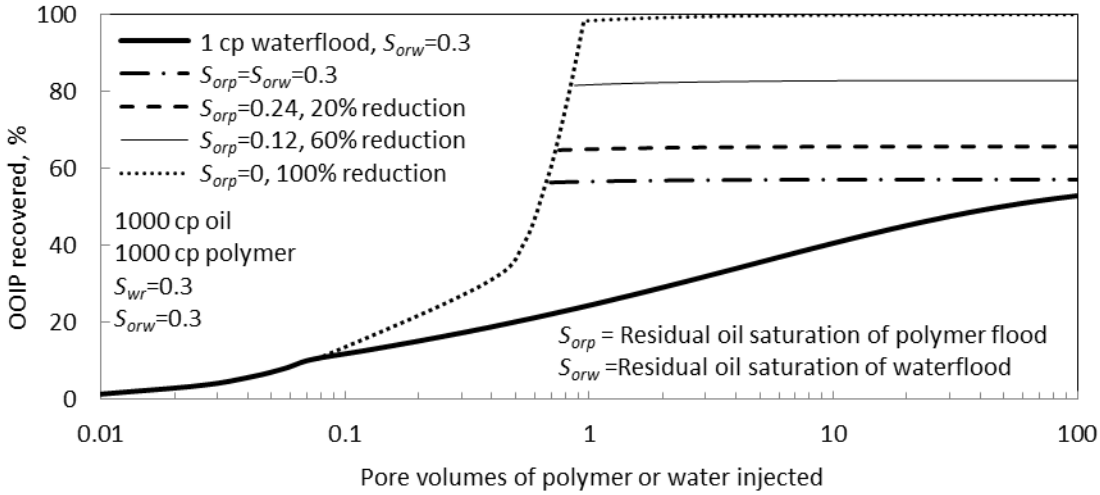

Fig. 2—1,000-cp polymer flood results for S_{orp} reduction, one layer. Base case.

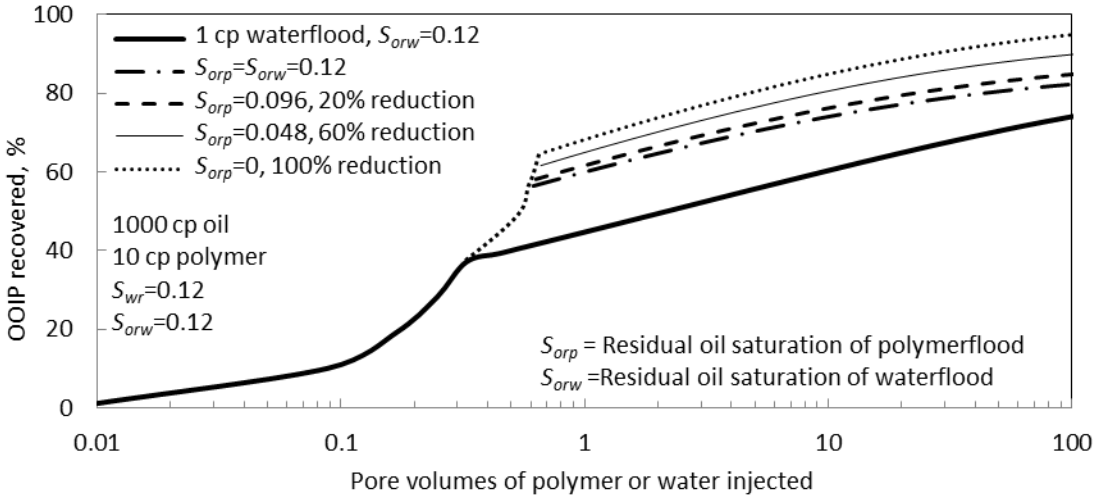

Fig. 3—10-cp polymer flood results for S_{orp} reduction, one layer. North Slope case.

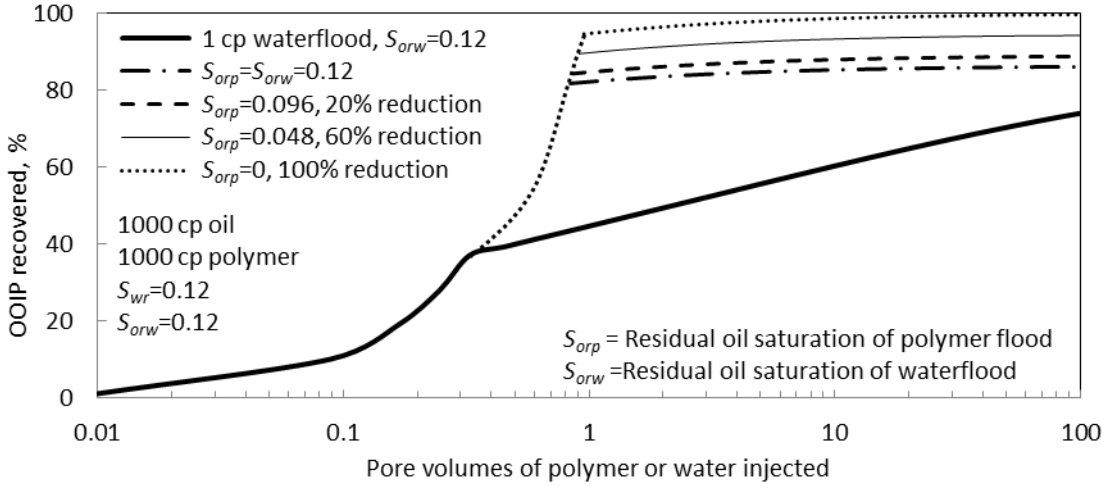

Fig. 4—1,000-cp polymer flood results for S_{orp} reduction, one layer. North Slope case.

Effect of Heterogeneity

The effect of heterogeneity was analyzed by considering two layers with and without crossflow between the layers. Both layers had equal thickness with k_1=1 darcy, ϕ_1=0.3, k_2=0.1 darcy, ϕ_2=0.3. All other parameters and conditions were the same as those used in the one-layer case. For the no-crossflow case, displacements in the individual layers were treated separately and then combined to yield the overall displacement efficiency (Green and Willhite 1998). The free-crossflow case required application of vertical equilibrium between the layers (Zapata and Lake 1981, Lake 1989). For both the free-crossflow and no-crossflow cases, spreadsheets were used to solve the fractional flow equations. Examples of these spreadsheets can be found in Seright 2010c.

Fig. 5 shows the one-layer North Slope case for 100-cp polymer displacing 1,000-cp oil. Figs. 6 and 7 illustrate the free-crossflow and no-crossflow North Slope cases for 100-cp polymer displacing 1,000-cp oil. The difference in incremental oil recovery between no S_{orp} reduction and

100% S_{orp} reduction was moderate for the one-layer case (11% OOIP) and was smaller for both the free-crossflow (8% OOIP) and no-crossflow (6% OOIP) cases. With the increase in heterogeneity (i.e., the two-layer cases), a reduction of S_{orp} has a smaller effect, compared to that seen for one layer.

At low mobility ratios, the two-layer, free-crossflow recovery curves can approach those for one homogeneous layer. A comparison of Figs. 4 and 8 demonstrates this finding for 1,000-cp polymer displacing 1,000-cp oil.

Table 1—% OOIP recovered after 1 PV injection for displacing 1,000-cp oil.

Polymer viscosity, cp	S_{orp} reduction, %	OOIP recovered, %	
		One layer (Base case)	One layer (North Slope case)
1	0 (S_{orp}=S_{orw})	24	45
	20	27	46
	60	32	48
	100 (S_{orp}=0)	37	51
	Incremental increase	(37-24)100/24=54%	(51-45)100/45=13%
10	0 (S_{orp}=S_{orw})	41	61
	20	45	63
	60	54	66
	100 (S_{orp}=0)	64	70
	Incremental increase	(64-41)100/41=56%	(70-61)100/61=15%
100	0 (S_{orp}=S_{orw})	53	74
	20	60	77
	60	75	81
	100 (S_{orp}=0)	88	85
	Incremental increase	(88-53)100/53=66%	(85-74)100/74=15%
1000	0 (S_{orp}=S_{orw})	57	82
	20	65	85
	60	82	90
	100 (S_{orp}=0)	98	95
	Incremental increase	(98-57)100/57=72%	(95-82)100/82=16%

Table 2 lists the recovery values for 1,000-cp oil at 1 PV injection of 1-cp water, 10-cp, 100-cp and 1,000-cp polymer. Along with Figs. 6 and 7, Table 2 explains the effects of heterogeneity and S_{orp} reduction on oil recovery. For no-crossflow and free-crossflow cases during an unfavorable displacement, the effect of S_{orp} reduction on oil recovery was noticably less than that in one layer. For an unfavorable displacement and a given set of conditions, the free-crossflow case provided the lowest recoveries. As the displacement became more favorable, recovery efficiency improved more for the free-crossflow case than the no-crossflow case. During

injection of the most viscous polymer solution, the free-crossflow case closely followed the behavior seen when only one layer was present.

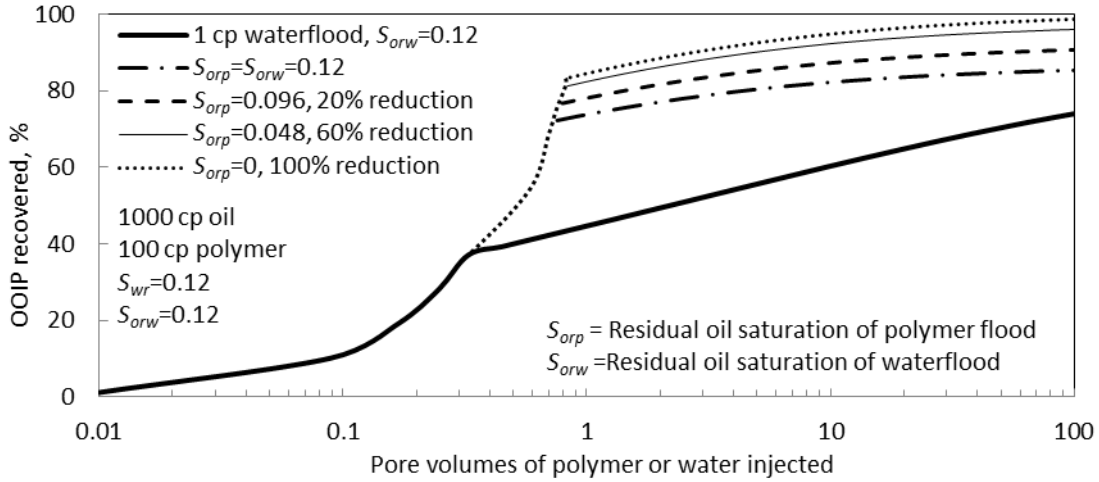

Fig. 5—100-cp polymer flood results for one homogeneous layer. North Slope case.

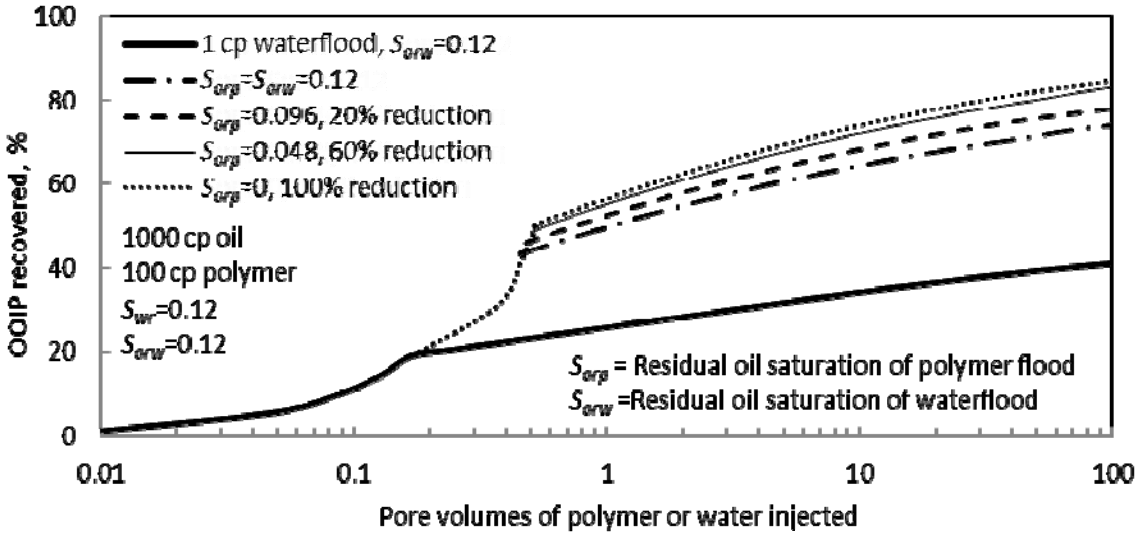

Fig. 6—100-cp polymer flood results for two layers. Free crossflow. North Slope case.

Our findings are consistent with the behavior that was observed by others (Coats et al. 1971, Craig 1971, Zapata and Lake 1981, Sorbie and Seright 1992). As the displacement becomes more favorable, crossflow cases achieve higher recovery compared to no-crossflow cases. For unfavorable displacements, no-crossflow cases achieve higher recovery than free-crossflow cases.

For the analyses of two-layered systems above, the permeability ratio, k_1/k_2, was fixed at a value of 10. We considered other permeability ratios, including 2 and 5. Figs. 9 and 10 explain the effects of heterogeneity and S_{orp} reduction on oil recovery by considering different permeability ratios for 1,000-cp oil displaced by 100-cp polymer (North Slope parameters). Fig. 9 describes the free-crossflow case, comparing the extreme cases of no S_{orp} reduction and 100% reduction (to S_{orp} =0). At 1 PV injection of polymer with free crossflow, the effect of S_{orp}

reduction on oil recovery diminished with increased permeability ratio: i.e., by 10.5% OOIP at k_1/k_2=1, by 10.5% OOIP at k_1/k_2=2, by 7.5% OOIP at k_1/k_2=5, and by 6.5% OOIP at k_1/k_2=10. No-crossflow cases (described by Fig. 10) exhibit a similar trend for increasing heterogeneity. At 1 PV injection of polymer with no crossflow, the effect of S_{orp} reduction on oil recovery diminished with increased permeability ratio: i.e., by 10.5% OOIP at k_1/k_2=1, by 9.3% OOIP at k_1/k_2=2, by 6.9% OOIP at k_1/k_2=5, and by 5.6% OOIP at k_1/k_2=10. Thus, the effect of S_{orp} reduction on oil recovery becomes less significant for both free-crossflow and no-crossflow cases with increasing reservoir heterogeneity.

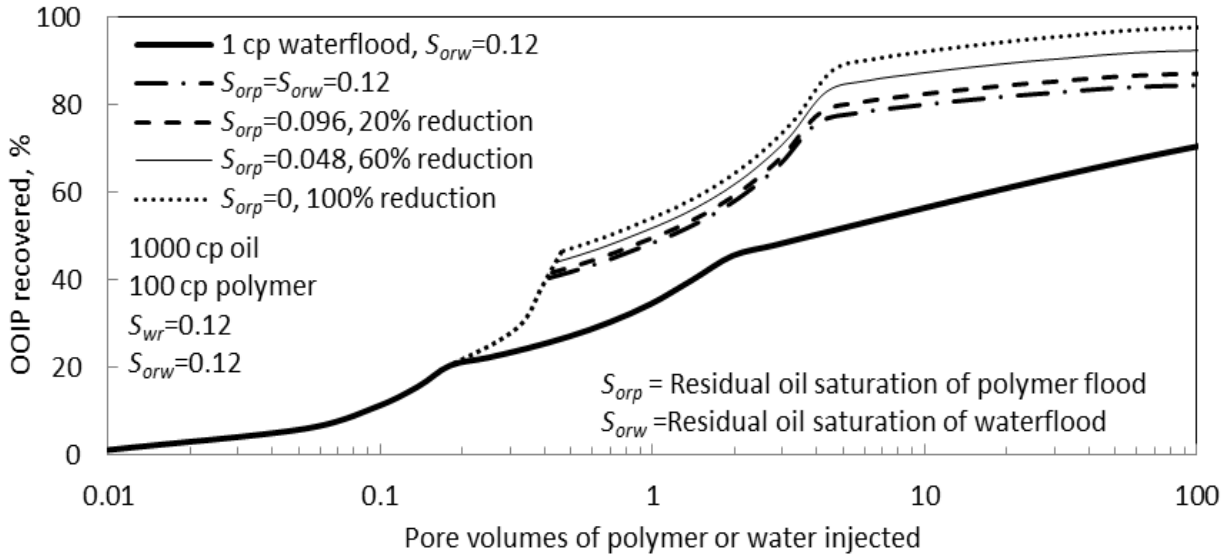

Fig. 7—100-cp polymer flood results for two layers. No crossflow. North Slope case.

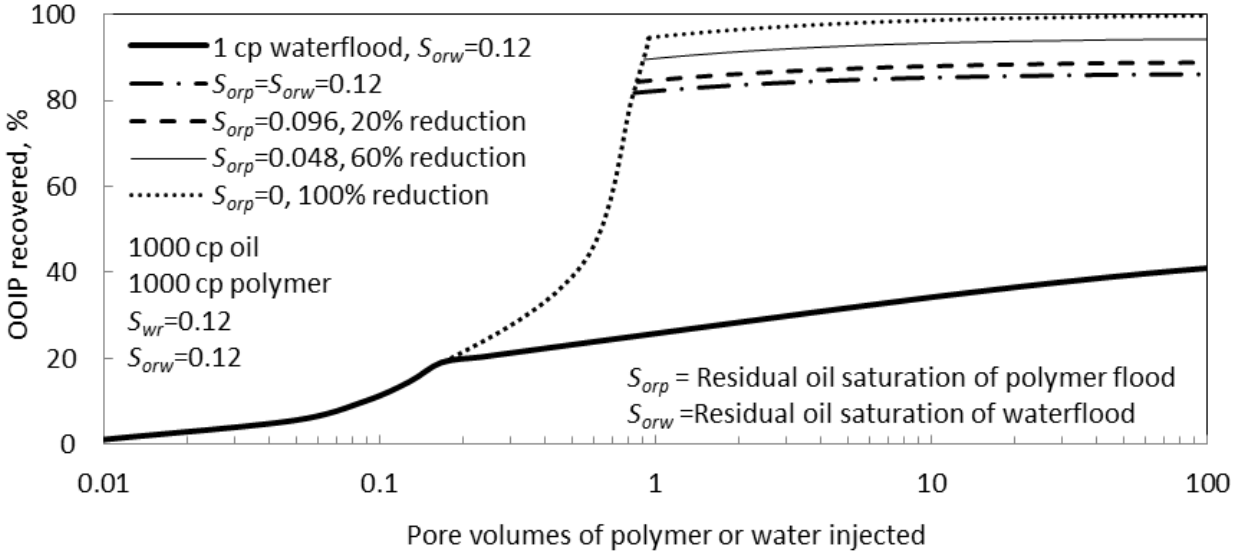

Fig. 8—1,000-cp polymer flood results for two layers. Free crossflow. North Slope case.

Table 2—% OOIP recovered after 1 PV injection for displacing 1,000-cp oil (North Slope case).

Polymer viscosity, cp	S_{orp} reduction, %	OOIP recovered, %		
		One layer	Two layers, no crossflow	Two layers, free crossflow
1	0 (S_{orp}=S_{orw})	45	34	26
	20	46	35	27
	60	48	36	28
	100 (S_{orp}=0)	51	38	30
	Max. difference	(51-45)=6	(38-34)=4	(30-26)=4
10	0 (S_{orp}=S_{orw})	61	43	35
	20	63	45	36
	60	66	47	38
	100 (S_{orp}=0)	70	50	40
	Max. difference	(70-61)=9	(50-43)=7	(40-35)=5
100	0 (S_{orp}=S_{orw})	74	49	52
	20	77	51	54
	60	81	54	55
	100 (S_{orp}=0)	85	57	58
	Max. difference	(85-74)=11	(57-49)=8	(58-52)=6
1000	0 (S_{orp}=S_{orw})	82	53	82
	20	85	54	85
	60	90	57	90
	100 (S_{orp}=0)	95	59	95
	Max. difference	(95-82)=13	(59-53)=6	(95-82)=13

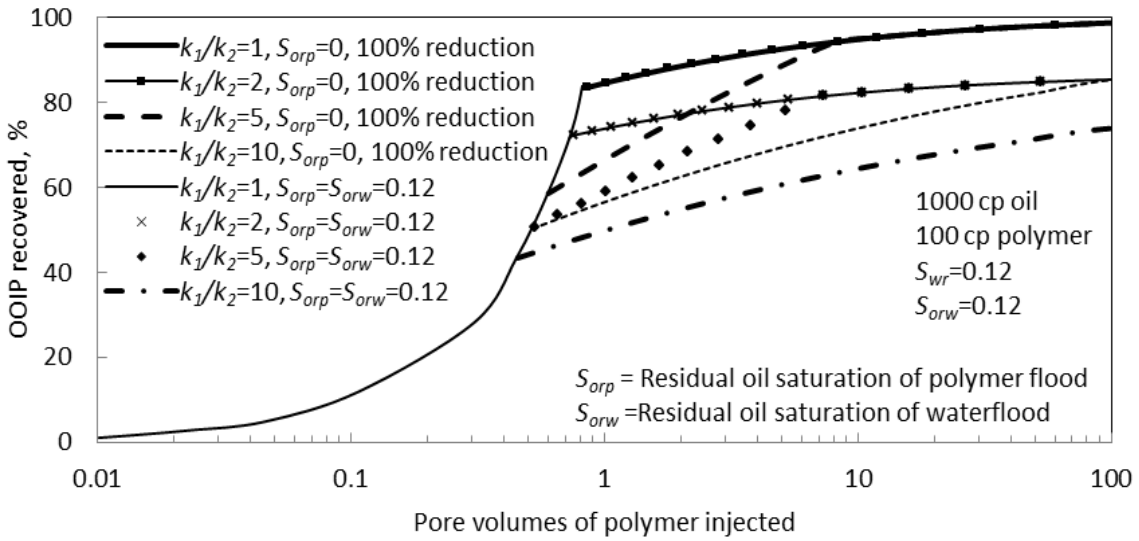

Fig. 9—Effect of heterogeneity. Free crossflow. North Slope case.

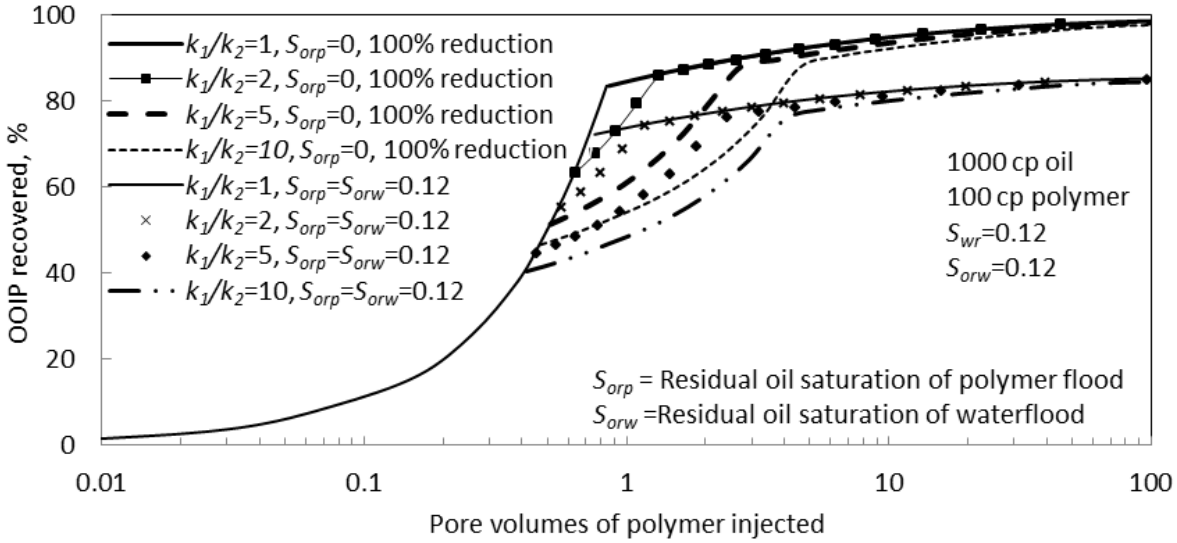

Fig. 10—Effect of heterogeneity. No crossflow. North Slope case.

Polymer Flooding After a Waterflood

Seright (2010b) explained how a polymer flood can be effective for recovery of viscous oils even if the reservoir is extensively waterflooded before application of the polymer flood. We extended this analysis for a polymer flood that reduces the residual oil saturation to a value lower than that possible by a waterflood. The bottom thick solid line in Fig. 11 shows oil recovery projections for continuous water injection (with 1-cp water), while all other curves show projections for continuous polymer solution injection (with 100-cp polymer). Depending on the extent of S_{orp} reduction (0%, 20%, 60%, 100%), different recovery projections were obtained for a polymer flood. In this figure, flow was linear, one homogeneous layer was present, porosity was 0.3, the reservoir contained 1,000-cp oil at connate water saturation (S_{wr}=0.12) and our "North Slope" parameters were used. The near-vertical line segments that connect the continuous-water-injection to the continuous-polymer-injection curves show cases where polymer flooding was initiated after injecting the specified volumes of water (from 1 to 10 PV). To explain this curve, consider the case of 1 PV delay. When 100-cp polymer is injected into the one-layer reservoir, oil recovery follows the bottom waterflooding curve for 1.75 PV (i.e., 1 PV associated with water injection plus 0.75 PV delay associated with polymer propagating through the reservoir). After that point, a 0.355-PV oil bank (for no S_{orp} reduction, S_{orp}=0.12) arrives at the production well, the oil recovery rate increases significantly, and the recovery curve jumps to join the continuous-polymer-injection curves. All other PV delays (2, 5, and 10 PV) followed a similar behavior. When a polymer flood reduced the residual oil saturation, the size of the oil bank increased. For 1 PV delay, the size of the oil bank increased from 0.355 to 0.526 PV when the polymer flood was able to achieve 100% S_{orp} reduction. With increased size of the pre-polymer waterflood (Fig. 11), the oil bank diminished, but the effect of S_{orp} reduction on oil bank formation remained constant and was equal to the PV of oil bank between 0% reduction (where the oil recovery projection joined the continuous polymer flood) and 100% reduction (extreme cases). Note that Fig. 11 is similar to Fig. 5 (North Slope case, one layer, 100-cp polymer displacing 1,000-cp oil). The oil bank size mentioned above (between 0% reduction and 100% reduction) is the same as the difference in oil recovery (in terms of PV) between the extreme

cases in Fig. 5. The key point is that even though the oil bank decreases with increasing size of the pre-polymer waterflood, the effect of S_{orp} reduction on oil bank is independent of the waterflood bank size. In other words, the oil bank formed due to reduction of S_{orp} by a polymer flood is the same for polymer as a secondary flood or a tertiary flood (after a waterflood).

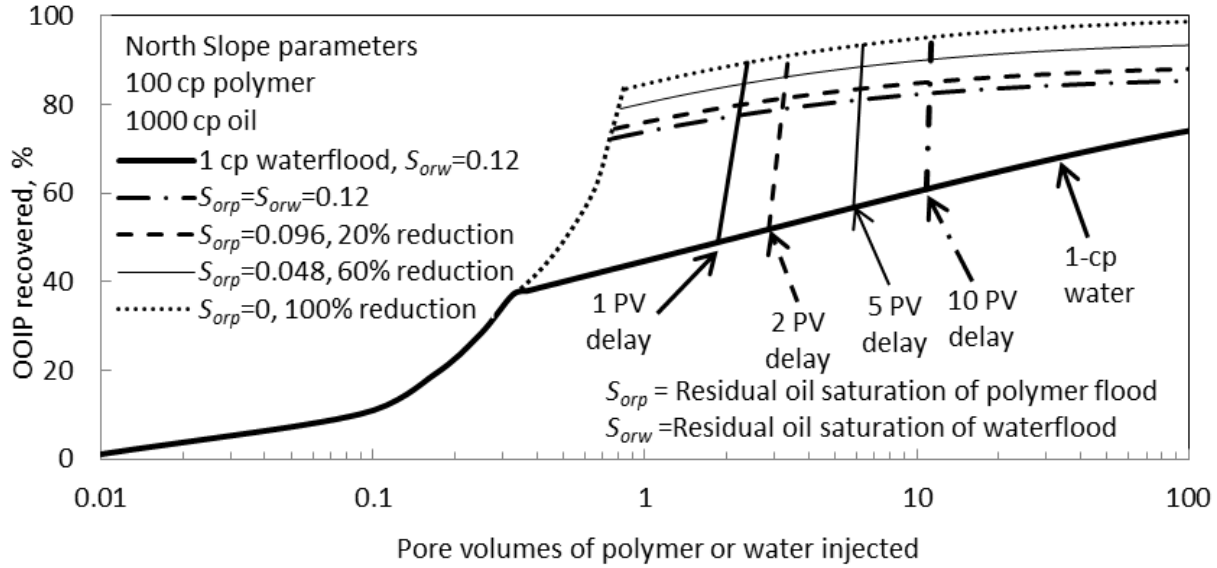

Fig. 11—Injection of 100-cp polymer, initiated after waterflooding of specified PV, 1 layer.

Conclusions

1. If a polymer flood of viscous oil is able to decrease the residual oil saturation (below that expected for a waterflood), a significant amount of additional oil can be recovered, compared to the case where polymer does not reduce S_{or}.
2. As expected, the impact of S_{or} reduction by a polymer flood on oil recovery is more pronounced in reservoirs where residual oil saturations are high at the start of polymer flooding.
3. The impact of S_{or} reduction diminishes with increasing degree of heterogeneity.
4. A polymer flood can be effective for recovery of viscous oils even if the reservoir is extensively waterflooded before application of the polymer flood. A reduction in S_{or} was beneficial for all waterflood delays that we examined.

3. RHEOLOGY OF A NEW SULFONIC ASSOCIATIVE POLYMER IN POROUS MEDIA

Introduction

In polymer floods or chemical floods where polymer is needed for mobility control, the cost-effectiveness of the polymer is a major concern. Cost-effectiveness is determined by the polymer cost and the resistance factor provided by the chosen polymer solution at conditions found deep within a reservoir (i.e., low fluid velocities, reservoir temperature, etc.). Resistance factor is the effective viscosity of the polymer solution in porous media, relative to water (i.e., water mobility divided by polymer solution mobility). Partially hydrolyzed polyacrylamides (HPAM) and xanthan polysaccharides have been the dominant polymers used in enhanced oil recovery (EOR). If polymers are identified that are more cost-effective than these traditional EOR polymers, field applications of chemical floods could become much more widespread.

Associative polymers have been investigated as a possible substitute for HPAM polymers in EOR applications (Evani 1984, Bock et al. 1988, McCormick and Johnson 1988, Taylor and Nasr-El-Din 1998, 2007, Buchgraber et al. 2009, Dupuis et al. 2010). In particular, Taylor and Nasr-El-Din (1998, 2007) extensively reviewed the literature for synthesis and performance of associative polymers. For hydrophobically associative polymers, incorporation of a small fraction of hydrophobic monomer into an HPAM polymer is intended to promote intermolecular associations and thereby enhance viscosities and resistance factors. At moderate concentrations (e.g., 0.05% to 0.5%), these polymers (with 0.1-7% hydrophobic monomer) can provide substantially higher viscosities than equivalent-molecular-weight polymers without hydrophobic groups (Bock et al. 1988, McCormick and Johnson 1988).

A number of issues have inhibited widespread application of associative polymers for EOR. In some cases, the increase in viscosity with increasing polymer concentration is abrupt (Bock et al. 1988, McCormick and Johnson 1988)—leading to concerns about controlling the performance of the polymer during flooding operations. If small changes in concentration cause large changes in viscosity, small operational errors could accentuate injectivity problems if polymer concentrations are higher than the target and could provide insufficient mobility control if polymer concentrations are low.

A second concern is the ability of associative polymers to penetrate deep into a reservoir. Compositions have been identified that show a maximum in plots of viscosity versus shear rate (Bock et al. 1988, Kujawa et al. 2004, Maia et al. 2009). Apparently, within a certain range of shear rates, the polymer becomes sufficiently extended to promote intermolecular interactions over intramolecular interactions. The polymer complexes that form by associative polymers certainly enhance viscosity and can provide high resistance to flow for a short distance in porous media. However, an important unresolved issue with many associative polymers is whether the enhanced viscosity characteristics can be propagated deep into a reservoir. Most previous studies of these polymers have used short cores with no internal pressure taps for their evaluations of behavior in porous media: 1.3-2.54 cm for Bock et al. (1988), 2.54 cm for Evani (1989), 13 cm for Dong and Wang (1995), 7 cm for Kun et al. (2004), 9 cm for Maia et al (2009). With such short cores (and no internal pressure taps), resistance factors that appear high may simply reflect plugging.

Argillier et al. (1996) and Volpert et al. (1997) concluded that hydrophobically associative polymers show multilayer adsorption on clays and siliceous minerals. Consistent with this

finding, Maia et al. (2009) observed that resistance factors for an associative polymer increased continuously with increased throughput in sandstone cores. Kun et al. (2004) and Lu et al. (2008) provided evidence of velocity- and history-dependent retention and resistance factors for associating polymers in sandpacks. Several authors (Eoff et al. 2005, Zhao et al. 2006) proposed utilizing highly adsorbing associating polymers to reduce rock permeability for acid diversion and conformance improvement. During a study of associative polymers in 10-cm-long cores with two internal pressure taps, Dupuis et al. (2010) noted a "minority polymeric species" that provided high resistance factors but that propagated very slowly through the cores. They felt that their observations were inconsistent with the classic view of multilayer adsorption of a polymer. Of course, if an associative polymer complex is removed (either by adsorption or mechanical entrapment) after flowing a short distance in a porous media, its mobility reduction benefits cannot be expected to materialize far from a wellbore where most oil is displaced. Work is needed in longer cores to assess whether the beneficial properties of associative polymers can be propagated deep into a porous medium.

In this chapter, we examine the rheology (both in a viscometer and in porous media) for a new sulfonic hydrophobically associative polymer. This sulfonated polymer has a lower hydrophobe content (and higher molecular weight) than most associative polymers that were previously investigated for EOR. Consequentally, it does not exhibit viscosities that are noticeably higher than those for the HPAM analog. Nevertheless, as will be shown, it provides significantly higher resistance factors in porous media than HPAM. Furthermore, its associative properties are not so great that polymer propagation through porous media is impaired. For studies in porous media in this work, a wide range of flux (0.1 to 100 ft/d), polymer concentration (500-2,500 ppm), and core permeability (300-13,000 md) are investigated. Throughout this study, comparisons are made with the performance of a commercially available HPAM. Our goals were to establish (1) whether the associative polymer provided superior resistance factors, compared with HPAM, (2) whether these enhanced resistance factors are expected to propagate deep into a reservoir, and (3) the resistance of the associative polymer to mechanical degradation, compared with HPAM.

Polymers Examined and Viscosity Behavior

The new hydrophobically associative polymer was provided by SNF Floerger: Superpusher DP/C1205, Lot GC 2882/6 (hereafter called AP or the "associative polymer"). This polymer is an anionic-polyacrylamide-based tetra-polymer that has associative properties as described by Gaillard et al. (2010). Typically, the hydrophobic monomer content ranges from 0.025 to 0.25 mol%. Molecular weights (Mw) range from 12-17 million g/mol, and the total anionic content is between 15 and 25 mol%. Less than 8 mol% sulfonic monomer is present. The associative polymer was made by a process derived from micellar polymerization, but the "hydrophobic" monomer used was amphiphilic and dissolved very well in water. A slight amount of surfactant was used as a process aid, but the final amount of remaining surfactant did not exceed 0.25% of the final polymer product, and for the solutions prepared here, had a concentration in brine of less than 10 parts per million (ppm)—well below any critical micelle concentration.

During our studies, the brine contained 2.52% total dissolved solids (TDS), specifically with 2.3% NaCl and 0.22% $NaHCO_3$. The studies were performed at 25°C. This brine and temperature are representative of those associated with a large polymer flood in Canada. Comparisons will be made with the performance of a conventional HPAM, SNF Flopaam 3830S (Lot X 1899). This polymer has a molecular weight of 18-20 million g/mol and a degree of hydrolysis of 35-40%. Hereafter in this report, we call this polymer, "HPAM." Polymer solutions

were prepared using the standard method for preparing laboratory HPAM solutions. A vortex was established in a beaker of brine using a magnetic stir bar. The polymer powder was sprinkled onto the vortex shoulder to individually wet the polymer particles. After adding the polymer, the stir rate was reduced but kept at a level sufficient to keep the hydrating polymer particles suspended and separated. Compared with the HPAM, the associative polymer generally took longer to dissolve in the 2.52%TDS brine (which contained no divalent ions). In a brine that contained calcium (2.3% NaCl, 0.23% $CaCl_2$), the dissolution time for the associative polymer was about 30% longer than without calcium. (However, this time could be reduced by optimizing the polymer composition for a calcium-containing brine.) The associative polymer solutions could exhibit viscosities that depend on mixing time and shear history during the dissolution period.

For both polymers, viscosity (determined using an Anton Paar Physica MCR 301 viscometer) versus shear rate and polymer concentration is plotted in Fig. 12. For polymer concentrations of 500 ppm, 900 ppm, 1500 ppm and 2,500 ppm in 2.52% TDS brine, viscosity versus shear rate was quite similar for the HPAM and associative polymers. Fig. 13 demonstrates that the elastic modulus (*G'*), loss modulus (*G"*), and complex viscosity behavior was also very similar for the two polymers.

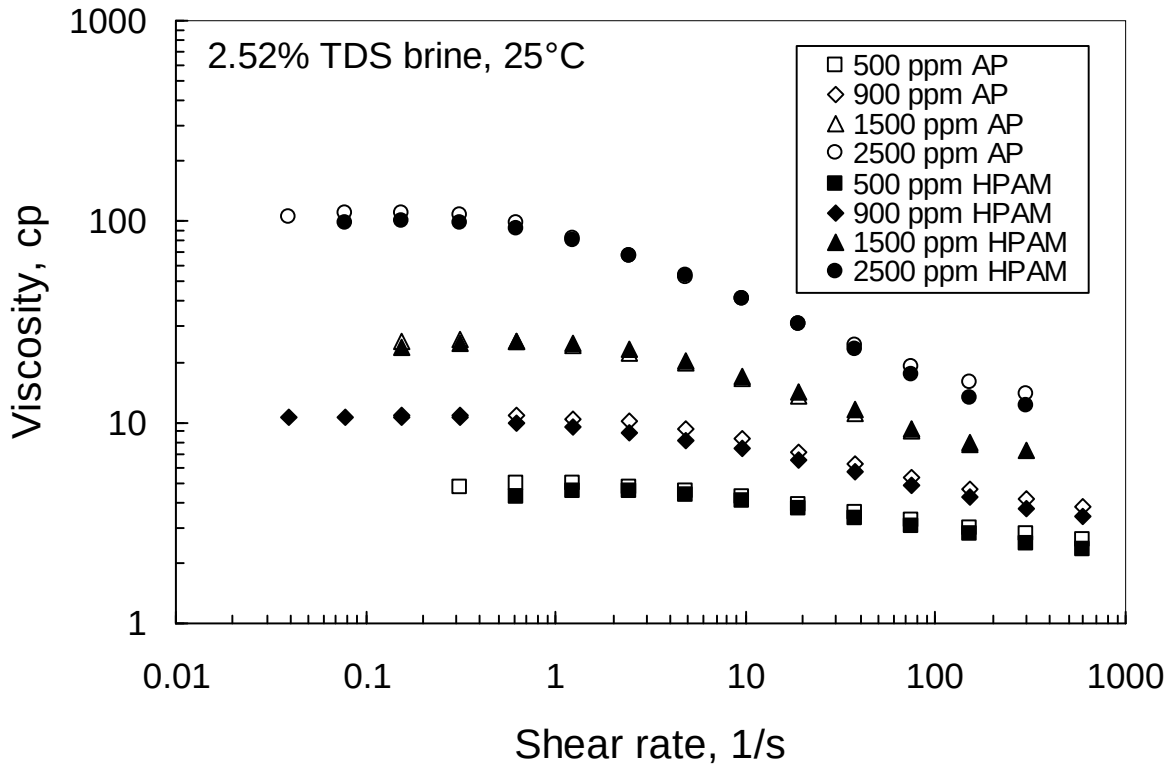

Fig. 12—Viscosity versus shear rate and concentration.

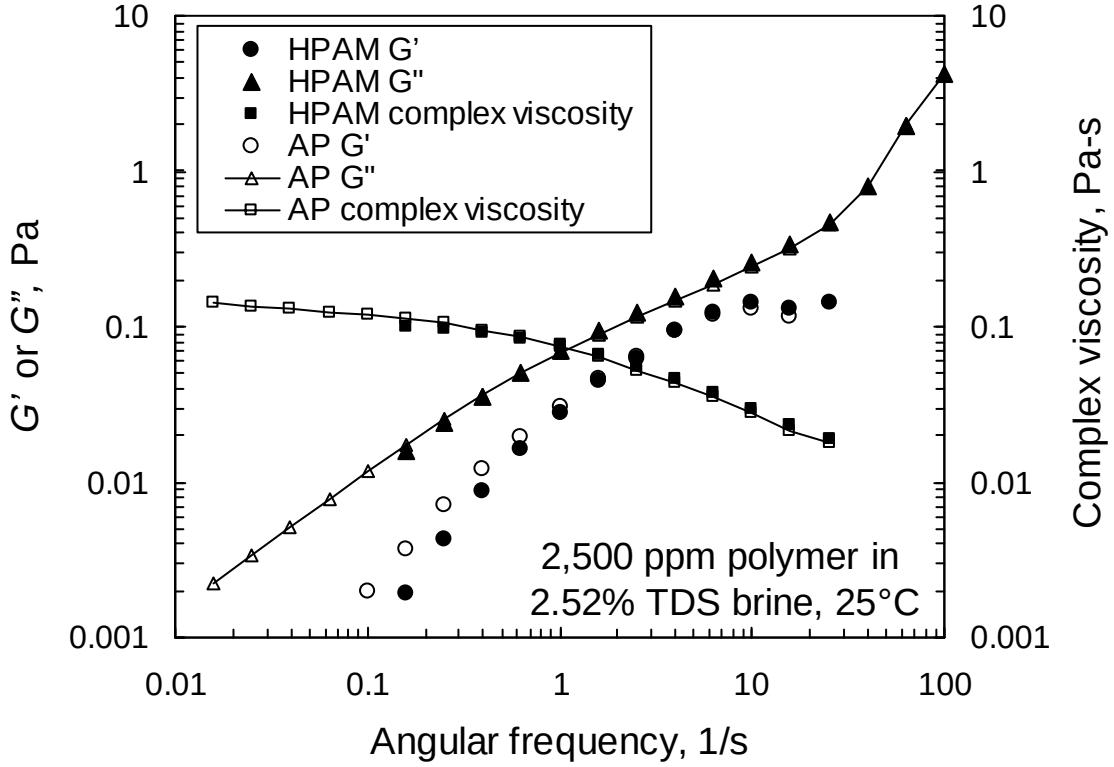

Fig. 13—*G'*, *G"*, and complex viscosity.

Face Plugging

Filter Tests. Our previous work (Seright *et al*. 2009) identified a filter test that allows comparison of the face-plugging characteristics for polymers. In this test, a Millipore AP10™ filter pad is placed in a filter holder upstream of a 10 μm polycarbonate (Sterlitech Track Etch™) membrane filter (both 13 mm in diameter). Using a fixed pressure drop across the filter holder, we record filter cake resistance (calculated using the Darcy equation, with units of cm-cp/darcy) versus throughput (volume of fluid injection per filter area, in cm^3/cm^2.) Fig. 14 compares filtration results for HPAM (solid symbols) and the associative polymer (open symbols). Notice that both polymers show excellent filterability at lower concentrations (1,000 ppm or lower), but plugged within 70 cm^3/cm^2 throughput at higher concentrations (1,500 ppm). Plugging characteristics of the associative polymer appear to be no worse than those of HPAM. The fact that plugging behavior for both polymers was severe with 1,500-ppm polymer, but not with lower concentrations may be explained using the bridging-adsorption concepts described by Zitha et al. (2001).

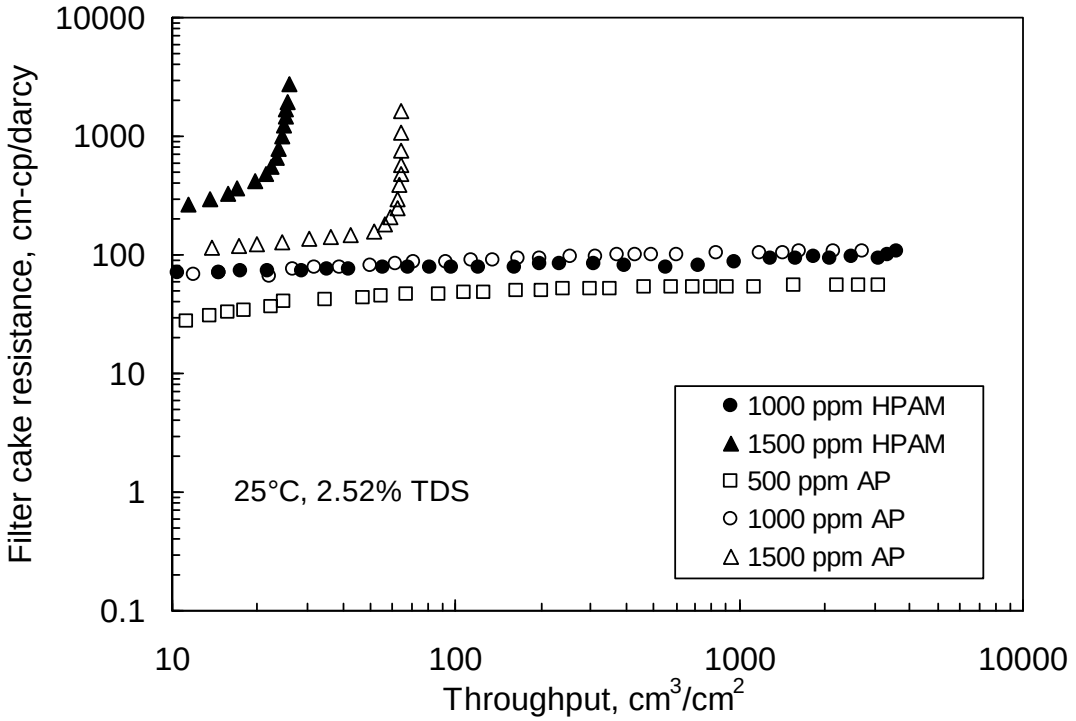

Fig. 14—Filter test results.

Core Face Plugging. Several experiments examined the level of face plugging that occurred during injection of large volumes of associative polymer solutions through a 363-md Berea sandstone core and through a 12,313-md porous polyethylene core. Both of these 13-14-cm-long cores had two internal pressure taps that divided the cores into three sections. By monitoring pressure drops and resistance factors in the various core sections we could assess the level of face plugging as a function of polymer solution throughput. After injecting 97 pore volumes (PV) or 580 cm^3/cm^2 of the associative polymer solutions (with concentrations up to 2,500 ppm) through the 12,313-md core, resistance factors in the first core section were no higher than in the second or third core sections. Similarly, after injecting 51 PV or 248 cm^3/cm^2 of associative polymer solutions (again with concentrations up to 2,500 ppm) through the 363-md core, resistance factors in the first core section were no higher than in the second or third core sections. Thus, no significant face plugging was observed for the associative polymer solutions. Details of these tests can be found in Seright 2010.

Pore Plugging

Resistance Factor versus Flux and Concentration. Fig. 15 plots resistance factor as a function of flux in each of the three core sections for injection of 500-ppm associative polymer in a Berea sandstone core. (Details of our equipment and methods can be found in Seright et al. 2010 and Seright 2010.) At a given flux, the resistance factors were reasonably consistent in the three core sections. The resistance factors were somewhat higher in the third core section, which argues against plugging of the inlet face. Consistent with normal HPAM behavior (Seright *et al.* 2010), a strong shear thickening was seen at moderate-to-high flux values and Newtonian or a slight shear-thinning behavior was seen at low flux values.

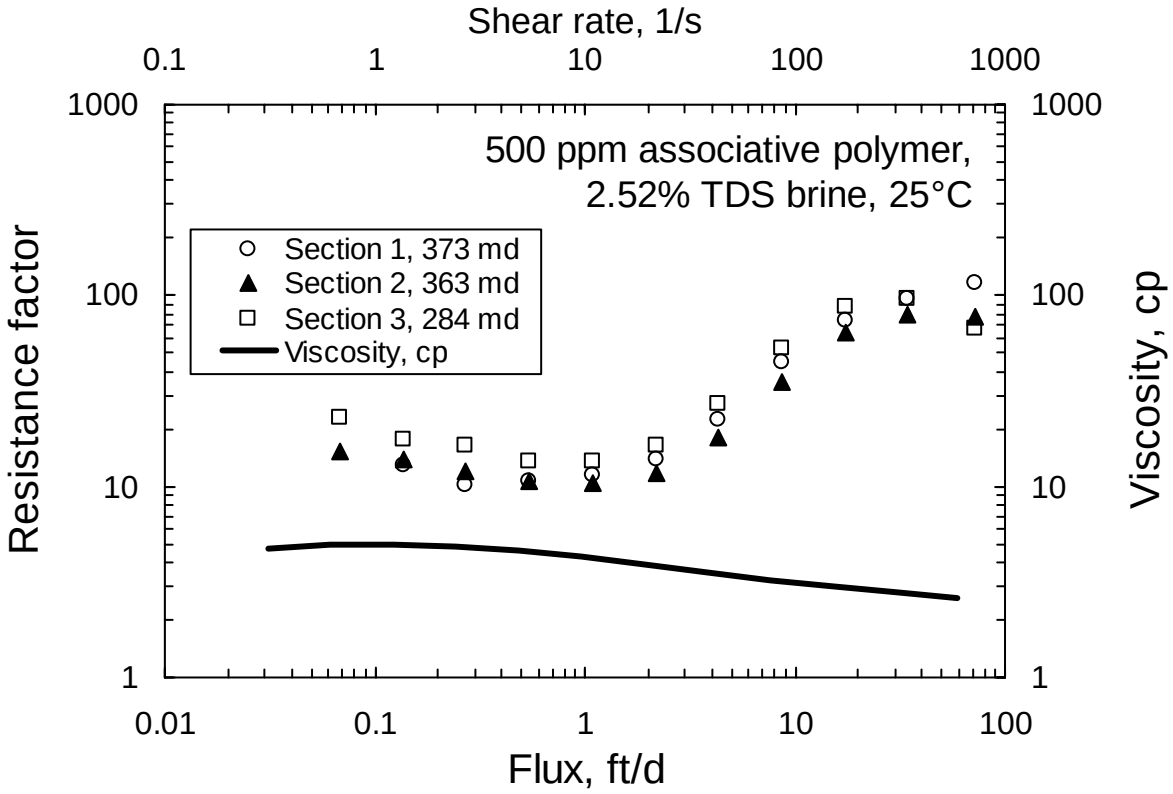

Fig. 15—500-ppm associative polymer viscosity and resistance factor in Berea sandstone.

Fig. 15 also plots viscosity versus shear rate for 500-ppm associative polymer (solid curve). Note that at all flux values, resistance factors were considerably greater than expectations from viscosity measurements. This behavior was noted in both Berea and porous polyethylene for all (fresh) associative polymer concentrations tested. Interestingly, for conventional HPAM and xanthan polymers, resistance factors at low fluxes were reasonably consistent with expectations from viscosity measurements unless a pore-plugging effect occurred (Seright *et al*. 2010)—e.g., if the permeability was too low to accommodate the size of the highest molecular weight species within the polymer.

Fig. 16 confirms that for other associative polymer concentrations in 363-md Berea and 12,313-md polyethylene, the lowest resistance factors were noticeably greater than the highest measured viscosity (i.e., viscosity at 1.8 s^{-1}). If this result was caused by large polymer adsorption or retention, we might have expected different resistance factors in the hydrophilic 363-md Berea than in hydrophobic 12,313-md polyethylene. Fig. 17 also supports the idea that the higher than expected resistance factors may not be due to polymer adsorption or retention. In Fig. 17, resistance factors for selected concentrations (500, 900, 1,500, and 2,500 ppm) are plotted against the capillary bundle parameter, $u(1-\phi)/(\phi k)^{0.5}$, where u is flux in ft/d, k is permeability in md, and ϕ is porosity. For all four associative polymer concentrations, the behavior in 363-md Berea correlated well with that seen in 12,313-md polyethylene. For a given x-axis value, resistance factors should have been different in 363-md Berea than in 12,313-md polyethylene if polymer retention was important.

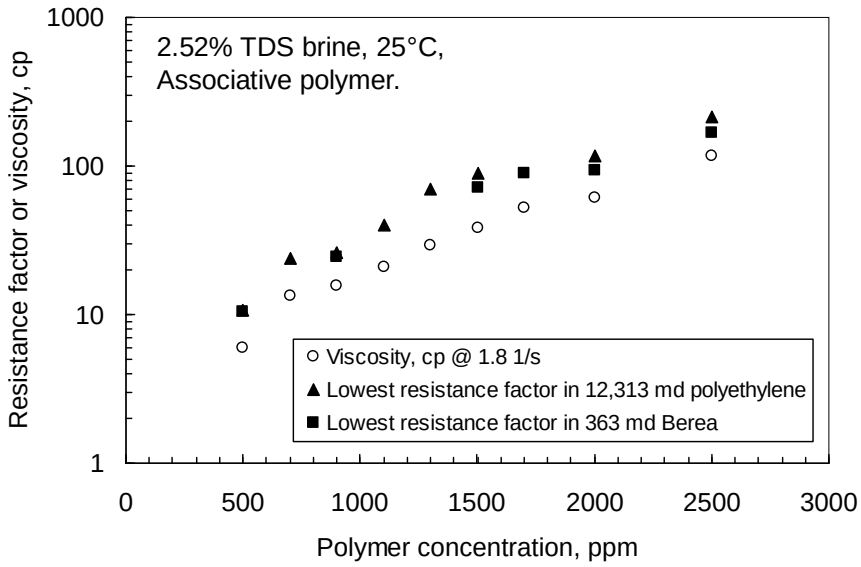

Fig. 16—Associative polymer resistance factors versus viscosities.

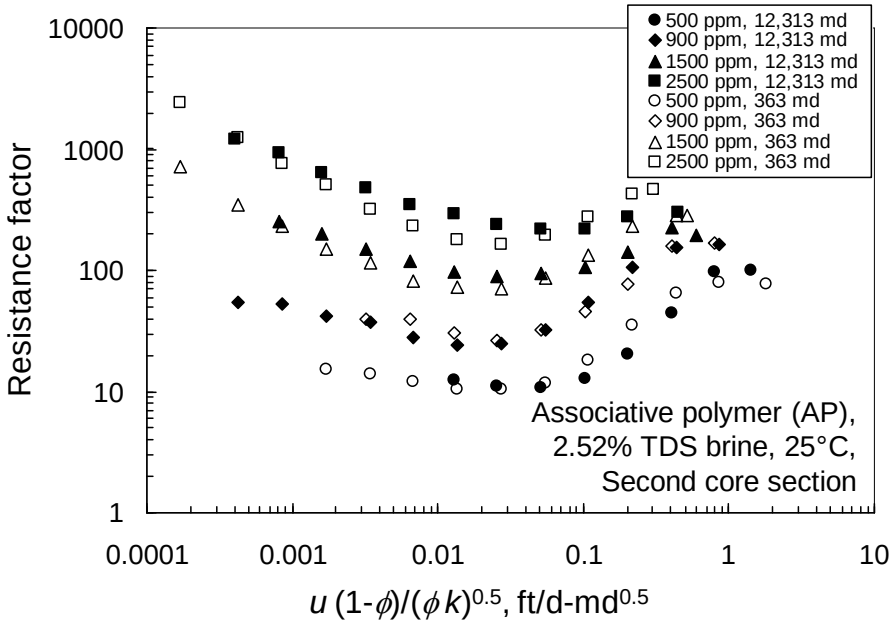

Fig. 17—Associative polymer resistance factor versus capillary bundle parameter.

If we assume that 363-md Berea has smaller pores and pore throats than 12,313-md polyethylene, we might expect pore plugging to be more severe in the less-permeable core—because particles of a given size should be more likely to plug small pores than large pores. Fig. 17 demonstrates that this expectation was not met. Ironically, Berea sandstone and porous polyethylene have very similar pore structures (Seright et al. 2006). Although the porosity and permeability for Berea sandstone and porous polyethylene are quite different, the pore size, pore throat size, and pore aspect ratio distributions are very similar. These facts may explain the similarity of behavior seen in Fig. 17 for the different porous media.

If a polymer particle (i.e., a polymer aggregate) was responsible for the higher-than-expected resistance factors, one might expect larger particles and/or a higher concentration of particles as the polymer concentration is increased. In turn, this occurrence should cause a higher ratio of resistance factor to viscosity as polymer concentration rises. This expectation was met at low fluid velocities. At a $u(1-\phi)/(\phi k)^{0.5}$ value of 0.0017, the ratio of resistance factor (from Fig. 17) to zero-shear viscosity (from Fig. 12) ranged from 3 for 500-ppm associative polymer to 5 for 2,500-ppm polymer. This ratio reached as high as 22 for 2,500-ppm polymer at a $u(1-\phi)/(\phi k)^{0.5}$ value of 0.00017. Interestingly, the ratio decreased substantially with increased velocity in porous media. When the $u(1-\phi)/(\phi k)^{0.5}$ value was raised to 0.027, the ratio was roughly 2 for all polymer concentrations between 500 and 2500 ppm (see Figs. 16 and 17). Apparently, flow through porous media at intermediate velocities disrupted polymer aggregates that form from hydrophobic associations.

Fig. 18 compares resistance factors in porous polyethylene for associative polymer versus HPAM. For all four concentration levels examined (~500 ppm, 900 ppm, ~1,500 ppm, and 2,500 ppm), resistance factors (at a given flux) were substantially greater for associative polymer than for HPAM. Specifically, 500-ppm associative polymer (solid circles) acts similar to 900-ppm HPAM (open triangles), and 900-ppm associative polymer (solid triangles) acts similar to 1,600-ppm HPAM (open squares).

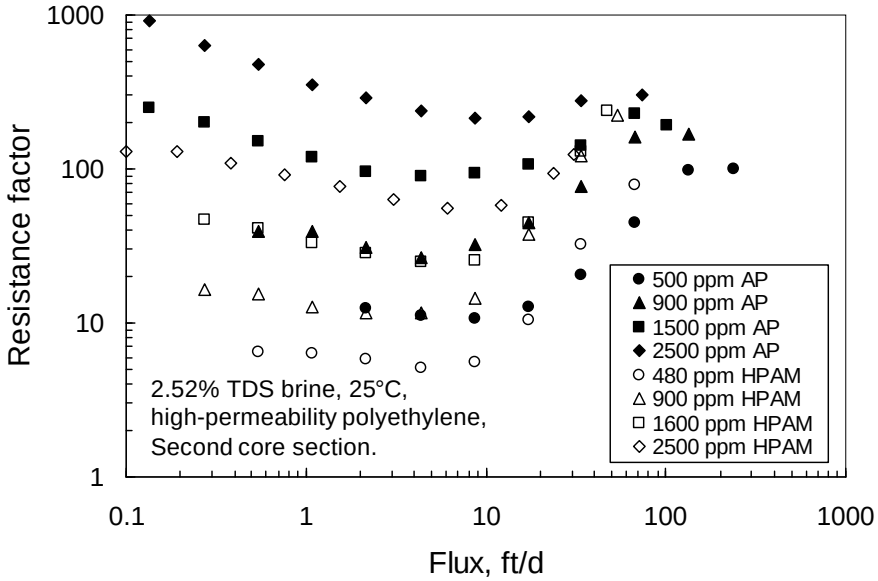

Fig. 18—Resistance factors in polyethylene: Associative polymer versus HPAM.

Residual Resistance Factors. At the end of associative polymer injection, many pore volumes of brine were injected to determine residual resistance factors in the Berea and polyethylene cores. After injecting 109 PV of brine into the polyethylene core, residual resistance factors were 1.9, 2.1, and 1.3 in the first, second, and third sections, respectively. This result is consistent with a suggestion of little to no significant pore plugging in the 12,313-md polyethylene core. However, after injecting 170 PV of brine into the Berea core, residual resistance factors were 13.0, 19.3, and 15.3 in the first, second, and third sections, respectively. This result suggests that some pore plugging or higher polymer retention may have occurred in the 363-md Berea core. In both cores, residual resistance factors were not sensitive to flow rate.

Mechanical Degradation

In previous work (Seright *et al*. 2010), when xanthan or HPAM resistance factors were higher than expected at moderate to low flux values, the effect was shown to be due to a high Mw polymer species. For both xanthan and HPAM, this species was removed by flow through a few feet of porous rock. For HPAM, the species was readily destroyed by mechanical degradation. Either way, the species was not expected to propagate deep into a reservoir to provide low-flux resistance factors that were substantially higher than expectations from viscosity measurements. During a study of a hydrophobically associative polymer, Dupuis *et al*. (2010) concluded that it contained a low-mobility (high-resistance-factor), high-Mw species that propagated significantly slower than other components of the polymer. We wondered whether mechanical degradation would reduce the high resistance factors that we observed.

We examined the effects of mechanical degradation by first forcing 6.4 liters of a 500-ppm associative polymer solution through a 13-cm long 347-md Berea core using a flux of 292 ft/d (resulting in a pressure gradient of 2,500 psi/ft). The effluent from this experiment was then re-injected (using a wide range of flow rates) into a new 78.2-cm long polyethylene core that had four equally spaced internal pressure taps. The porosity of this core was 44% and the pore volume was 390.6 cm^3. The permeabilities of the five 15.64-cm long core sections were 8,316, 11,554, 11,105, 11,222, and 10,370 md, respectively. Thus, the average permeability was 10,365 md. We repeated this experiment using 900-ppm, 1,500-ppm, and 2,500-ppm associative polymer solutions (in the same cores), where the pressure gradient was 2,500 psi/ft when forcing the solutions through the 347-md Berea core.

Since 2,500 psi/ft pressure gradient was a fairly extreme level of mechanical degradation, additional work with a lower level of mechanical degradation was performed. For these cases, the pressure gradient was 235 psi/ft when forcing the solutions through the 347-md Berea core. The effluent from this core was then injected into the polyethylene core using a range of flow rates. The same polymer concentrations and range of rates were used. All of these procedures were repeated using HPAM. Details of the results can be found in Seright 2010.

Comparison of Viscosity and Resistance Factor Losses. Table 3 lists viscosity and resistance factor losses experienced by HPAM and associative polymer solutions after being forced through the 347-md Berea sandstone core at either 235 psi/ft or 2,500 psi/ft. The third and fourth columns in this table list the percent of the original viscosity that was lost, as measured at a shear rate of 7.3 s^{-1} and 25ºC. The fifth and sixth columns in this table list the percent of the original resistance factor that was lost, as measured at a flux of 1 ft/d (in the middle section of the polyethylene core) and 25ºC. For both polymers at all concentrations, exposure to 235 psi/ft resulted in very little viscosity loss—from 0% to 8% of the original viscosity. Resistance factor losses for HPAM were modest (0-15%) after exposure to 235 psi/ft. However, resistance factor losses for the associative polymer were significant after exposure to 235 psi/ft—from 31-45%. For HPAM after exposure to 2,500 psi/ft, viscosity losses ranged from 5% to 17%. For the associative polymer after exposure to 2,500 psi/ft, viscosity losses were higher, ranging from 19% to 35%. Similarly, after exposure to 2,500 psi/ft, resistance factor losses were much greater for the associative polymer (53-71%) than for HPAM (9-41%).

Table 3—Losses after being forced through a Berea core at given pressure gradient.

Polymer	Concentration, ppm	Viscosity loss, % of original @ 7.3 s^{-1}		Resistance factor loss, % of original @ 1 ft/d	
		235 psi/ft	2,500 psi/ft	235 psi/ft	2,500 psi/ft
HPAM	500	1	11	4	31
Associative polymer	500	6	35	39	53
HPAM	900	2	17	0	24
Associative polymer	900	5	19	31	64
HPAM	1,500	0	10	15	41
Associative polymer	1,500	3	27	36	64
HPAM	2,500	1	5	0	9
Associative polymer	2,500	8	23	45	71

Figs. 19-22 compare resistance factor (in the middle polyethylene core section) versus flux for the associative polymer and HPAM at various polymer concentrations and levels of mechanical degradation. In all four figures (i.e., at 500-, 900-, 1,500-, and 2,500-ppm polymer), the low-flux resistance factors for fresh associative polymer (solid circles) were considerably greater than (typically twice) those for fresh HPAM (open circles). Second, for all but the highest concentration, low-flux resistance factors for associative polymer that was degraded using 235 psi/ft (solid triangles) were about the same as those for fresh HPAM (open circles). Third, for all four concentrations, the low-flux resistance factors for associative polymer that was degraded using 2,500 psi/ft (solid squares) were the same or less than those for HPAM that was degraded using 2,500 psi/ft (open squares). Fourth, the shear-thickening behavior (i.e., increase in resistance factors) at moderate to high flux values for fresh and 235-psi/ft-degraded HPAM was more pronounced than that for fresh and 235-psi/ft-degraded associative polymer.

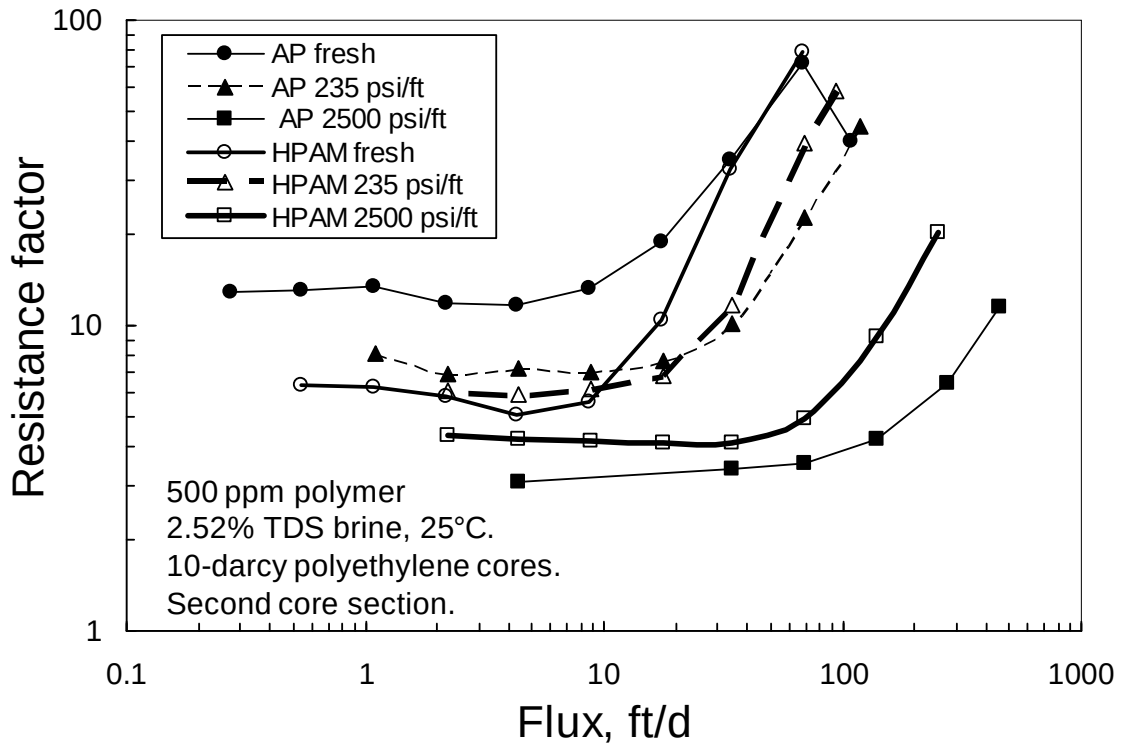

Fig. 19—Resistance factors for 500-ppm polymer: Associative polymer versus HPAM.

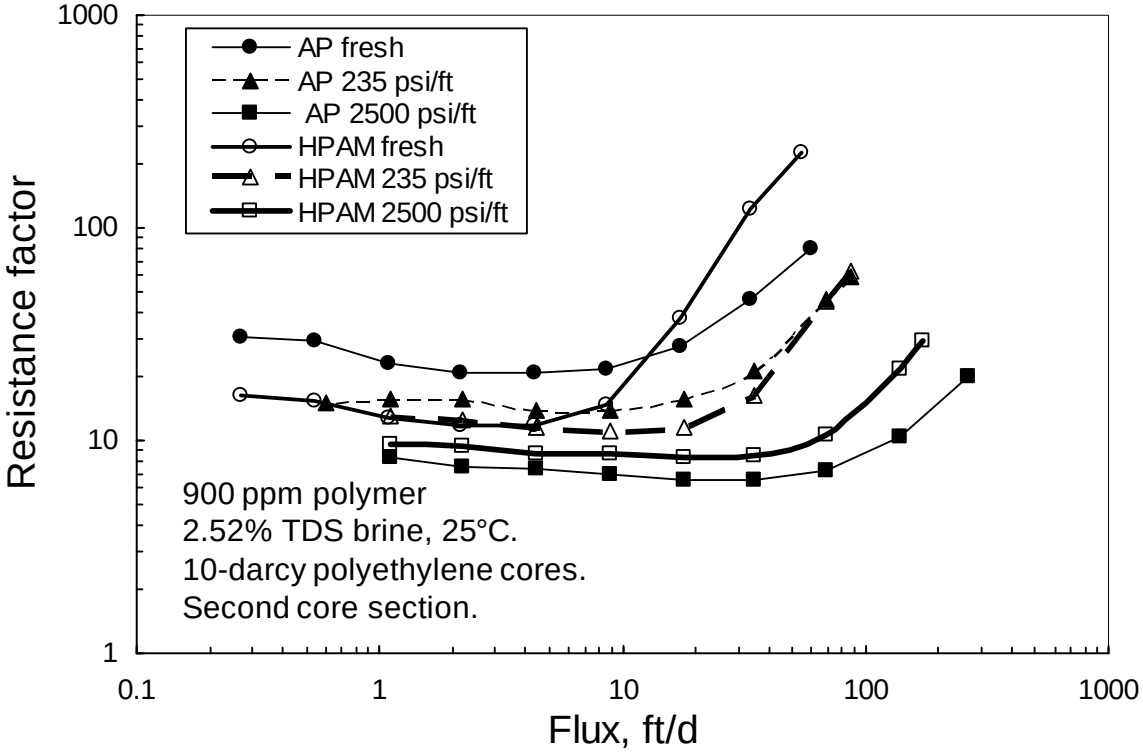

Fig. 20—Resistance factors for 900-ppm polymer: Associative polymer versus HPAM.

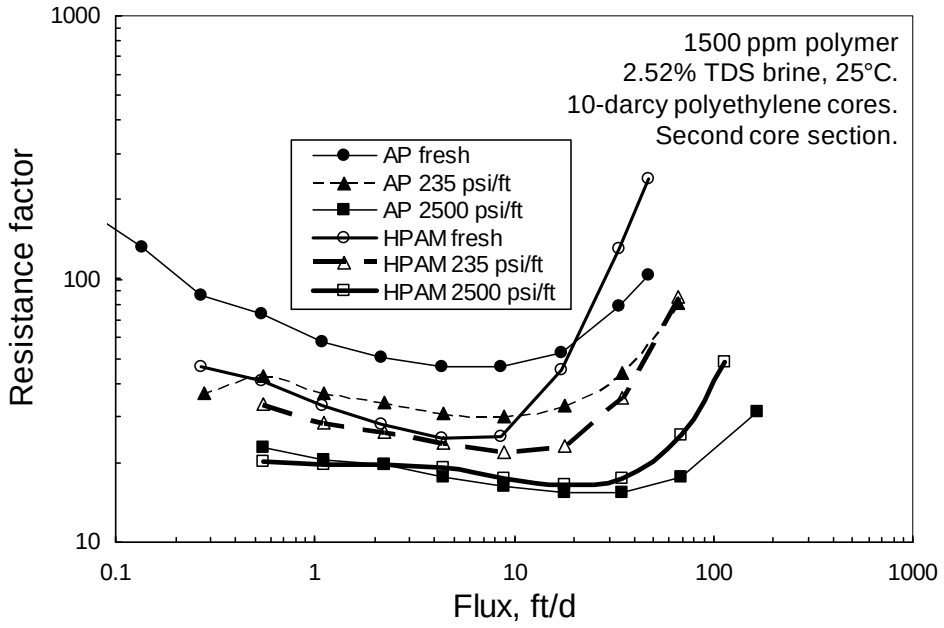

Fig. 21—Resistance factors for 1,500-ppm polymer: Associative polymer versus HPAM.

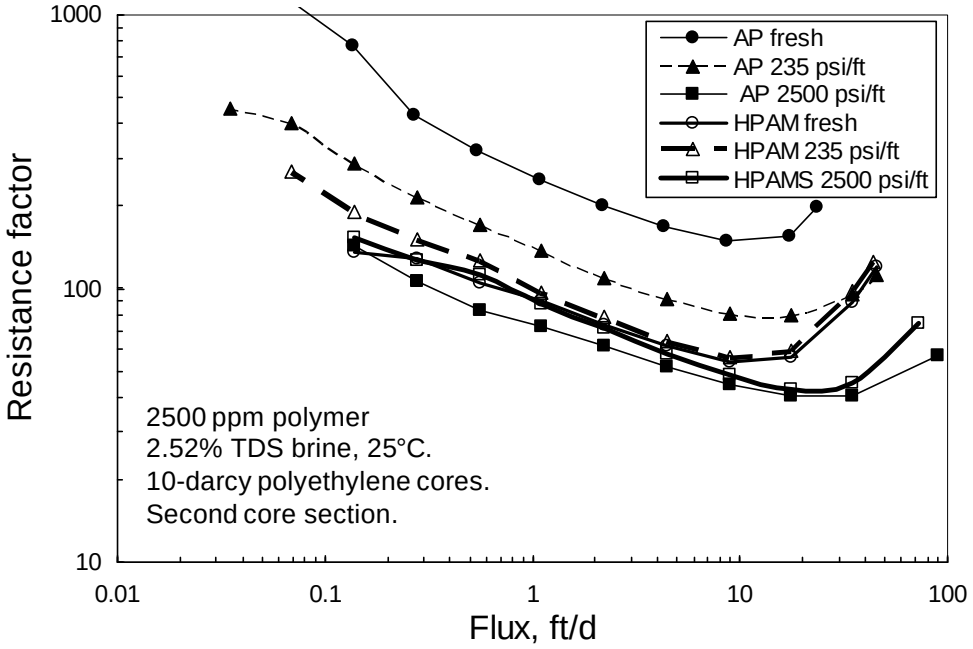

Fig. 22—Resistance factors for 2,500-ppm polymer: Associative polymer versus HPAM.

For the HPAM cases (fresh, 235 psi/ft, and 2,500 psi/ft), the low-flux resistance factors were usually the same or just slightly greater than expectations from the low-shear-rate viscosities. To quantify this point, Fig. 23 plots the ratio of (resistance factor at 1 ft/d flux in the middle polyethylene core section) to (shear rate at 7.3 s^{-1}) for the two polymers, with different polymer concentrations and different levels of mechanical degradation. For all cases with HPAM

concentrations up to 1,500 ppm, the low-flux resistance factor was only 0 to 33% greater than the low-shear-rate viscosity. For all cases (fresh, 235 psi/ft, and 2,500 psi/ft) with 2,500-ppm HPAM, the resistance factor at 1 ft/d was about twice the viscosity at 7.3 s^{-1}. However, a more detailed examination of the resistance-factor-versus-flux curves and the viscosity-versus-shear-rate curves (which can be found in Figs. 49, 53, and 55 of Seright 2010b) revealed that the low-flux resistance factors were actually just slightly above the low-shear-rate viscosities. Similarly, for cases with associative polymer concentrations up to 1,500 ppm that had been exposed to 2,500 psi/ft, the low-flux resistance factor was only 0 to 32% greater than the low-shear-rate viscosity. For associative polymer solutions that were exposed to 235 psi/ft, the low-flux resistance factors were 1.6-3.3 times greater than the low-shear-rate viscosity. For fresh, undegraded associative polymer solutions, the low-flux resistance factors were 2.5-5.6 times greater than the low-shear-rate viscosity. Thus, even after exposure to 235 psi/ft, associative polymer solutions provided low-flux resistance factors that were significantly greater than expectations from viscosity values.

Table 3 and Figs. 19-23 reveal that the associative polymer was more sensitive to mechanical degradation than the HPAM. For comparison, after being forced through a 1.3-cm-long Berea core at high rates, Bock et al. (1987) found that 1,500-ppm associative polymer with 0.75% hydrophobic monomer (octylacrylamide) and 20-30% AMPS (in brine with 3.3%TDS) experienced a significantly smaller loss of viscosity than a normal HPAM. Compared with Bock's polymer, our associative polymer had less than one-third the hydrophobe and sulfonic monomer content. For an associative polymer with 0.1% hydrophobic monomer, Dong and Wang (1996) found the level of shear degradation (as judged by viscosity loss induced by a Waring blender) was about the same as for other HPAM solutions.

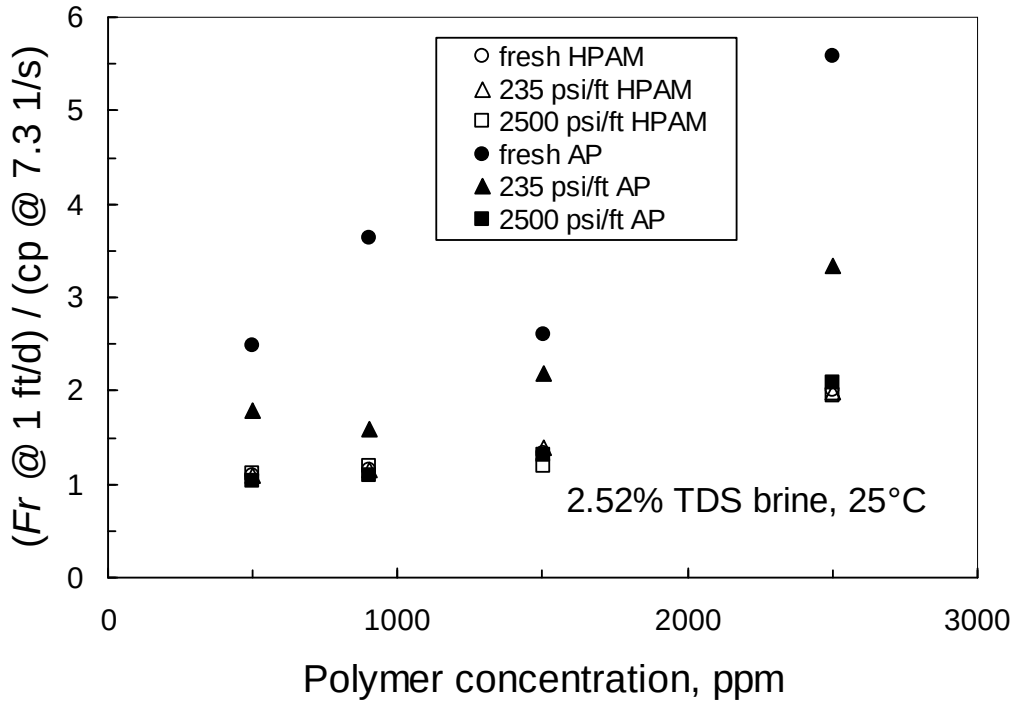

Fig. 23—Low-flux resistance factors relative to low-shear-rate viscosities.

Will the High Resistance Factors Propagate Deep into Porous Rock?

Cores with Lengths up to 78 cm. In previous work, no permeability dependence of resistance factors was noted for HPAM in 13-15-cm long Berea sandstone cores with permeabilities of 269 md or above (Seright 2009). In permeable polyethylene cores, we did not observe any length dependence of resistance factors for any concentration or level of mechanical degradation when using HPAM (see Figs. 46-53 of Seright 2010b). This point is, perhaps, made most effectively in Fig. 24, which plots resistance factors for a fresh 2,500-ppm solution of HPAM in the five sections of the 78.2-cm-long 10-darcy polyethylene core. In short (13-14 cm) Berea sandstone or porous polyethylene cores, we also saw no length dependence of resistance factors for the associative polymer (see Figs. 28, A-1, A-3 to A-13 of Seright 2010b).

A set of experiments was performed in a 78.09-cm-long porous polyethylene core. In this case, the porosity was 0.377, and the pore volume was 343 cm^3. The core had two internal pressure drops that divided the core into three sections of equal length (i.e., 26.03 cm each). The section permeabilities were 7,295, 10,144, and 8,717 md, respectively. After saturating with brine, we injected 1 PV of 500-ppm associative polymer at 108 ft/d. Over the next 3.4 PV, we determined resistance factor for progressively lower flux values. Then, 13.2 PV more of polymer solution were injected, where resistance factor versus flux was determined at the end of the injection process. Fig. 25 demonstrates that 500-ppm associative polymer showed the same behavior for the entire course of this experiment. So whatever phenomenon that caused the resistance factors to be 2-3 times the value expected from viscosity measurements (solid curve in Fig. 25), it did not seem to change the rheology in porous media over the course of injecting many pore volumes of polymer solution.

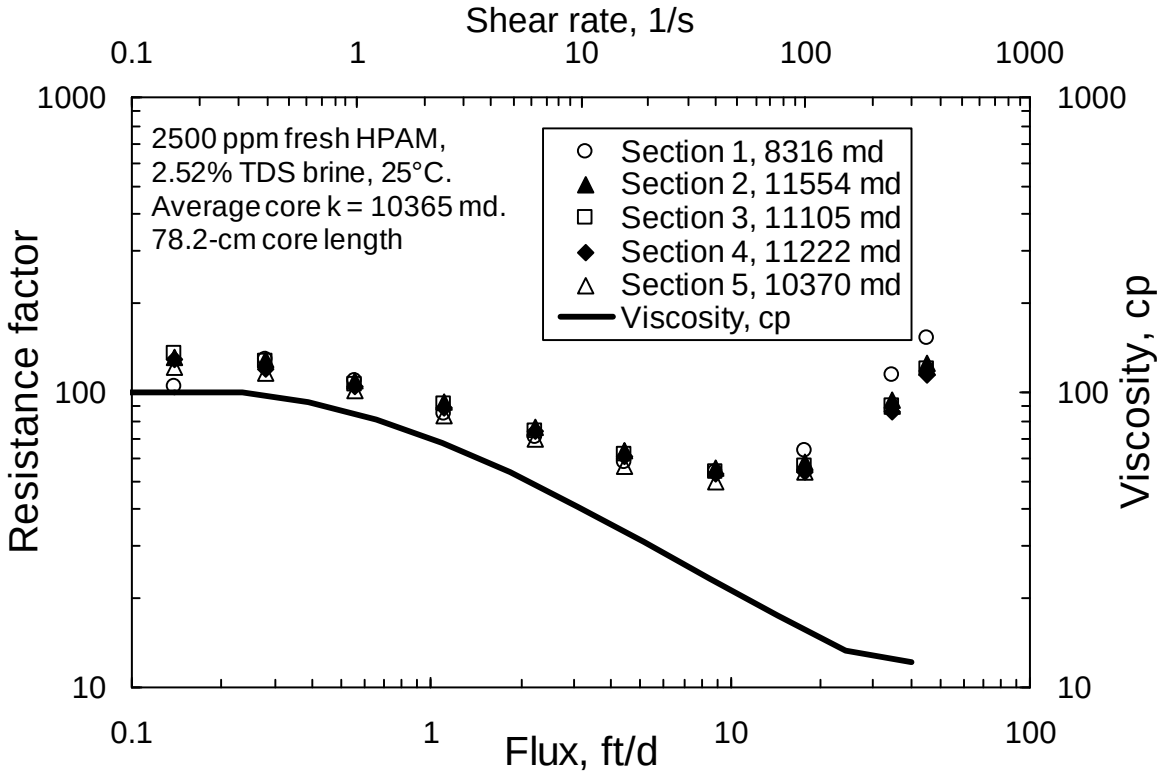

Fig. 24—Resistance factors for fresh 2,500-ppm HPAM.

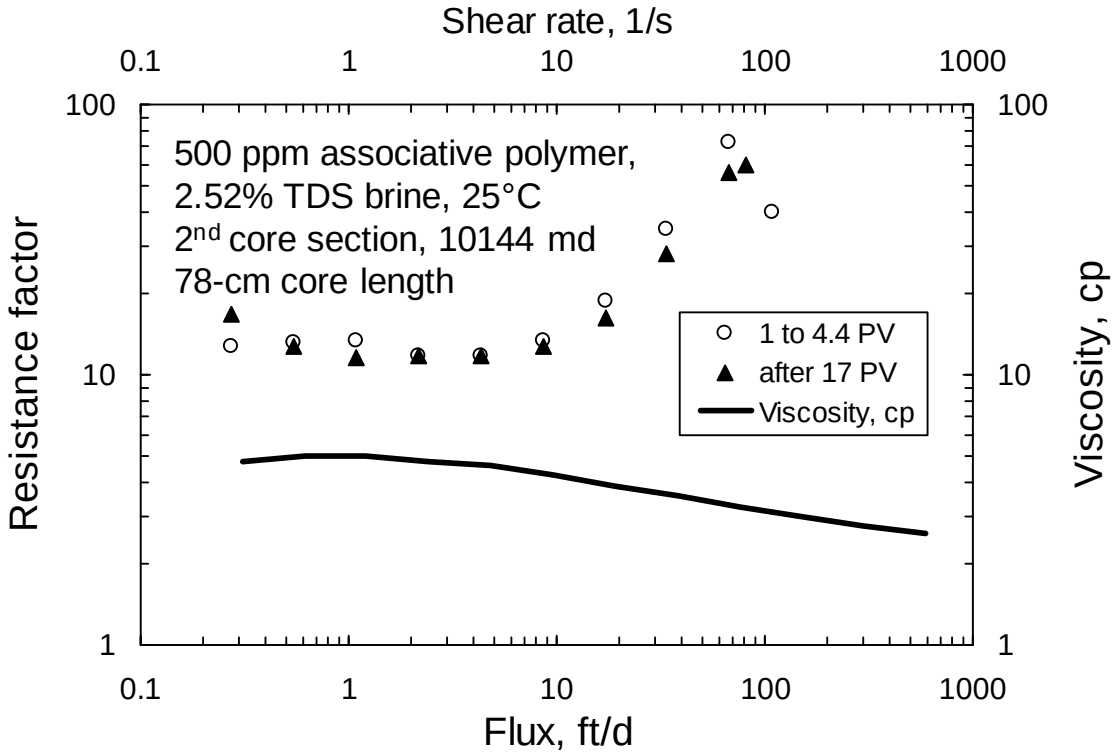

Fig. 25—500-ppm associative polymer resistance factors at beginning versus end of the experiment.

Propagation in a 157.5-cm Polyethylene Core. An experiment was performed in a 157.5-cm-long porous polyethylene core that had five equally spaced internal pressure taps. These taps divided the core into six sections, each with 26.25 cm length. The last two sections were combined to make one 52.5-cm-long section, thus reducing the total number of core sections to five. The permeabilities of these five sections were 12.25, 16.56, 9.59, 10.88, and 10.11 darcys, respectively. The composite average permeability of the core was 11.2 darcys. The core cross-sectional area was 11.04 cm^2, and the core pore volume was 754 cm^3. We injected 15.7 PV of 500-ppm AP (in 2.52% TDS brine) using a fixed flux of 7.13 ft/d. Subsequently, we injected 110 PV (83 l) of brine to flush the polymer from the core. Then, 8 PV of 500-ppm AP was injected again using a fixed flux of 7.13 ft/d. This procedure allowed determination of polymer retention and inaccessible pore volume for the core.

Fig. 26 plots resistance factors in the five core sections as a function of volume for the first 15.7 PV of polymer solution injected. Fig. 27 amplifies the first two PV of Fig. 26. Examination of the curves suggests that two species of polymer propagated through the core—a fast species that arrived at the end of the first core section after 0.23 PV and a much slower species that caused resistance favors to steadily increase for many PV. This concept is consistent with that proposed by Dupuis et al. (2010). The first polymer species provided a resistance factor plateau of 7-8 after 1 PV. The second species ultimately provided a resistance factor of 260 (over 60 times the value expected from viscosity measurements). After the first stage of polymer injection, 110 PV of brine was injected—resulting in ultimate residual resistance factors of 1.8, 3.6, 3.3, 2.8, and 2.4 in the five core sections, respectively. We suspect that the residual resistance factors could have been driven to lower values with more brine throughput.

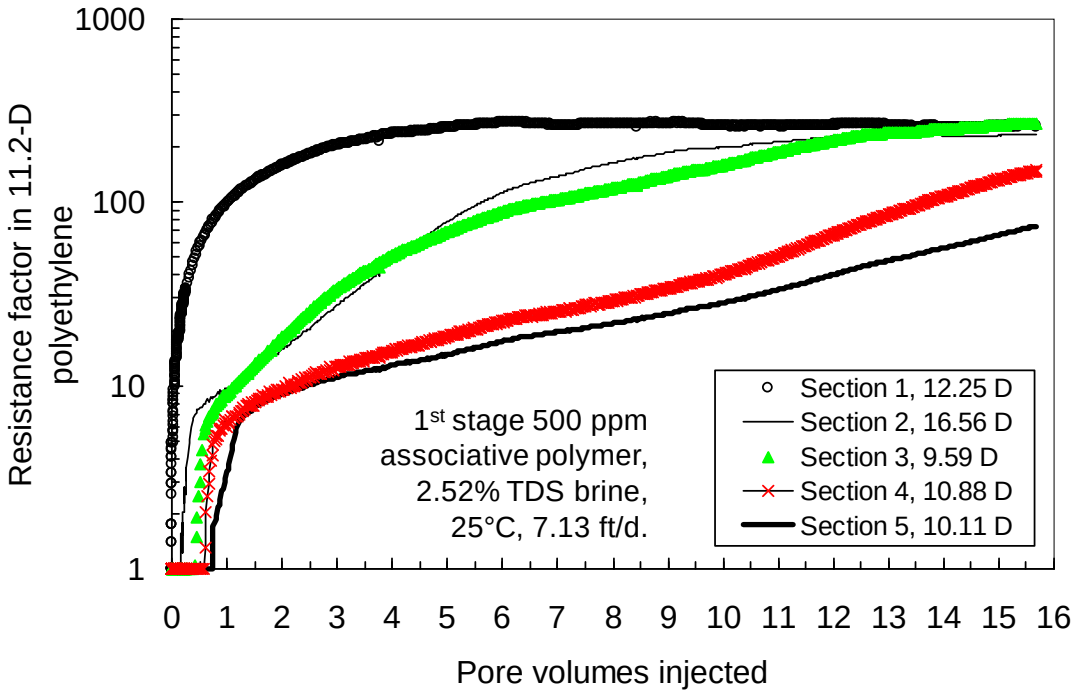

Fig. 26—Resistance factors during 1st injection of 500-ppm AP at 7.13 ft/d into 11.2-D polyethylene.

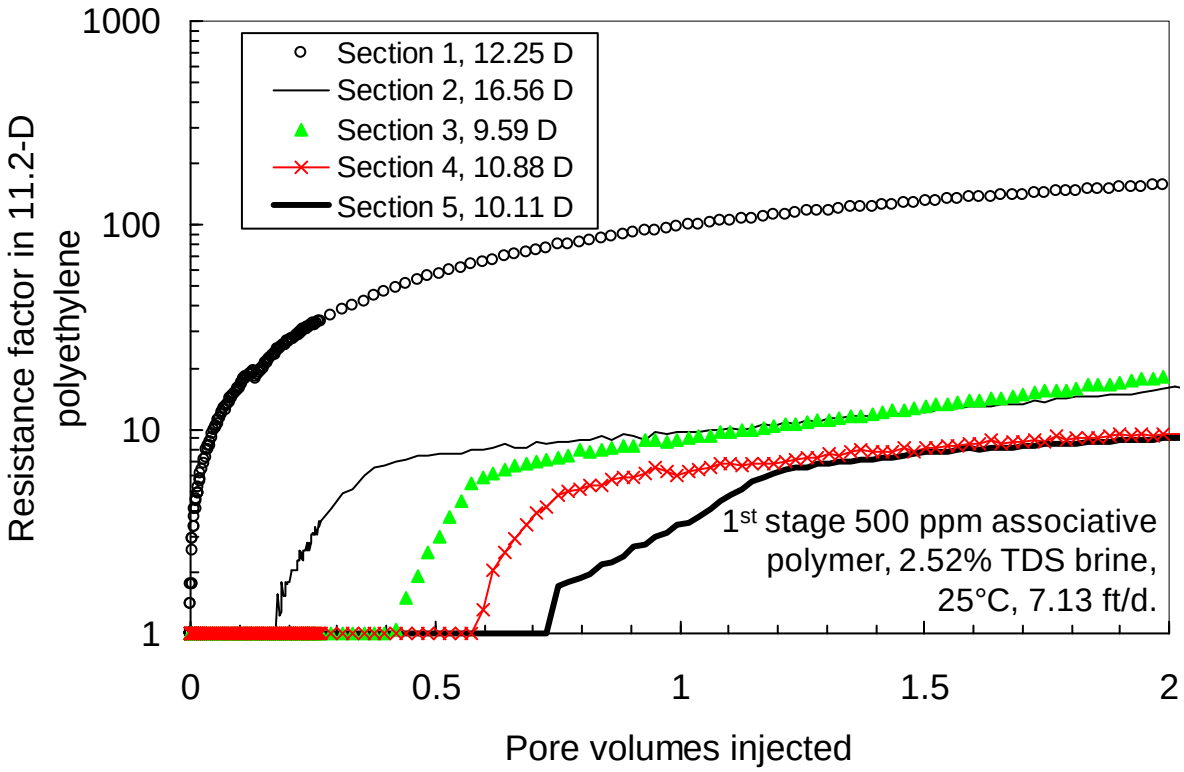

Fig. 27—Closer look at the first 2 PV of Fig. 26.

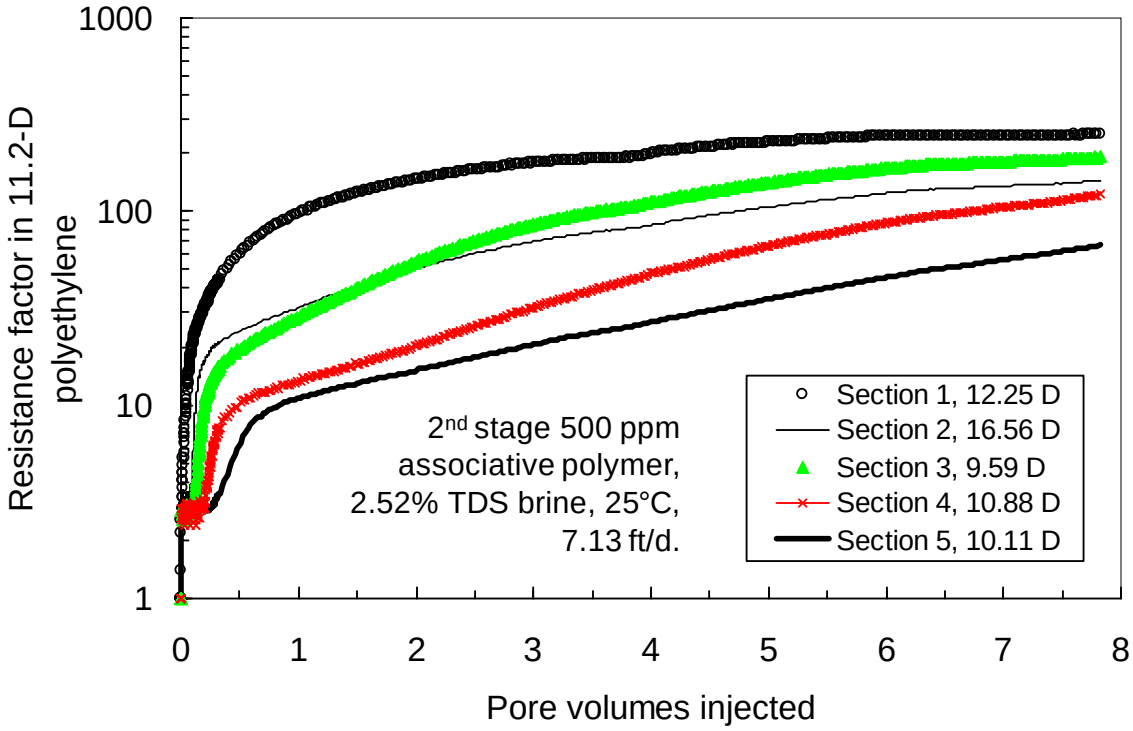

Fig. 28—Resistance factors during 2nd injection of 500-ppm AP at 7.13 ft/d into 11.2-D polyethylene.

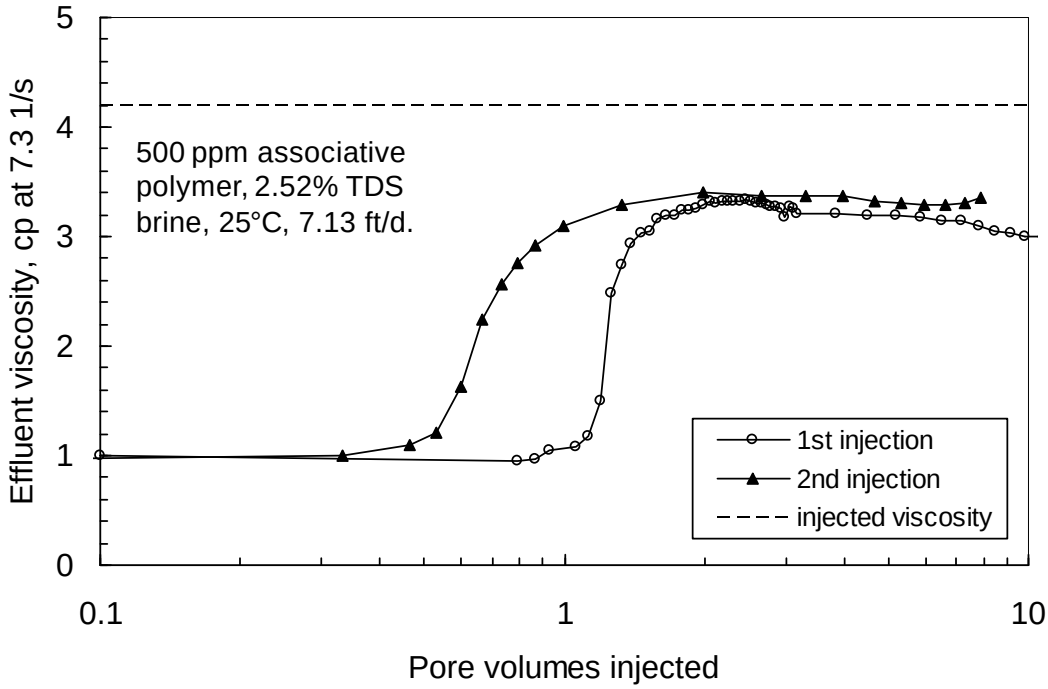

Fig. 29—Effluent viscosities.

Fig. 28 plots resistance factors in the five core sections as a function of volume for the second stage (8 PV) of polymer solution injection. Just as with the first polymer injection, a fast polymer species and a slow polymer species appeared to propagate through the core. The fast species arrived at the end of the core before 1 PV—where it provided resistance factors ranging from 10 in the fifth core section to over 20 in the second core section. During both the first and second stages of polymer injection, resistance factors in all core sections were at least twice the viscosity value after 1 PV of polymer injection. This result indicates that the higher-than-expected resistance factors can propagate effectively.

Fig. 29 plots viscosities of the effluent during the two stages of polymer injection. During both stages, the effluent viscosity only reached 3.3-3.4 cp—i.e., 20% less than the injected concentration of 4.2 cp. Apparently, passage through the core at low velocity either disrupted or removed some of the associative polymer species. Fig. 29 indicates that the viscous polymer front (associated with the fast polymer species) reached the end of the core after 1.24 PV during the first stage of polymer injection and after 0.72 PV during the second stage. Assuming that polymer retention sites were occupied during the second stage of polymer injection, the front arrival at 0.72 PV indicates an inaccessible pore volume value of 0.28 (i.e., 1-0.72). The difference between the front arrivals during the first and second stages of polymer injection gives an indication of polymer retention (at least for the fast species)—(1.24-0.72 PV)*(500x10^{-6} g polymer cm^3)*(754 cm^3/PV)/(1002.11 g of core) = 196 µg/g. A careful examination of the front arrivals in Figs. 26-29 indicates that the retention and inaccessible PV values were fairly consistent through all five core sections—i.e., the level of polymer retention did not depend on distance travelled. The observed retention level was comparable to that for HPAM. These observations provide hope that the fast species and the higher-than expected resistance factors can propagate deep into a reservoir.

For the second, slower polymer species, ~4 PV of injection were required for the resistance factors in the first core section (i.e., the first 1/6 of the core) to level out during both stages of polymer injection (Figs. 26 and 28)—suggesting that about 24 PV of injection are required for the slow species to fill the core. This result can be used to estimate a retention level of 9,000 µg/g—over 40 times greater than that for the fast species. The ultimate resistance factors associated with this slow species was about 260. Upon first consideration, this high value seems inconsistent with the resistance factor of 12 that was observed at the same flux after 17 PV in Fig. 25. However, note that Figs. 26-28 report values measured at a fixed flux over a wide range of polymer throughput. In contrast, the values in Fig. 25 were determined within a short range of throughput, during which fluid velocities varied over a wide range. Conceivably, exposure to high flux values (in Fig. 25) may have disrupted polymer structures that might form during a constant low flux of 7.13 ft/d. In other words, the polymer retention level (and therefore resistance factor values) might vary with fluid velocity. Future work will be needed to establish whether the high resistance factors that develop at low flux values will present problems with injectivity and polymer transport.

Although the coreflood results could be interpreted to indicate that two polymer species exist in the associative polymer, some information is inconsistent with this view. The associative polymer is not a mixture of two different macromolecules. The product is obtained by radical polymerization, and due to the manufacturing process, drift of compositions can occur. Each macromolecule contains the four monomers used as raw materials for the synthesis. However, the percentage of each monomer can differ from one molecule to the next due to differences in

reactivity. Also, molecular weights differ from one molecule to the next. Thus, a continuous distribution of polymer compositions and structures can exist. This view is consistent with the gradual rise in resistance factors (with increasing pore volume throughput) in Figs. 26-28. If only one slow species was present, step changes in resistance factors might be expected (e.g., at 6 PV, 12 PV, 18 PV, etc.).

One might expect that size exclusion chromatography (SEC) could distinguish whether the associative polymer contained one, two, or multiple polymer species. However, the associative polymer has a very high molecular weight (around 12-15 million g/mol by intrinsic viscosity measurement). To our knowledge, there is no standard column for SEC to handle such polymers.

Propagation in a 122-cm Berea Sandstone Core. An experiment was performed in a 122-cm-long Berea sandstone core that had four equally spaced internal pressure taps. These taps divided the core into five sections, each with 24.4 cm length. The permeabilities of these five sections were 116, 142, 143, 145, and 121 md, respectively. The composite average permeability of the core was 132 md. The core cross-sectional area was 14.52 cm^2, and the core pore volume was 329.7 cm^3. We injected 3.5 PV of 500-ppm AP (in 2.52% TDS brine) using a fixed flux of 2.17 ft/d. Fig. 30 plots resistance factors in the five core sections as a function of volume injected. The figure indicates polymer arrival at the end of the five core sections after 0.42, 0.84, 1.29, 1.90, and 2.7 PV. This rate of AP propagation was noticeably slower than that in 11.2-D polyethylene (Figs. 26 and 27). Nevertheless, it still suggests that the AP may have the ability to penetrate deep into the porous rock of a reservoir. Note in the last two core sections that the resistance factors leveled out at a resistance factor of 25—6 times the value expected from viscosity measurements. (We planned to inject brine and another polymer bank to determine retention and inaccessible pore volume. Unfortunately, the core broke.)

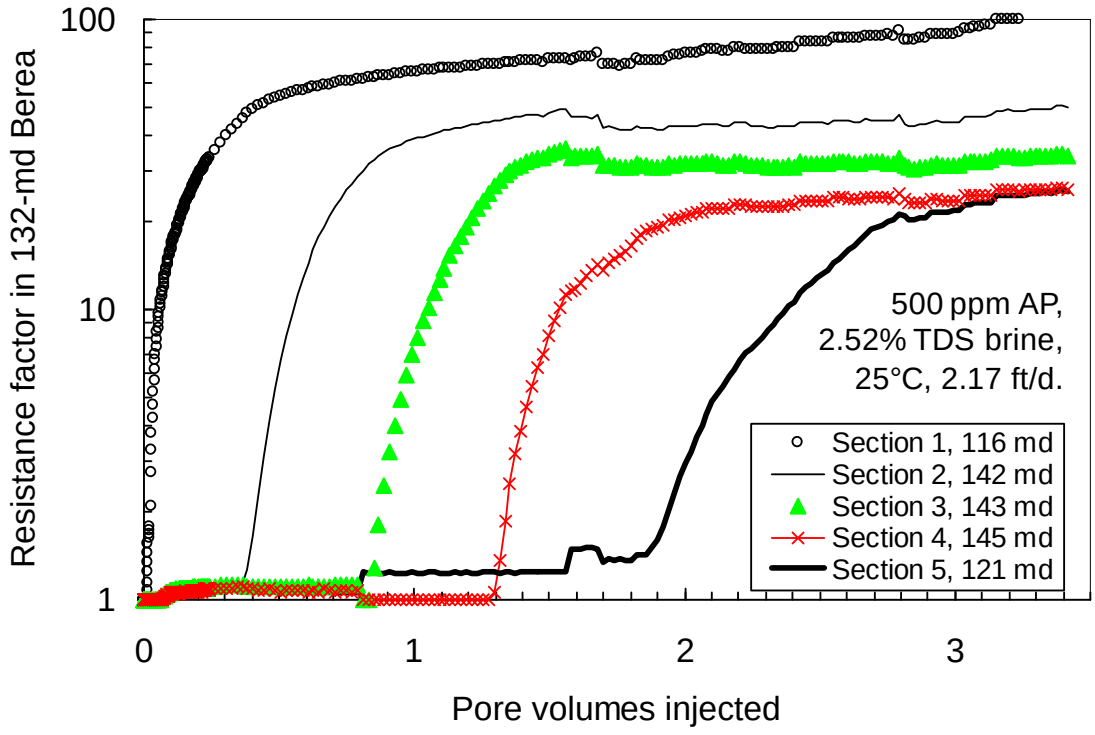

Fig. 30—Resistance factors during injection of 500-ppm AP at 2.17 ft/d into 132-md Berea.

Conclusions

This investigation compared the hydrophobically associative polymer, C1205, and the conventional HPAM, 3830S, for potential use in polymer flooding.

1. Rheological properties (viscosity versus concentration and shear rate, elastic modulus versus frequency, loss modulus versus frequency) were similar for the two polymers (in a 2.52% TDS brine at 25°C).
2. Both HPAM and the associative polymer show excellent filterability at lower concentrations (1,000 ppm or lower), but plugged within 200 cm^3/cm^2 throughput at higher concentrations (1,500 ppm).
3. In cores with multiple sections, we saw no evidence of face plugging for either polymer at any concentration. This was true in both 347-md Berea sandstone and 10-12-darcy porous polyethylene.
4. Plots of resistance factor versus flux (after normalization for permeability using the capillary bundle correlation) matched well for a broad range of permeability.
5. Associative polymer solutions were noticeably more turbid than those of HPAM.
6. In Berea sandstone and porous polyethylene cores, low-flux resistance factors for fresh associative polymer were at least twice those for HPAM.
7. Both polymers showed modest (0-8%) viscosity losses (at 7.3 s^{-1}) after exposure to 235 psi/ft pressure gradient in a core. However, associative polymer solutions experienced 31-45% loss in low-flux resistance factor, whereas HPAM solutions experienced only 0-15% loss. After 235 psi/ft, low-flux resistance factors for associative polymer solutions were often similar to those for fresh HPAM solutions.
8. After exposure to 2,500 psi/ft pressure gradient, associative polymer solutions experienced 19-35% viscosity loss, whereas HPAM solutions experienced 5-17% viscosity loss. After 2,500 psi/ft, low-flux resistance factors for associative polymer solutions were the same or less than those for HPAM solutions.
9. Results from propagation studies in long polyethylene and sandstone cores suggest that higher-than-expected resistance factors (typically at least twice the values expected from viscosity measurements) can propagate deep into a reservoir.
10. Consistent with previous research (Dupuis et al. 2010), the associative polymer appears to contain a species that propagates through porous rock at rates comparable to those for HPAM and a second species (or perhaps multiple species) that moves much slower and creates much higher resistance factors.

4. A COMPARISON OF POLYMER FLOODING WITH IN-DEPTH PROFILE MODIFICATION

Introduction

Heterogeneity is well known to reduce sweep efficiency during waterflooding and other flooding processes. Depending on the nature of the heterogeneities, a number of methods are available to improve sweep efficiency. For example, if continuous impermeable barriers separate high-permeability watered-out strata from less-permeable oil-productive strata, one can use cement, mechanical methods, or certain chemical plugging agents to block off the offending high-permeability zones (at the wellbore) so that injected water only enters and displaces oil from the less-permeable zones. As another example, if a fracture or fracture system causes direct channeling between wells, gels can be extruded deep into the fractures to allow subsequently injected fluid to be diverted to displace oil from the rock matrix (Sydansk and Romero-Zeron 2011). This study is directed at a third scenario, where fluids can crossflow between strata but fractures do not contribute significantly to channeling. Improving sweep efficiency for this case is generally acknowledged as considerably more challenging than that for the first two cases (Seright *et al.* 2003).

Polymer Flooding. Polymer flooding is one method to attack this difficult problem (Willhite and Seright 2011). Fig. 31 illustrates the benefits of a polymer flood in a two-layered system with free crossflow. This figure shows five displacements of water by red-dyed polymer solutions, with xanthan solutions ranging in concentration from 0 ppm to 2,000 ppm and viscosities (at 11 s^{-1}, 25°C) ranging from 1 to 75 cp. In each case, the plexiglass-encased beadpack had dimensions of 238 cm x 11.6 cm x 1.3 cm. A 5.8-cm high layer of 150-μm glass beads comprised the bottom layer, while a 5.8-cm high layer of 500-μm glass beads acted as the top layer. The top layer was 11.2 times more permeable than the bottom layer. No flow barrier existed between the layers. Fig. 31 shows the position of the polymer fronts in the bottom layer at the time when the polymer reached a fixed position in the top layer. The figure clearly shows the benefit of a polymer flood. As the viscosity of the injected fluid increases, sweep efficiency in the less-permeable layer increases. (Details of these experiments can be found in Sorbie and Seright 1992. Videos of these laboratory experiments may be viewed at http://baervan.nmt.edu/randy/.)

Gels for In-Depth Profile Modification. When gels and other blocking agents were proposed to improve sweep in stratified reservoirs with crossflow, it was commonly stated or implied that the material exclusively entered and reduced permeability in high-permeability strata, thereby diverting subsequently injected water into less-permeable oil-bearing strata (Needham and Doe 1987, Chang *et al.* 2006, Choi *et al.* 2010). Unfortunately, this view ignores penetration into and permeability reductions in less-permeable strata (Seright 1988, Sorbie and Seright 1992, Sydansk and Romero-Zeron 2011). In Fig. 31, one can easily envision that if the polymer solution suddenly gelled, the reduction in flow capacity in the low-permeability layer may be greater than in the high-permeability layer. This expectation is confirmed experimentally in Fig. 32 and in additional videos of experiments at http://baervan.nmt.edu/randy/. After polymer placement, injected water forms severe viscous fingers that channel exclusively through the high-permeability layer.

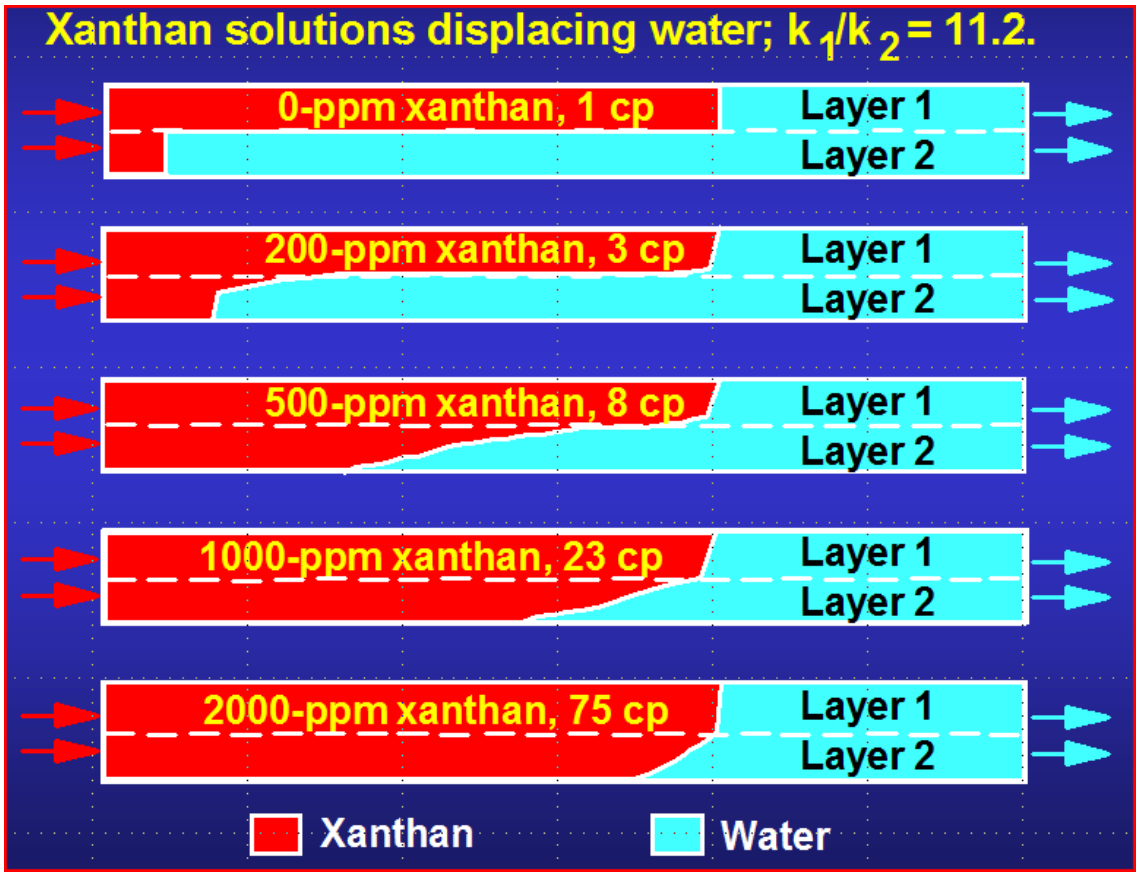

Fig. 31—Polymer flood improving sweep in a two-layer system with free crossflow.

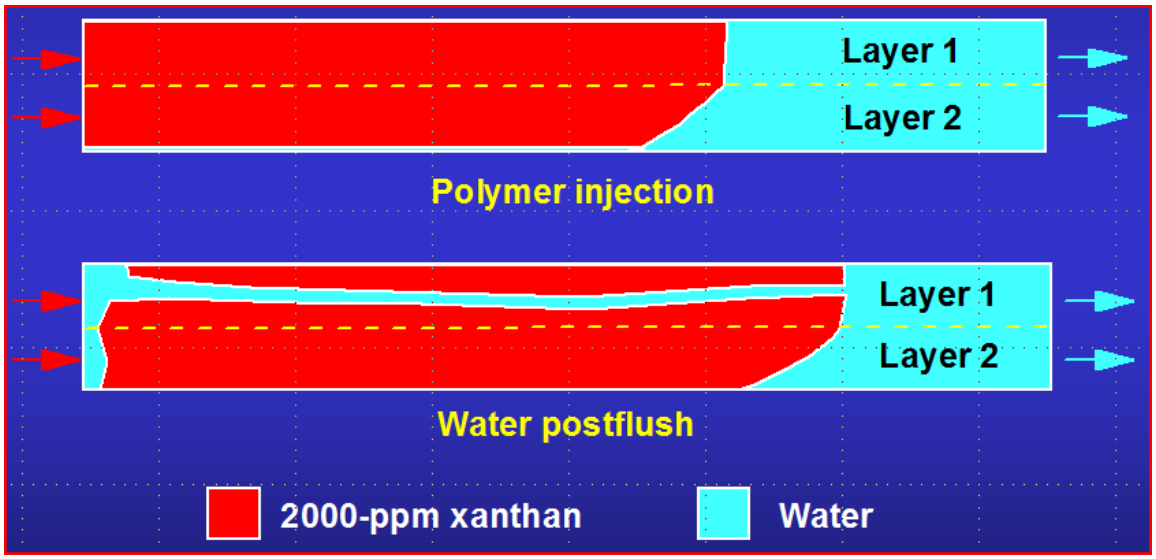

Fig. 32—Water injection following polymer injection for the bottom case in Fig. 31.

Water Postflush Following Placement of a Water-Like Gelant. To get around the problem illustrated in Fig. 32, an idea was conceived that used a water postflush following placement of a water-like gelant (Fletcher *et al.* 1991, Sorbie and Seright 1992). Fig. 33 illustrates the idea. During waterflood operations, assume that injected water has reached a production well by following a high-permeability pathway. Presumably, considerable mobile oil remains in less-permeable strata. For the first step of the gel treatment, a gelant with a water-like viscosity is injected (Fig. 33a). Because of the low viscosity of the gelant, penetration into the less-permeable zones is minimized (Seright 1988, Sorbie and Seright 1992). Second, water is injected to displace the water-like gelant away from the wellbore (Fig. 33b). Enough water must be injected so that the rear of the gelant bank in the most-permeable zone outruns the front of the gelant bank in an adjacent less-permeable zone. In the third step of the process, the gelation or permeability reduction occurs (Fig. 33c). Finally, if the gel treatment is applied in a waterflood injection well, water injection is resumed (Fig. 33d). Hopefully, a pathway will be available for water to crossflow from the high-permeability zone into the less-permeable zone(s) so that sweep efficiency can be improved.

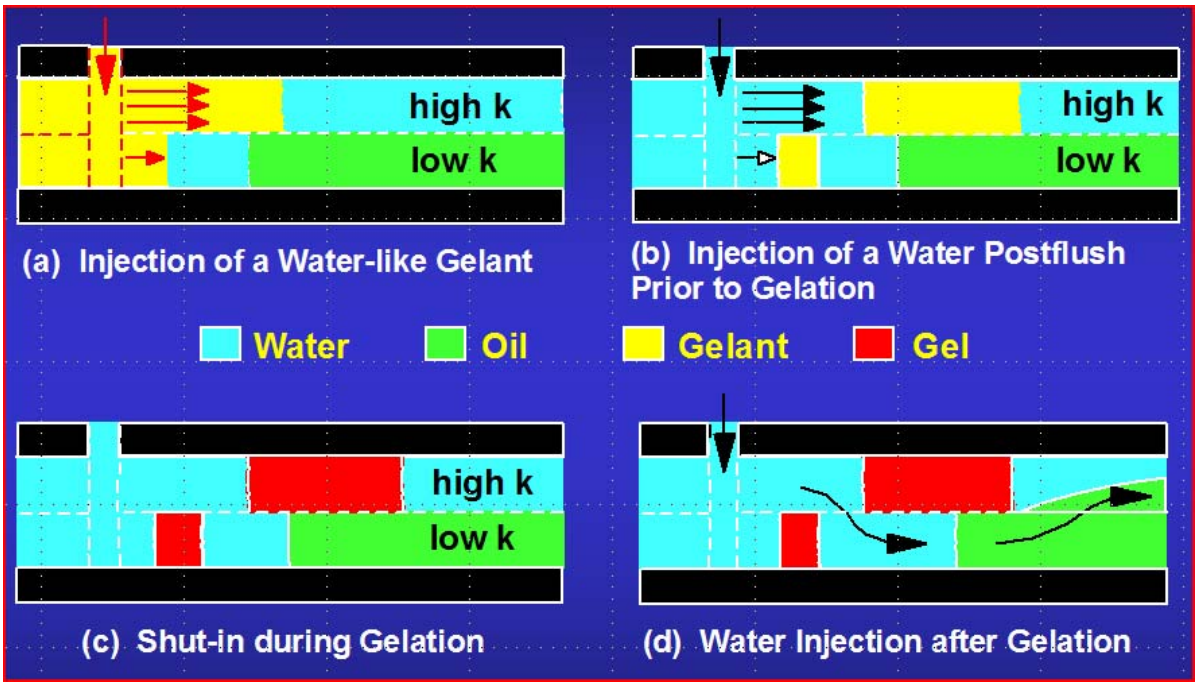

Fig. 33—Use of a water post-flush with a water-like gelant.

If this scheme is feasible, it could provide favorable injectivity. During water injection after gelation, much of the water leaving the wellbore should enter the most-permeable zone. If the cross-sectional area is relatively large in the region where water cross flows from the high-permeability zone into the low-permeability zone, injectivity losses from the gel treatment could be minimized. In contrast, conventional gel treatments (i.e., those with no postflush prior to gelation) in unfractured injection wells should cause significant injectivity losses. The "incremental" oil from this scheme could be recovered relatively quickly. Oil displaced from the less-permeable zones can crossflow into the most-permeable zone, where it can flow more rapidly to the production well.

A number of limitations should be recognized for this scheme. First, the gel treatment will not improve sweep efficiency beyond the greatest depth of gelant penetration in the reservoir. Once beyond the gel bank in the most-permeable zone, fluids can crossflow back into the high-permeability channel. This provides an incentive to maximize the depth of gelant penetration in the high-permeability channels.

Gelation time can be an important factor that limits the depth of gelant penetration in a reservoir. If the offending channel consists of a very permeable rock matrix, then very long gelation delays (many months) may be needed in order to achieve large depths of gelant penetration.

The applicability of this scheme depends on the sweep efficiency in the reservoir prior to the gel treatment. In injection wells, the scheme is expected to work best if sweep efficiency was very poor prior to the gel treatment. Then, the water that is diverted into the less-permeable strata should primarily displace oil. In contrast, if sweep efficiency was high prior to the gel treatment or if gelant penetration is insufficient in the high-permeability channel, there may be little or no oil to displace in the less-permeable zones.

In light-oil reservoirs, one very important limitation is that the viscosity and resistance factor of the gelant must not be too large. Viscous gelants will penetrate to a greater degree into the less-permeable zones (see Fig. 31). Furthermore, prior to gelation, viscous gelants will crossflow continuously from the high-permeability channel into the adjacent less-permeable zones. This creates a barrier of viscous gelant in the less-permeable zones all along the interface with the high-permeability channel. When a water postflush is injected, the barrier hinders crossflow of water from the high-permeability channel into the less-permeability zones. Thus, viscous fingers from a water postflush will break through the viscous gelant bank in the high-permeability channel before breakthrough in less-permeable zones. This can render the process ineffective. In viscous oil reservoirs, it is conceivable that this limitation could be relaxed. In addition, the viscosity and resistance factor of the gelant should not increase much during injection of either the gelant or the water postflush. Any increase in gelant resistance factor during this time will drive additional gelant into the less-permeable zones, and thereby, jeopardize the process.

Use of a Thermal Front. A variation of the idea in Fig. 33 is illustrated in Fig. 34. Cold water is sometimes injected into hot reservoirs, creating a thermal front that moves through the reservoir more slowly and evenly than the displacement front (Fletcher *et al.* 1991). If a gelant is injected that is activated by heat, a plug might form in the high-permeability layer after the formulation passes the thermal front (Fig. 34). With proper planning, no plug will form in the less-permeable layer because the gelant never reaches the thermal front (so the gelant never experiences a high enough temperature to react and form a gel). The reader should recognize that the scheme in Fig. 34 is subject to all the advantages and limitations that were mentioned above for Fig. 33. The concept in Fig. 34 was field tested in the Kuparuk field on the North Slope of Alaska in the early 1990s. Aluminum-crosslinked HPAM was the gelant (Pritchett *et al.* 2003). Although world-class engineering was used during project design and implementation, permeability reduction was felt to have been confined to the region of the injection well because of aluminum retention (Pritchett *et al.* 2003).

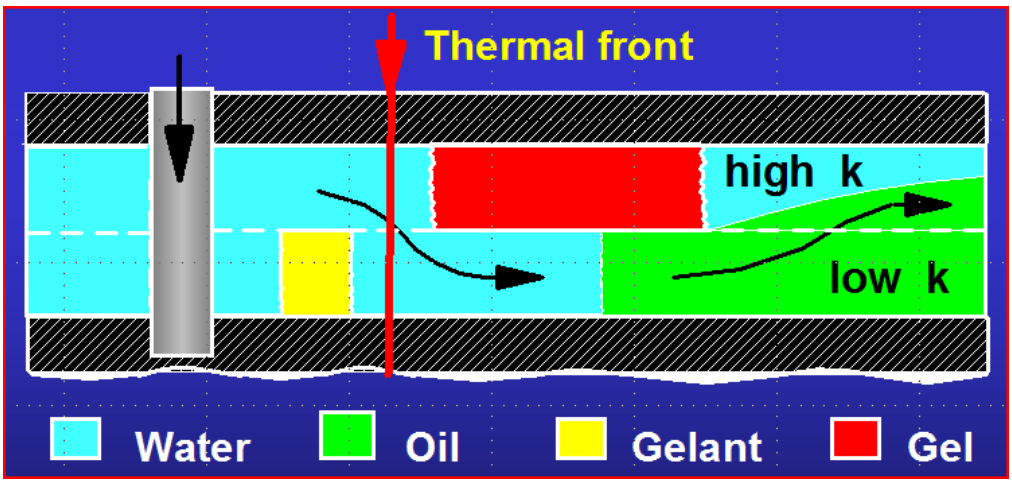

Fig. 34—Modified idea, exploiting a thermal front.

In recent years, a variation of the above concept has been commercialized (Chang *et al.* 2002, Frampton *et al.* 2004). We will refer to this as in-depth "popping" technology, because it uses polymer particles that "pop" or swell when activated. The material consists of crosslinked sulfonate-containing microparticles (0.1-3 μm in diameter) with both labile and stable internal crosslinks (Frampton *et al.* 2004). The kernel particles are manufactured as a 30% dispersion in light mineral oil. This dispersion is diluted along with a surfactant (surfactant/polymer ratio of 1:2 to 1:3) to prepare polymer concentrations from 3,000 ppm to 4,500 ppm (Pritchett *et al.* 2003, Ghaddab *et al.* 2010). Cost for the polymer was indicated to be $5.71/lb in 2003 (Pritchett *et al.* 2003). The activation is typically accomplished by exposure to elevated temperature. Consequently, this technology has been advocated and applied in cases where cold water has been injected into a warm/hot reservoir—i.e., where a thermal front exists in the reservoir. The polymer particles are injected with the intention that they will pass the thermal front and "pop" first in the high-permeability watered-out zones, thus diverting subsequently injected water/fluids into the less-permeable oil zones. Resistance factors estimated for the "popped" polymer ranged from 11 to 350 (Frampton *et al.* 2004, Ohms *et al.* 2010, Husband *et al.* 2010). The reader should realize that from a reservoir engineering viewpoint, this concept has the same advantages/limitations as the postflush concept described in Fig. 33. Field applications of the process have occurred in Indonesia (Pritchett *et al.* 2003), Argentina (Yanez *et al.* 2007), Alaska (Ohms *et al.* 2010, Husband *et al.* 2010), and Tunisia (Ghaddab 2010). Ohms *et al.* (2010) reported injecting ~40,000 lbs of polymer (38,000 bbl with 3,300-ppm polymer), and recovering ~60,000 bbl of oil. Husband *et al.* (2010) reported injecting ~200,000 lbs of polymer (190,000 bbl with 3,000-ppm polymer) into three wells, and recovering ~500,000 bbl of oil.

Methods and Assumptions

The question raised in this study is: When is the above in-depth profile modification process a superior choice over conventional polymer flooding? We made several attempts to address this question using both analytical and simulation methods (Akanni 2010, Zhang 2010, Appendix A). This study presents our most refined effort. All three of our efforts assumed that the in-depth popping material had the same viscosity as water prior to activation. This assumption is optimistic and will push our analysis results in favor of in-depth profile modification (compared with traditional polymer flooding). In reality, prior to activation, the popping material exhibits viscosities/resistance factors that are 2 to 7 times higher than water (Chang *et al.* 2002, Pritchett

et al 2003). As demonstrated in Fig. 31, increased viscosity promotes crossflow of the gelant into the less-permeable layers and diminishes or eliminates the ability of post-flush water to be diverted into the less-permeable layer (Fig. 32). For the in-depth profile-modification process, Sorbie and Seright (1992) suggested that the maximum allowable viscosity/resistance factor during placement is ~0.3 times the permeability contrast.

All three of our efforts assumed that the popping material caused no permeability reduction in the less-permeable zone. Again, this is an optimistic assumption that will favor in-depth profile modification over traditional polymer flooding. All of our efforts also assumed that (1) activation of the popping material occurred instantaneously, (2) permeability was reduced to zero in the high-permeability path where the popping material was activated, and (3) the permeability reduction was permanent. In reality, the popping material reduces permeability by factors from 11 to 350 (Frampton *et al.* 2004, Ohms *et al.* 2010, Husband *et al.* 2010). Also, the resistance associated with the popped polymer bank goes through a peak (with time and throughput) and shows some degree of movement through porous media (Chang *et al.* 2002, Frampton *et al.* 2004). This behavior is what might be expected. If the particles pop to become hydrated polymer molecules in solution, the resistance factors reflect the viscosity of 3,000-4,500-ppm polymer solutions. For a time, this viscous polymer bank in the high-permeability zone (hopefully) will allow much of the subsequently injected brine to be diverted into less-permeable zones. However, eventually, the brine will finger through this viscous polymer bank (as in Fig. 32). Thus, our assumption of a permanent block in the high-permeability layer is optimistic and will favor in-depth profile modification over traditional polymer flooding. Capillary pressure and gravity were also neglected during all of our efforts. Also, no dispersion was allowed at the boundaries of the popping-agent bank. Furthermore, in all our analyses, polymer rheology was Newtonian; polymer retention balanced inaccessible pore volume; and polymer did not reduce residual oil saturation below that for water flooding. Flow was generally linear between one injection well and one production well. (However, during the two simulation efforts, radial flow was assumed in the two well grid blocks.) The relative permeability characteristics that we used were:

$$k_{rw}=k_{rwo}\,[(S_w-S_{wr})/(1-S_{or}-S_{wr})]^{nw} \quad (5)$$

$$k_{ro}=k_{roo}\,[(1-S_{or}-S_w)/(1-S_{or}-S_{wr})]^{no} \quad (6)$$

$$k_{rwo}=0.1,\ k_{roo}=1,\ S_{or}=0.3,\ S_{wr}=0.3,\ nw=2,\ no=2 \quad (7)$$

Using the ECLIPSE simulator, Akanni (2010) examined a two-layer reservoir with permeability contrasts ranging from 2:1 to 20:1 and with oil/water viscosity ratios ranging from 1 to 10,000. He assumed relatively large popping-agent bank sizes and examined the effect of popping-agent bank positioning on recovery. He concluded that in-depth profile modification would have its greatest opportunity to compete with polymer flooding if the permeability contrast between layers was high. As expected, he concluded that placement of larger popping-agent banks in the high-permeability layer would enhance oil recovery, but economics would likely favor use of small popping-agent banks. He also concluded that higher recovery values favored positioning the popped bank in the middle of the high-permeability layer or somewhat towards the producer (i.e., not near the injector). Some concerns were raised about the simulations during the benchmarking process. Akanni (2010) was unable to match accepted

expectations during waterflooding (i.e., prior to application of polymer flooding or in-depth profile modification). In particular, as the water/oil mobility ratio increases, accepted reservoir engineering predicts that recovery efficiency in a stratified reservoir should become progressively worse for the case of free crossflow than for the case of no crossflow (Craig 1971). Instead, the simulation predicted that waterflood recoveries for the crossflow and no-crossflow cases were similar, even at high mobility ratios. We presume that this deficiency was due to our inexperience with simulation (at the PRRC). However, we noted this same behavior with two other simulators (using other personnel).

Consequently, an effort was made to attack our problem using strictly analytical means (i.e., no simulator). In that analysis, Zhang (2010, AppendixA) confirmed that in-depth profile modification had the best opportunity to compete with polymer flooding when the permeability contrast between layers was high. In-depth profile modification also benefited when the high-permeability layer was much thinner than the less-permeable layer. The study also indicated that use of small popping-agent banks would be most desirable (economically) when displacing low-viscosity oils. More viscous oils are expected to require larger popping-agent banks.

For both of the previous approaches, at the start of polymer injection or popping-agent placement, we assumed that the high-permeability layer was at residual oil saturation and the low-permeability layer was at connate water saturation. We also assumed that the popping agent was placed instantaneously. Both of these assumptions are unrealistic. Consequently, a new analysis was performed by an expert in simulation of chemical flooding processes. This analysis assumed that (1) the reservoir was initially at connate water saturation, and (2) one pore volume (PV) of water was injected before beginning either polymer or popping-agent injection. For the in-depth profile-modification cases in the new analysis, the popping-agent material acted simply as a continued waterflood until the popping-agent bank reached its desired location. For example, if a small bank of popping agent was to be placed in the center of the high-permeability layer, we assumed that (1) the reservoir (i.e., both layers) was at connate water saturation initially, (2) one PV of water was injected, (3) an additional amount of fluid (1-cp popping-agent pre-gel material followed by water) was injected to allow the popping-agent bank to reach the center 5% of the high-permeability layer, (4) the popping-agent bank was then instantaneously set into place to reduce permeability in the center 5% of the high-permeability layer to zero, and (5) finally, the waterflood was continued with the new block in place.

In order to verify the correctness of our previous efforts, we used a simulator from CMG. Our experienced simulation person was able to confirm credible behavior during benchmarking waterflood simulations. Subsequently, we examined oil recovery efficiency for the two processes (in-depth profile modification versus polymer flooding) as a function of (1) permeability contrast (up to 10 fold), (2) relative zone thickness, (3) oil viscosity (up to 1,000 cp), (4) polymer solution viscosity, (5) polymer or blocking-agent bank size, and (6) relative costs for polymer versus blocking agent. In Figs. 35-41, we plot the percent of original mobile oil in place that was recovered as a function of PV injected. Results from the first PV of injection were not included because they were all the same for a given figure (because 1 PV of water was injected at the start of all cases). In each figure, the thin solid curve (with no symbols) represents the waterflood-only curve, and the thick solid curves represent the case where polymer solutions (10, 40, or 100 cp) were injected beginning after 1 PV of waterflood. The other three curves in each figure show cases where 5%, 35%, or 90% of the high-permeability layer (HP-PV) was blocked with popping-agent gel (after the initial waterflood).

Effect of Oil Viscosity

We first examine the effects of oil viscosity. Our initial interest in this topic was motivated by a question as to whether in-depth profile modification would be preferred over polymer flooding for reservoirs on Alaska's North Slope that contained somewhat viscous oils (100-1,000 cp). Figs. 35-37 show recovery projections (expressed as the percent of the original mobile oil that was in place) versus pore volumes injected for oil viscosities of 10 cp, 100 cp, and 1,000 cp, respectively. For each case in these figures, the high-permeability layer (Layer 1) was 10 times more permeable than the low-permeability layer (k_1/k_2=10), the low-permeability layer (Layer 2) was 9 times thicker than the high-permeability layer (h_2/h_1=9), and water viscosity was 1 cp. In all cases, waterflooding occurred between 0 and 1 PV—then the alternative process was implemented. In each of the following figures, the thin black curve (without symbols) shows the results for continued waterflooding, which provided the lowest recovery in all cases.

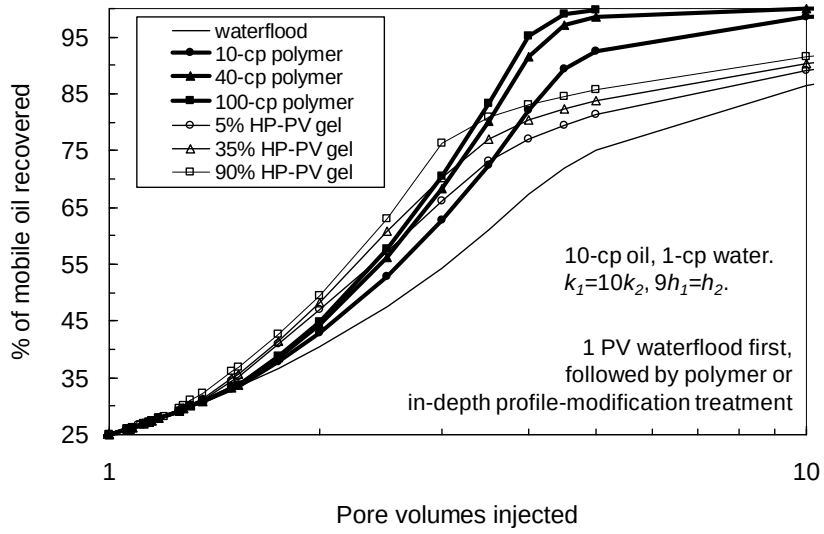

Fig. 35—Recovery with k_1/k_2=10 and h_2/h_1=9. 10-cp oil.

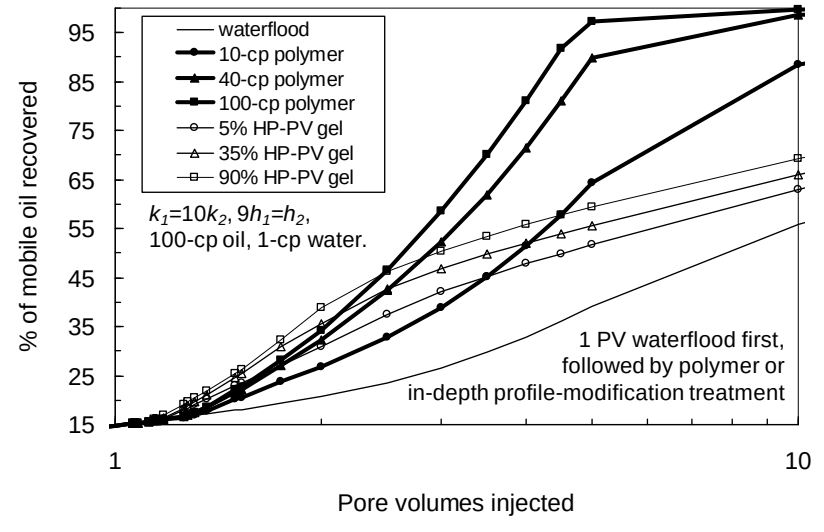

Fig. 36—Recovery with k_1/k_2=10 and h_2/h_1=9. 100-cp oil.

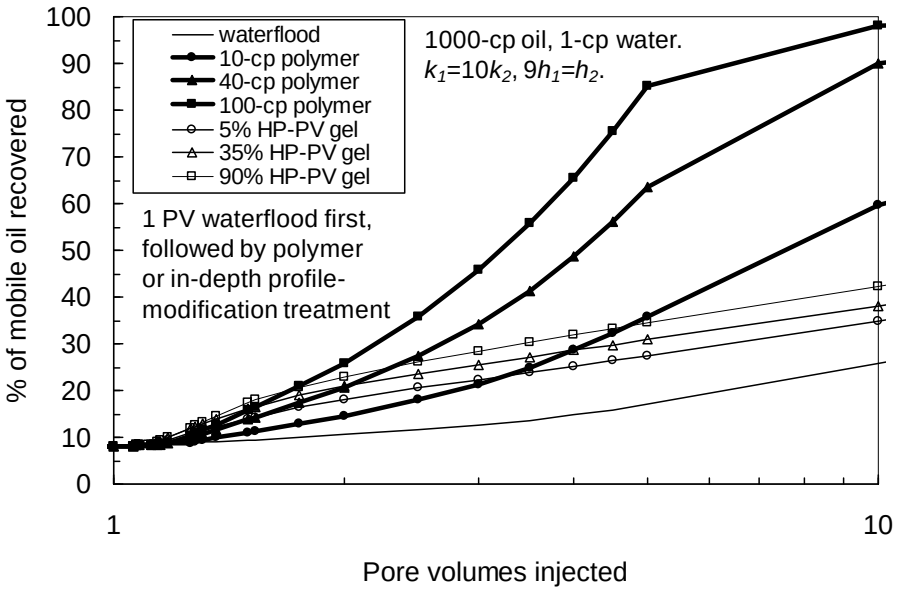

Fig. 37—Recovery with k_1/k_2=10 and h_2/h_1=9. 1,000-cp oil.

The thick black curves in Figs. 35-37 show results from polymer floods with 10-cp, 40-cp, or 100-cp polymer. These results are quite in-line with expectations (Seright 2010b).When displacing 10-cp oil (Fig. 35), injecting a 10-cp polymer solution provides a noticeable improvement over waterflooding. Additional recovery is seen using 40-cp or 100-cp polymer, but the incremental benefit diminishes substantially with increased polymer viscosity. In contrast, for the 100-cp and 1,000-cp oils (Figs. 36 and 37), substantially greater recovery is seen with the more viscous polymer solutions.

In Figs. 35-37, the thin lines with open symbols show results for various bank sizes (5% to 90% in the high-permeability layer) for the in-depth profile-modification process. Interestingly, in all three figures, a 90% popping-agent bank only recovered modestly more oil than a 5% bank. There are several reasons for this. First, for the more viscous oils, during water injection after placement of the popping agent, sweep efficiency is poor in the thick less-permeable zone. Viscous fingering within the less-permeable layer (i.e., adjacent to the popped material in the high-permeability layer) strongly affects the incremental recovery. Second, because we assumed that permeability dropped to zero when the popping agent activated, oil reserves in the blocked portions of the high-permeability layer were lost. The magnitude of the loss is directly proportional to the size of the popping-agent bank. One can argue that this loss of reserves is unrealistically pessimistic, since water can actually viscous finger into the popping-agent bank and displace some of that trapped oil. However, this error is offset by our overly optimistic assumption that the blocking action is permanent in the high-permeability layer. As will be seen shortly, the relatively modest effect of popping-agent bank size on recovery will result in economics favoring the use of small banks. This observation is consistent with what is currently advocated by the vendor of this in-depth profile-modification technology.

Note that in-depth profile modification provides higher oil recovery values (for a given PV) than polymer flooding between 1 and 3 PV. Even for this PV range, the recovery values are, at best, only modestly greater than for polymer flooding. At high PV values (>4PV), polymer flooding always provides higher recovery values.

Effect of Permeability Contrast

Along with Figs. 35-37, Figs. 38 and 39 demonstrate the effect of permeability contrast on the performance of in-depth profile modification versus polymer flooding. Permeability contrast was 10:1 in Fig. 36, 5:1 in Fig. 38, and 2:1 in Fig. 39. For all three cases, oil viscosity was 100 cp, and the low-permeability layer was nine times thicker than the high-permeability layer. A comparison of Figs. 36 and 38 reveals that the enhanced recovery using in-depth profile modification (over 10-cp polymer flooding) diminishes significantly as the permeability contrast drops from 10:1 to 5:1. Fig. 39 (2:1 permeability contrast) shows no benefit of in-depth profile modification over 10-cp polymer flooding, for any popping-agent bank size. These results are qualitatively consistent with the results from our earlier analytical effort (Zhang 2010, Appendix A) and with the results from the first simulation effort using ECLIPSE (Akanni 2010).

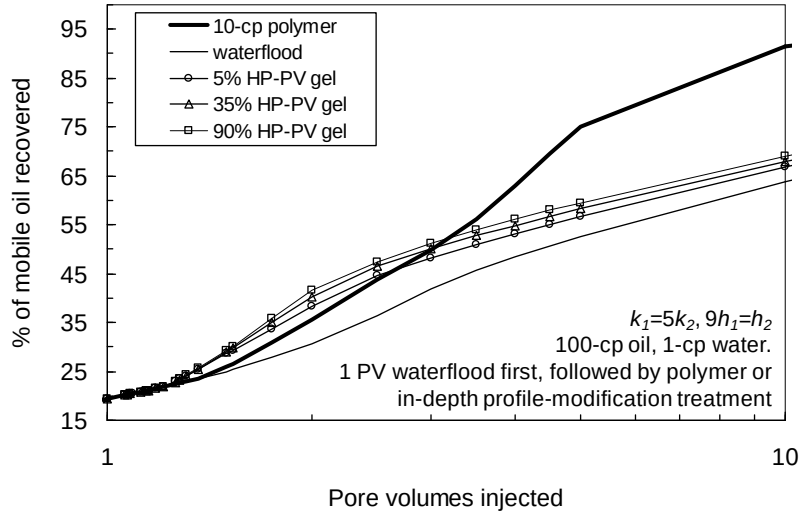

Fig. 38—Recovery with k_1/k_2=5 and h_2/h_1=9. 100-cp oil.

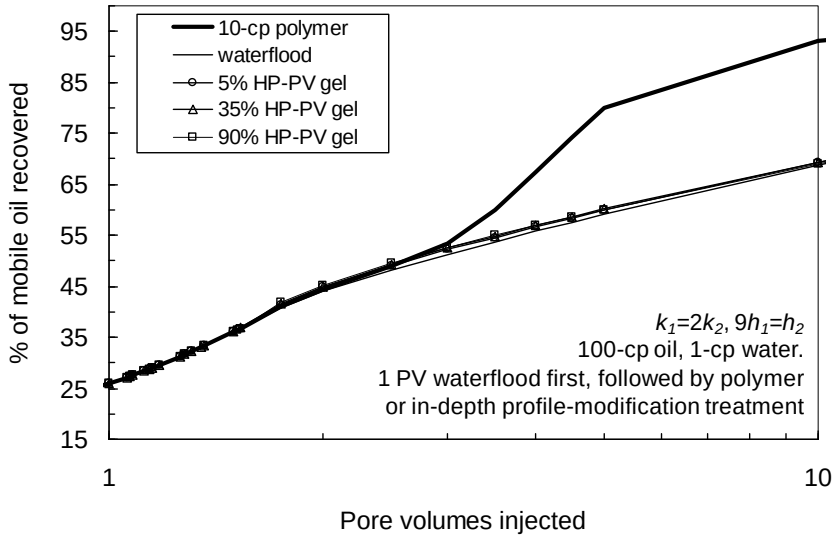

Fig. 39—Recovery with k_1/k_2=2 and h_2/h_1=9. 100-cp oil.

Effect of Layer Thickness

Along with Figs. 35-37, Figs. 40 and 41 demonstrate the effect of layer thickness on the performance of in-depth profile modification versus polymer flooding. The thickness ratio (low-permeability layer to high-permeability layer) was 9:1 in Fig. 36, 3:1 in Fig. 40, and 1:1 in Fig. 41. For all three cases, oil viscosity was 100 cp, and the high-permeability layer was ten times more permeable than the low-permeability layer. For large popping-agent bank sizes (e.g., 35% or 90%), in-depth profile modification showed enhanced recovery (over 10-cp polymer flooding) for thickness ratios of 9:1 and 3:1 (Figs. 36 and 40). However, the benefit occurred over a narrower range of PV for a 3:1 thickness ratio (1.3-2.5 PV in Fig. 40) than for a 9:1 thickness ratio (1.2-4 PV in Fig. 36). For a 1:1 thickness ratio, Fig. 41 shows that 10-cp polymer flooding was superior to in-depth profile modification. The results reveal that in-depth profile modification is most appropriate for high permeability contrast (e.g. 10:1) and high thickness ratios (e.g., less-permeable zones being 9 times thicker than high-permeability zones). These results are qualitatively consistent with the results from our earlier analytical effort (Zhang 2010, Appendix A).

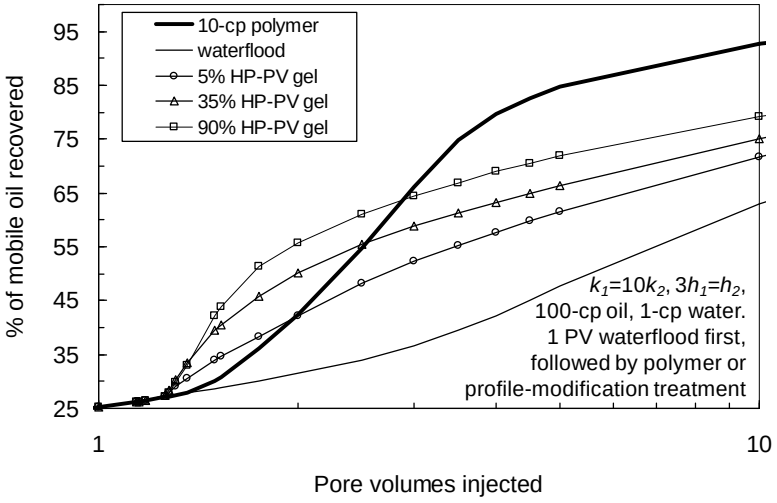

Fig. 40—Recovery with k_1/k_2=10 and h_2/h_1=3. 100-cp oil.

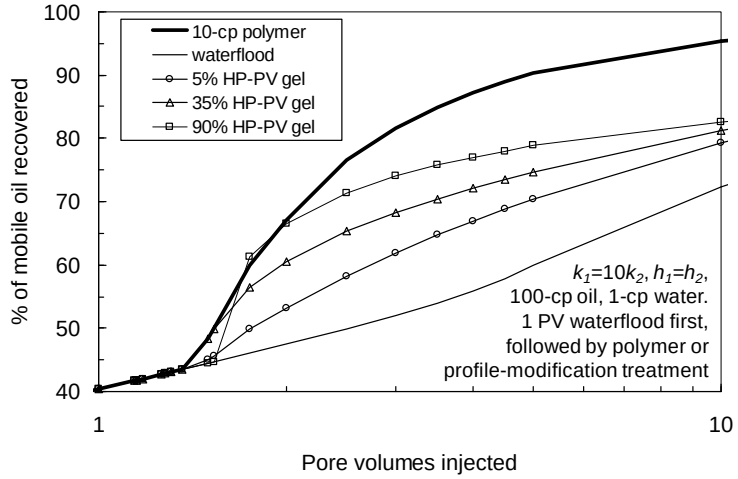

Fig. 41—Recovery with k_1/k_2=10 and h_2/h_1=1. 100-cp oil.

Cost Considerations

The popping-agent process typically uses high concentrations of polymers (e.g., 0.3%-0.45%) and surfactants (e.g., 0.1%-0.2%), resulting in a cost (per weight of chemical) that is several times higher than for conventional polymer flooding (Pritchett *et al.* 2003, Ghaddab *et al.* 2010). The polymer used in the popping-agent process (an internally crosslinked HPAM) is a specialty polymer and therefore more expensive (on a per weight basis) than HPAM. In the following analysis, we will focus on the most-favorable case for in-depth profile modification, with a permeability contrast (k_1/k_2) of 10:1 and a thickness ratio (h_2/h_1) of 9:1. Oil was assumed to have a value of \$50/bbl; water was assumed to cost \$0.25/bbl; HPAM was assumed to cost \$1.50/lb; a 10-cp HPAM solution required 0.1% polymer; a 40-cp HPAM solution required 0.2% polymer; a 100-cp HPAM solution required 0.3% polymer; and the popping-agent block was assumed to require 0.3% concentration of popping-agent polymer. Our assumptions about viscosity versus HPAM concentration are conservative in favor of the in-depth profile-modification process. This level of viscosification by HPAM would be valid if the injection water was saline (e.g., as in seawater). If less saline water were used, a higher viscosity would be achieved with less polymer. For example, at Daqing, 0.1% HPAM yields solution viscosities from 20 to 50 cp (Wang *et al.* 2008b). For a given PV of fluid injected, a relative profit was calculated as the total value of the oil produced minus the total cost of fluid injected (water, polymer, popping-agent material). In these figures, we assumed that the cost of the popping-agent material was expended immediately at the start of popping-agent injection—explaining the sudden drop in relative profit at 1 PV for the popping-agent cases.

The cost comparisons are shown in Figs. 42-44. These figures assume that the popping-agent material costs \$5.71/lb (per Pritchett *et al.* 2003) and 0.3% popping polymer was used in the popping bank. For an oil viscosity of 10 cp (Fig. 42), small popping-agent treatments appeared modestly more profitable than polymer flooding in the range from 2-4 PV. Note that the smallest popping-agent bank was always more profitable than the larger banks. Although large popping-agent banks result in higher oil recoveries (Figs. 35-37), their high cost negates that benefit (open triangles in Fig. 42). This result is consistent with the current advocacy of the popping-agent vendor. A table in the center of Fig. 42 compares the percent of the original mobile oil that was recovered after 5 PV for various cases. Note that the ultimate recoveries for polymer flooding were higher than for in-depth profile modification. Although the smallest popping-agent bank (5% of the PV in the high-permeability layer) provided a higher profitability (i.e., at 3 PV), its ultimate recovery factor was significantly less than for 10-cp polymer flooding. Also note that 10-cp polymer flooding provided a higher profitability than any of the other cases at 5 PV—where the profitability peak occurred. After 5 PV, profitability for polymer flooding decreased because the value of the oil produced was less than the value of the polymer injected. For the popping-agent cases, profitability did not decrease after 5 PV because no additional popping-agent material was purchased or injected. As mentioned earlier, this projection is overly optimistic because the blocking effect from the popping material will deteriorate with time (Chang *et al.* 2002, Frampton *et al.* 2004).

For 100-cp oil (Fig. 43), the economics for a 5% PV popping-agent treatment appears only slightly better than for a 40-cp polymer flood for a short range between 1 and 2.5 PV. However, recovery efficiencies are dramatically lower for the popping agent treatment (51.8% versus 89.8% in the center table of Fig. 43). For 1,000-cp oil, the 40-cp and 100-cp polymer solutions appear superior to in-depth profile modification for virtually all cases (Fig. 44).

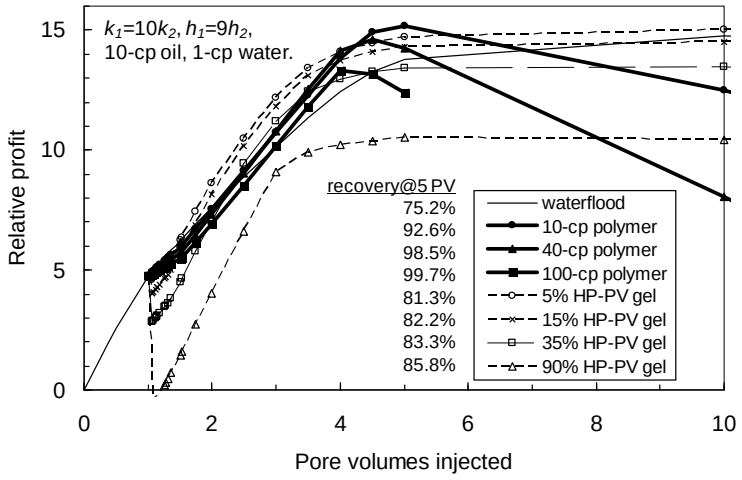

Fig. 42—Relative profit for various cases: 10-cp oil.

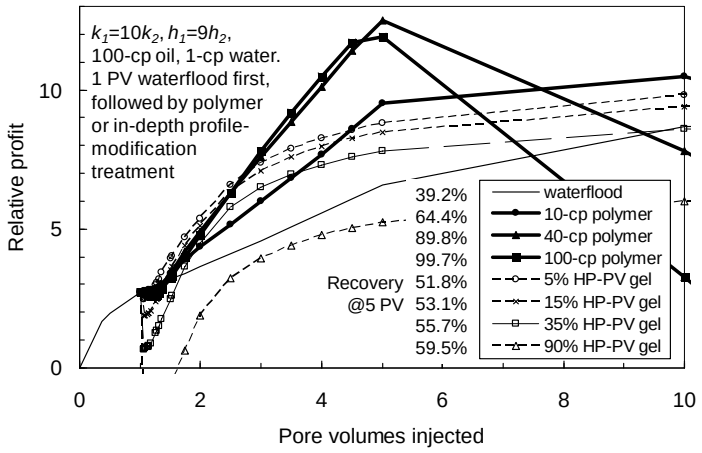

Fig. 43—Relative profit for various cases: 100-cp oil.

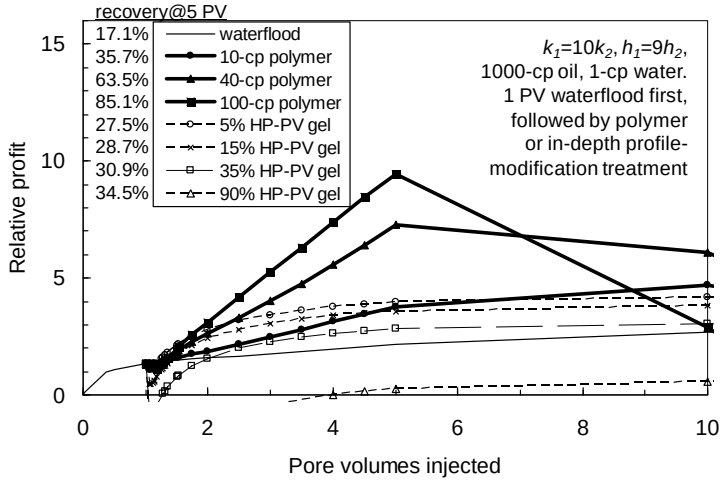

Fig. 44—Relative profit for various cases: 1000-cp oil.

Fig. 45 compares cases where the popping-agent material costs differing amounts. In all cases, Layer 1 was 10 times more permeable and 9 times thinner than Layer 2, and oil viscosity was 10-cp. For the cases with in-depth profile modification, the bank size was 5% PV (in the high-permeability layer). The middle dashed curve (labeled "1X cost) shows the case where the popping-agent concentration was 0.3% and the popping-agent cost was $5.71/lb. The "1.5X cost" case in Fig. 45 assumes that the total popping-agent cost was 1.5 times more expensive (e.g., as in Pritchett *et al.* 2003, where 0.45% popping-agent concentration was used). The "0.5X cost" case in Fig. 45 assumes that the total popping-agent cost was half as expensive (e.g., if a breakthrough in price reduction can be accomplished). All other assumptions were the same as in Fig. 42, with a small popping-agent bank (5% of the PV in the high-permeability layer). The primary message from Fig. 45 is that popping-agent performance was not highly sensitive to popping-agent cost, presumably because the bank size was so small. However, even though short-term economics (i.e., before 4 PV in Fig. 45) may favor small in-depth profile modification, a longer view (i.e., at 5 PV where the peak of profitability occurred) favored polymer flooding. Also, the relative simplicity of the polymer flooding process favors it over in-depth profile modification.

During a personal communication with R.H. Lane (June 16, 2011), we learned that Seyidov and Lane (2010) performed a relevant simulation study of "deep diverting gels." This study assumed that the blocking agent could be effectively placed in a multilayered reservoir with crossflow. They observed a number of results that were consistent with our findings. Their study concluded that "although higher ultimate recovery was achieved with a polymer flood, the combination of delayed production response and large polymer amounts used adversely impacted polymer flood economics." They also found that treatment size and oil viscosity were important variables in determining the effectiveness of these treatments.

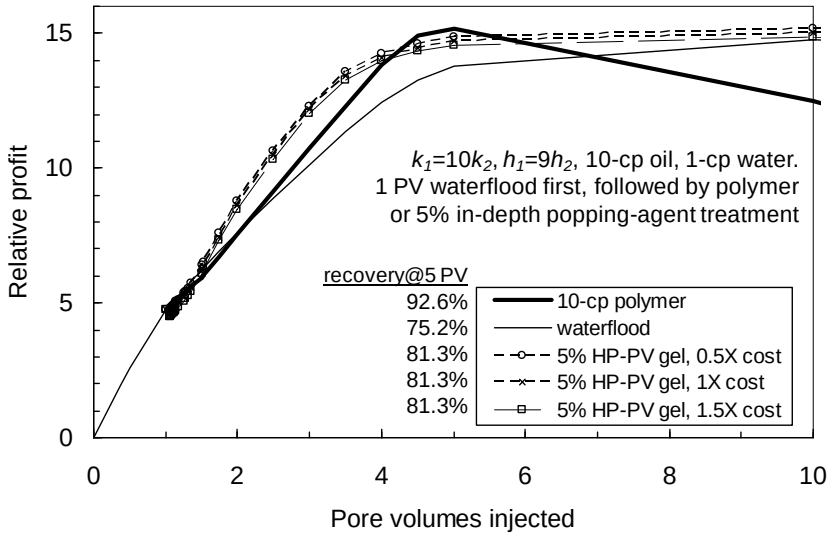

Fig. 45—Relative profit assuming various popping-agent material costs.

Injectivity Considerations

Concern about injectivity losses was a key motivation that was given for choosing in-depth profile modification over polymer flooding. The concern is that injectivity losses associated with injection of viscous polymer solutions will result in prohibitive losses in oil production rate.

However, most waterflood and polymer flood injectors are thought to be fractured (Van den Hoek *et al.* 2009, Khodaverdian *et al.* 2009, Wang *et al.* 2008a, Seright *et al.* 2009). Fractures are especially likely to be present in hot reservoirs with cold-water injectors (Fletcher *et al.* 1991). Even when injecting concentrated, viscous polymer solutions (i.e., 200-300 cp), injectivity has not been a problem in field applications (Wang *et al.* 2011) because fractures extend to accommodate the viscosity and rate of fluid injected. Of course, the key concerns when injecting above the parting pressure are to not allow fractures to (1) extend so far and in a direction that causes severe channeling and (2) extend out of zone. If these concerns can be mitigated, under the proper circumstances, injection above the parting pressure can significantly (1) increase polymer solution injectivity and fluid throughput for the reservoir pattern, (2) reduce the risk of mechanical degradation for polyacrylamide solutions, and (3) increase pattern sweep efficiency (Trantham *et al.* 1980, Wang *et al.* 2008a, Seright *et al.* 2009). Using both field data and theoretical analyses, these facts have been demonstrated at the Daqing Oilfield in China, where the world's largest polymer flood is in operation (Wang *et al.* 2008a).

Additional Considerations

If small banks of popping-agent are injected (e.g., ~5% PV in the high-permeability layer), a significant amount of mixing and dispersion may occur as that bank is placed deep within the reservoir (Lake 1989)—thus, diluting the bank and potentially compromising the effectiveness of the blocking agent. Also, as mentioned earlier, since the popping material provides a limited permeability reduction (i.e., 11 to 350) and the popped-material has some mobility, the blocking bank eventually will be diluted and compromised by viscous fingering (Chang *et al.* 2002, Frampton *et al.* 2004).

Another consideration is the possibility of re-treatment for the in-depth profile-modification process. During a second or subsequent treatment, the presence of a block or partial block in the high-permeability layer will (1) divert new popping-agent into less-permeable zones during the placement process and (2) inhibit placement of a new block that is located deeper in the reservoir than the first block. These factors may compromise any re-treatment using in-depth profile modification.

A third additional consideration concerns the initial diagnosis of the problem. The assumption in this study and with some of the previous treatments is that fractures or fracture-like features were not responsible for significant channeling in the reservoir. However, if the mobility ratio is favorable during waterflooding (i.e., low viscosity oil) and the maximum permeability contrast is modest (e.g., 4:1), one has to wonder why the water/oil ratio is high (e.g., <20) if the oil recovery factor is low. For this type of case, one may want to reconsider whether fractures are important to channeling. If so, traditional gel treatments (Sydansk and Romero-Zeron 2011) may warrant consideration.

Conclusions

Our analyses revealed that in-depth profile modification is most appropriate for high permeability contrasts (e.g. 10:1), high thickness ratios (e.g., less-permeable zones being 9 times thicker than high-permeability zones), and relatively low oil viscosities. Because of the high cost of the blocking agent (relative to conventional polymers), economics favor small blocking-agent bank sizes (e.g. 5% of the pore volume in the high-permeability layer). Even though short-term economics may favor in-depth profile modification, ultimate recovery may be considerably less

than from a traditional polymer flood. A longer view may favor polymer flooding both from a recovery viewpoint and an economic viewpoint.

5. DO HPAM SOLUTIONS REDUCE S_{OR} DURING POLYMER FLOODING OF VISCOUS OILS?

Previous Literature

Conventional wisdom within the petroleum industry is that the ultimate residual oil saturation (S_{or}) for a polymer flood is the same as that for a waterflood (Tabor 1969, Lake 1989). Polymers have a negligible effect on oil-water interfacial tension, so no reduction of S_{or} is expected, compared with waterflooding. Several previous literature reports are consistent with this view in water-wet cores, especially with Berea and Bentheim sandstone (Schneider and Owens 1982, Pusch et al. 1987, Wreath 1989).

However, for conditions associated with the Daqing reservoir, researchers (Wang et al. 2000, 2001a, 2001b, Xia et al. 2004, Wu et al. 2007) argued that HPAM solutions reduced S_{or} by 6 to 15 saturation percentage points, even with waterfloods and polymer floods conducted at the same constant capillary number. Notably, Wu et al. (2007) observed that HPAM polymers reduced the waterflood S_{or} by up to 15 saturation percentage points (i.e., a S_{or} of 36.8% with waterflooding versus 21.75% for polymer flooding) using a constant capillary number of $5x10^{-5}$. The Daqing researchers observed reductions in S_{or} under oil-wet, weakly oil-wet, and mixed-wet conditions. They attributed the reduction in oil saturation to the viscoelasticity of high molecular-weight HPAM solutions—particularly associated with a polymer solution's normal stress difference. They did not observe the effect with Newtonian glycerin solutions. Ironically, the Daqing researchers reported reductions in S_{or} to about the same extent at low velocities in porous media as at high velocities (Wu et al. 2007). This result seems inconsistent with their proposed explanation, since viscoelasticity and normal stress differences vanish at low velocities.

Others have also reported reductions in S_{or} during polymer flooding in cores that were not water wet. Schneider and Owens (1982) found that HPAM floods resulted in 1% to 6% reductions in S_{or} in Berea that was treated with diesel oil to make the core oil wet. They also found that HPAM floods caused 6.5% to 8.4% reductions in S_{or} in Tensleep and Berea cores that were treated with "Surfasil" to induce oil-wettability.

Interestingly, reports also exist where polymer floods reportedly reduced S_{or} in water-wet cores. Zaitoun and Kohler (1987, 1988) observed that a nonionic polyacrylamide reduced S_{or} by 3% in water-wet Berea and Vosges sandstones. In Bentheim sandstone, Pusch et al. (1987) reported 1% to 4% reductions in S_{or} with xanthan and a Newtonian viscous sugar solution. We wonder if these observations were within experimental error of the S_{or} determinations.

Huh and Pope (2008) performed studies in water-wet Berea and Antolini sandstone cores. Their work indicated that HPAM solutions would not significantly reduce S_{or} in a homogeneous water-wet core that had previously been waterflooded to residual oil saturation. However, they also noted that when polymer flooding in a secondary-recovery mode (i.e., when the core had a high oil saturation at the start of the polymer flood), the S_{or} reached was notably less than for a waterflood. This effect was attributed to the ability of the polymer to maintain longer oil ganglia and more effective pore drainage before snap-off and trapping of residual oil.

For heterogeneous cores, two effects could appear to make the S_{or} lower after a polymer flood than after a waterflood. First, if insufficient water is flushed through the core to displace mobile oil from less-permeable pathways, one could be misled by the high water cut to believe that the core was near S_{or}. Improved volumetric sweep during a subsequent polymer flood could rapidly produce a small spike of mobile oil from the less-permeable pathways. Huh and Pope envisioned a second means by which a polymer flood could reduce S_{or} from a heterogeneous core—that is

the case where high-permeability pathways have been effectively flushed with water at the start of polymer injection, but the mobile oil saturation remains high in less-permeable pathways. In the high-permeability pathways, the final S_{or} from polymer flooding would be no different from that for the waterflood. However, in the less-permeable pathways, polymer flooding could drive the S_{or} to a lower value via the same mechanism mentioned at the end of the previous paragraph. During polymer flooding, Huh and Pope (2008) observed S_{or} reductions (relative to waterflooding) ranging from 2 to 22 saturation percentage points using heterogeneous Antolini cores and a constant capillary number of 4×10^{-6}.

Porous Polyethylene Cores

We are particularly interested in whether polymer flooding can reduce S_{or} when displacing a viscous North Slope crude (190 cp viscosity @ 25°C, 0.935 g/cm^3, provided by ConocoPhillips). Two 77.2-cm long porous polyethylene cores were used. Both had permeability ~10 darcys, porosity ~0.445, a flow cross section of 10.75 cm^2, and a pore volume of ~370 cm^3. Both had two internal pressure taps that divided the core into three sections of equal length (25.7 cm each). The cores were first saturated with a 2.52% TDS brine (2.3% NaCl, 0.22% $NaHCO_3$).

To avoid complications for heterogeneous cores that were described by Huh and Pope (last paragraph of the previous section), we wanted to use a homogeneous core. To test whether our porous polyethylene core material was homogeneous, a tracer study was performed on one of the cores. A brine bank with a low concentration of KI was injected and the effluent was monitored spectrophotometrically at a wavelength of 230 nm. The tracer results (Fig. 46, showing results for injection rates ranging from 500 to 2,000 cm^3/hr or from 37 to 146 ft/d) reveal that the core is quite homogeneous. The 50% tracer concentration was reached at 1 pore volume (PV), the tracer profile was reasonably symmetrical, and 100% tracer concentration was reached by 2 PV. In contrast for heterogeneous cores, a "tail" was observed where 100% tracer concentration was gradually approached over the course of many pore volumes. For example, for Huh and Pope's Antolini core, 100% tracer concentration had not been reached after injecting over 6 PV.

Polymer Injection after Waterflooding

Crude oil was injected to establish connate water saturation, S_{wr} (0.012 for Core 1 and 0.011 for Core 2). Then the cores were shut in for five days. (All experiments were performed at room temperature.) Next (Fig. 47), 11 PV of brine (2.52% TDS) were injected into Core 1, followed by 10 PV of 10-cp HPAM solution (1,020-ppm Flopaam 3830S in 2.52% TDS brine), followed by 5 PV of 100-cp HPAM solution (3,286-ppm Flopaam 3830S). During this sequence a fixed pressure drop of 50 psi (19.7 psi/ft) was maintained. The capillary number during these displacements was 1.77×10^{-5}.

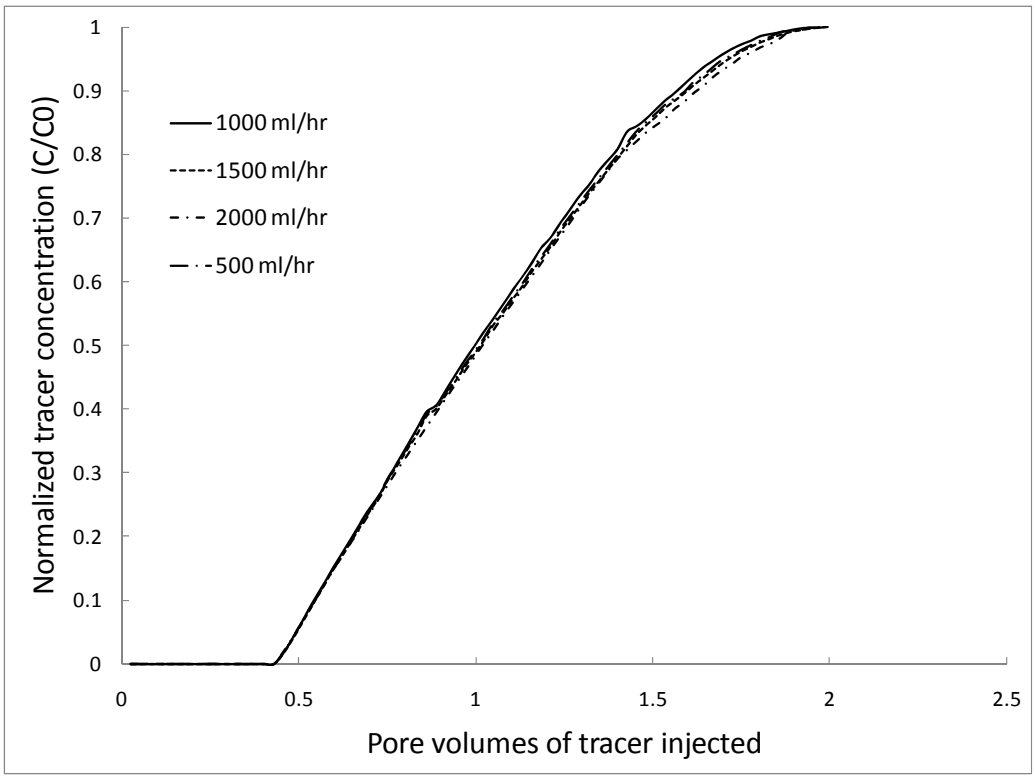

Fig. 46—Tracer results for a polyethylene core.

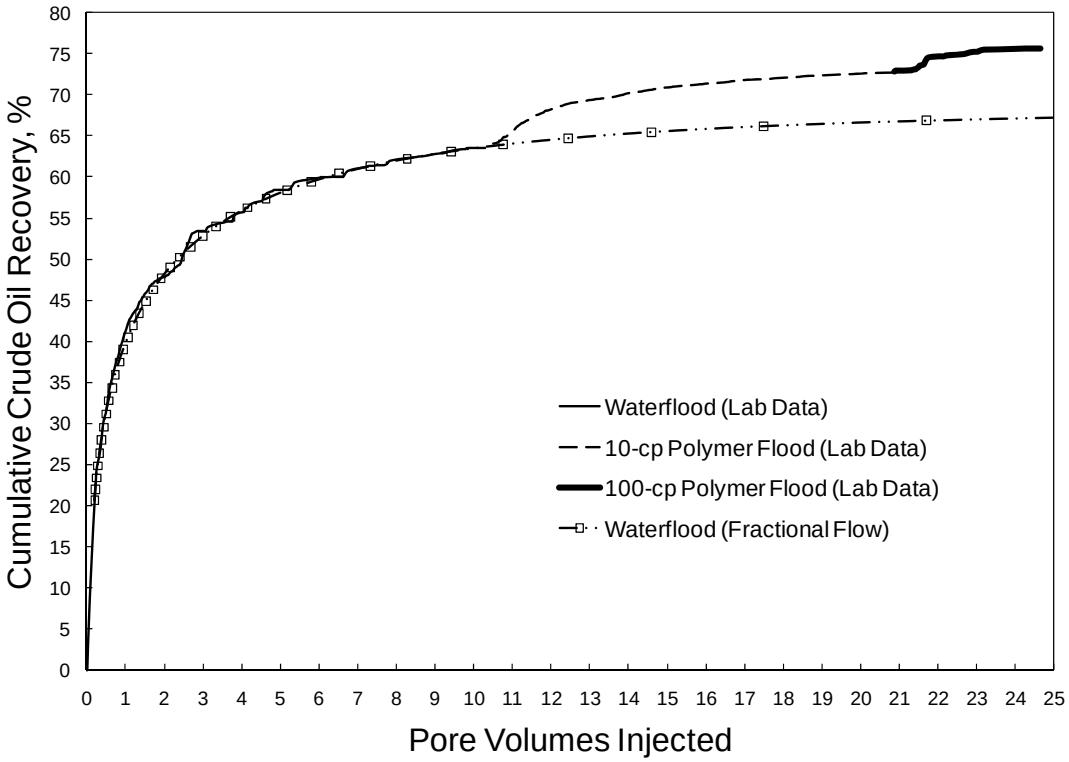

Fig. 47—Oil recovery during water and polymer injection in Core 1.

After injecting 11 PV of brine, 63.6% of the oil was recovered (thin solid curve up to 11 PV in Fig. 47). This experimental recovery curve was matched very well using fractional flow calculations with the following relative permeability characteristics:

$$k_{rw} = k_{rwo}\,[(S_w\text{-}S_{wr})/(1\text{-}S_{or}\text{-}S_{wr})]^{nw} = 0.055\,[(S_w - 0.012)/(1\text{-}0.31\text{-}0.012)]^{1.5} \quad \text{.....(8)}$$

$$k_{ro} = k_{roo}\,[(1\text{-}S_{or}\text{-}S_w)/(1\text{-}S_{or}\text{-}S_{wr})]^{no} = 0.8\,[(1 - 0.31 - S_w)/(1\text{-}0.31\text{-}0.012)]^{1.55} \quad \text{.....(9)}$$

This curve fit (dashed line with open squares in Fig. 47) reveals that the residual oil saturation (S_{or}) after waterflooding was 0.31. Subsequent injection of 10 PV of 10-cp HPAM solution (dashed curve without symbols in Fig. 47) increased the oil recovery level to 72.77% original oil in place (OOIP)—indicating that the S_{or} was reduced to 0.27 or less. The error bars on our measurements ($\pm$ 0.0026 PV) were such that 10-cp polymer injection definitively reduced S_{or}. The error bars were low primarily because of the large pore volume associated with our core (~370 cm^3).

The polyethylene cores were hydrophobic, so the observed reductions in S_{or} (by at least 4 saturation percentage points) were qualitatively consistent with other literature reports in oil-wet cores (Schneider and Owens 1982, Xia et al. 2004)

Polymer Injection as a Secondary Recovery Process

The previous experiments demonstrated that polymer flooding could reduce S_{or} after a hydrophobic core was waterflooded. Another set of experiments was performed in the second polyethylene core to assess how much polymer flooding reduces S_{or} when no waterflood was implemented before polymer injection. After saturating Core 2 with brine then oil, 10 PV brine was injected (bottom solid curve in Fig. 48), resulting in a recovery of 61.1% OOIP (compared with 63.6% OOIP seen during a similar waterflood in Core 1).

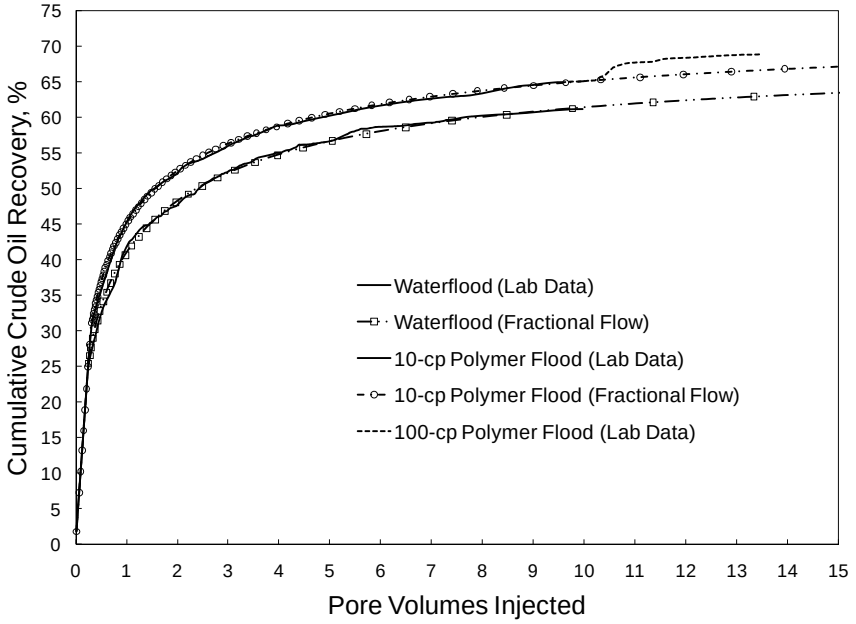

Fig. 48—Oil recovery during water and polymer injection in Core 2.

This experimental recovery curve was matched very well using fractional flow calculations with the following relative permeability characteristics:

$$k_{rw} = k_{rwo}\,[(S_w\text{-}S_{wr})/(1\text{-}S_{or}\text{-}S_{wr})]^{nw} = 0.05\,[(S_w - 0.011)/(1\text{-}0.32\text{-}0.011)]^{1.7} \quad \text{.....(10)}$$

$$k_{ro} = k_{roo}\,[(1\text{-}S_{or}\text{-}S_w)/(1\text{-}S_{or}\text{-}S_{wr})]^{no} = 0.8\,[(1 - 0.32 - S_w)/(1\text{-}0.32\text{-}0.011)]^{1.75} \quad \text{.....(11)}$$

This curve fit (open squares in Fig. 48) reveals that the residual oil saturation after waterflooding was 0.32. These relative permeability curves were quite similar to those associated with Core 1 (Eqs. 8 and 9).

After the waterflood, oil was injected to re-establish the connate water saturation. Next, 9.5 PV of 10-cp HPAM solution was injected (top solid curve in Fig. 48)—resulting in recovery of 64.9% OOIP. This experimental recovery curve was matched very well using fractional flow calculations with the following relative permeability characteristics:

$$k_{rw} = k_{rwo}\,[(S_w\text{-}S_{wr})/(1\text{-}S_{or}\text{-}S_{wr})]^{nw} = 0.35\,[(S_w - 0.011)/(1\text{-}0.26\text{-}0.011)]^{1.5} \quad \text{.....(12)}$$

$$k_{ro} = k_{roo}\,[(1\text{-}S_{or}\text{-}S_w)/(1\text{-}S_{or}\text{-}S_{wr})]^{no} = 1.0\,[(1 - 0.26 - S_w)/(1\text{-}0.26\text{-}0.011)]^{2.2} \quad \text{.....(13)}$$

This curve fit (open circles in Fig. 48) reveals that the residual oil saturation after waterflooding was 0.26. Thus, in a secondary recovery mode, the polymer flood reduced S_{or} by 6 saturation percentage points—compared with 4 saturation percentage points for polymer flooding after waterflooding. Comparison of Eqs. 8-13 reveals that the endpoint water and oil relative permeabilities were altered noticeable by the polymer flood. k_{rwo} was 0.35 for the polymer flood versus 0.05 for the waterflood. k_{roo} was 1.0 for the polymer flood versus 0.8 for the waterflood.

Just as during the floods in Core 1, a fixed pressure drop of 50 psi (19.7 psi/ft) was maintained. Again, the capillary number during these displacements was $1.77\text{x}10^{-5}$.

After the 10-cp polymer flood, 4 PV of 100-cp HPAM solution was injected (upper dashed curve in Fig. 48), increasing oil recovery to 68.8%.

Future studies will test whether these effects will be seen in water-wet porous media.

Conclusions

1. In a homogeneous hydrophobic porous polyethylene core at residual oil saturation (with a 190-cp North Slope crude after waterflooding), injection of a 10-cp HPAM solution (with a fixed capillary number of $1.77\text{x}10^{-5}$) reduced the residual oil saturation by at least four saturation percentage points (from 31% to less than 27%). Subsequent injection of 100-cp HPAM at the same capillary number appeared to reduce the residual oil saturation further.
2. In a second homogeneous hydrophobic porous polyethylene core at connate water saturation (i.e., highly saturated with a 190-cp North Slope crude), injection of a 10-cp HPAM solution (with a fixed capillary number of $1.77\text{x}10^{-5}$) reduced the residual oil saturation by six saturation percentage points compared to waterflooding (i.e., 26% versus 32%).

6. EFFECTS OF SALINITY AND DIVALENT CATIONS ON MECHANICAL DEGRADATION OF A NEW SULFONIC ASSOCIATIVE POLYMER

Following our previous studies of a new sulfonic associative polymer from SNF: Superpusher DP/C1205, Lot GC 2882/6 (hereafter called C1205, Seright 2010b), we examined the effects of salinity and divalent cations on mechanical degradation of C1205. Also, as in our second annual report (Seright 2010b), we contrasted those effects using a conventional HPAM: SNF Flopaam 3830S. Properties of these two polymers were described in our second annual report, and Table 4 compares these two polymers.

Table 4—Polymer properties.

Polymer	3830S	C1205
Molecular weight (M_w), million g/mol	18-20	12-17
Anionic content, mol %	35-40	15-25
Hydrophobe content, mol %	0	0.025-0.25

Polymer Solutions

The hydrophobic associative polymer (C1205) and conventional HPAM (3830S) were each dissolved in six brines: (1) 0.23% NaCl and 0.022% $NaHCO_3$, (2) 2.3% NaCl and 0.22% $NaHCO_3$, (3) 11.5% NaCl and 1.1% $NaHCO_3$, (4) 0.23% NaCl and 0.023% $CaCl_2$, (5) 2.3% NaCl and 0.23% $CaCl_2$, and (6) 11.5% NaCl and 1.15% $CaCl_2$. Twelve polymer solutions were prepared in total. When making each polymer solution, the polymer powder was carefully mixed with brine at room temperature using a magnetic stirrer at low stir rate until it was dissolved completely. All polymer solutions contained 1000-ppm polymer. Table 5 shows the ionic composition for each polymer solution.

Table 5—Polymer solution ionic compositions.

Sample No.	Ionic Composition	Polymer
1	0.23% NaCl + 0.022% $NaHCO_3$	1000-ppm C1205
2	0.23% NaCl + 0.022% $NaHCO_3$	1000-ppm 3830S
3	2.3% NaCl + 0.22% $NaHCO_3$	1000-ppm C1205
4	2.3% NaCl + 0.22% $NaHCO_3$	1000-ppm 3830S
5	11.5% NaCl + 1.1% $NaHCO_3$	1000-ppm C1205
6	11.5% NaCl + 1.1% $NaHCO_3$	1000-ppm 3830S
7	0.23% NaCl + 0.023% $CaCl_2$	1000-ppm C1205
8	0.23% NaCl + 0.023% $CaCl_2$	1000-ppm 3830S
9	2.3% NaCl + 0.23% $CaCl_2$	1000-ppm C1205
10	2.3% NaCl + 0.23% $CaCl_2$	1000-ppm 3830S
11	11.5% NaCl + 1.15% $CaCl_2$	1000-ppm C1205
12	11.5% NaCl + 1.15% $CaCl_2$	1000-ppm 3830S

Degradation Tests

Mechanical degradation was induced by forcing fresh polymer solutions (Table 5) through a polyethylene core plug using a wide range of flux rates (1 to 463 ft/d). The polyethylene core was 3.05 cm long with a porosity of 0.26, a pore volume of 4.1 cm^3, core cross-section of 5.06 cm^2, and an average permeability of 464 md. The core was saturated with the 2.52% TDS brine (2.3% NaCl, 0.22% $NaHCO_3$). Then, the core was flooded with 100 pore volumes (PV) of 2.52% TDS brine. Then 20 PV the polymer solution was injected to make sure that polymer retention in the core was satisfied. After saturating the core with this polymer solution, injection rates were varied over a wide range of flux rates (1 to 463 ft/d). For each polymer solution at each constant flux, one fluid sample was collected in a beaker at the outlet. The fluid samples were then used for viscosity and screen-factor measurements to determine the degree of mechanical degradation.

Viscosity Measurements

The viscosities of freshly prepared polymer solutions and effluent from the core at different flux rates were measured using an Anton PaarPhysica MCR 301 viscometer. During each measurement, shear rate changed from 0.01 to 1180 s^{-1}, and the effect of this change on solution viscosity was measured. The viscosity measured at 7.3 s^{-1} shear rate was used for common comparison. All measurements were made at 25°C. The percent loss of viscosity for each polymer effluent at each flux rate was calculated as the ratio of effluent viscosity to the initial viscosity of the polymer solution. The degree of mechanical degradation was quantified from the percent loss of viscosity.

Screen-Factor Measurements

Screen factor is defined as the ratio of the time required for a fixed volume of polymer solution to flow through a stack of five 100-mesh screens to the flow time required for the same volume of brine to pass through the screens. The screen factor device is simply two glass bulbs mounted into a glass tube. Therefore, screen factor is defined as below:

$$S_F = t_d / t_{ds} \quad (14)$$

Where, t_d is the flow time of the polymer solution, and t_{ds} is the flow time of the polymer-free brine.

Mechanical Degradation of the Associative Polymer (C1205)

Effect of Injection Rate. Fig. 49 describes effluent viscosities for 1,000-ppm C1205 solutions (in brine with 0.252% total dissolved solids, TDS) injected at various rates. As expected, the effluent viscosity decreased with increasing injection rate. The rheology of C1205 polymer solutions show conventional behavior: Newtonian behavior at low shear rates and shear thinning at intermediate shear rates and near-Newtonian behavior at very high shear rates. These observations were consistent with results reported by Bock et al. (1988) and Zaitoun et al. (2011). Bock et al. (1988) concluded that the viscosity of an associative polymer can show a complex response to shear rate, depending on concentration. For an acrylamide copolymer with 0.75 mol % N-octylacrylamide, as polymer concentrations increased above 3,000 ppm, regions of Newtonian behavior, shear thickening and shear thinning were observed as shear rate increased. This complex behavior was due to shifting the relative amounts of inter- and intra-molecular associations (Bock et al. 1988; Taylor et al. 1998). No shear thickening behavior was

observed with C1205 in our work—perhaps because we used only 1,000-ppm polymer or perhaps because C1205 contained significantly less hydrophobe than Bock's polymer (<0.25% versus 0.75%).

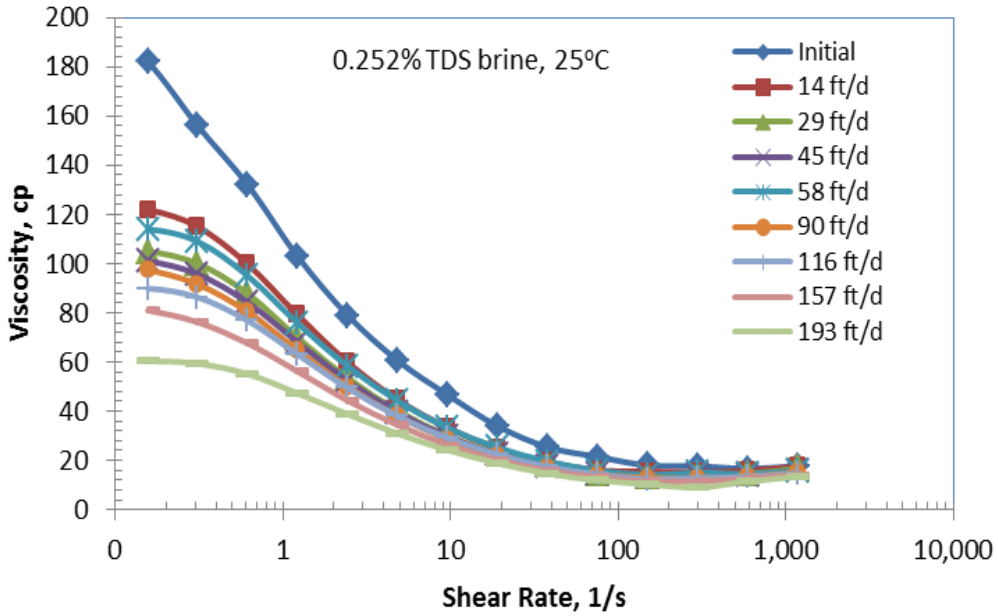

Fig. 49—Effluent viscosity versus shear rate and flux.
1,000-ppm C1205 in 0.23% NaCl, 0.022% $NaHCO_3$.

Effect of Salinity. Fig. 50 is a plot of effluent viscosity versus flux through the 464-md polyethylene core for 1,000-ppm C1205 polymer solutions with 0.252%, 2.52% and 12.6% total dissolved solids. As ionic strength increases, the dramatic initial viscosity drop indicates that C1205 shows sensitivity to brine salinity. For example, as ionic strength increased from 0.252% to 2.52% TDS, the initial solution viscosity dropped from 45.6 cp to 10.2 cp, which was a 77.6 percent loss. Previous work (Bock et al. 1988; McCormick et al. 1988; Taylor et al. 1998) concluded that the viscosity of associating polymers increased in the presence of salts, especially at higher polymer concentrations. However, the viscosity behavior of C1205 did not show the same trend, probably due to its low hydrophobic content and low polymer concentration.

Fig. 51 and Fig. 52 plot percent loss of viscosity and screen factor versus flux for C1205 polymer solutions. The percent loss of screen factor for C1205 increased with ionic strength. However, the percent loss of viscosity did not increase with salinity. The polymer solution with 0.252% TDS showed the most severe mechanical degradation, although its ending viscosity was 3-4 times higher than more saline solutions (see Fig. 50).

Our observations for C1205 contrast with those of Maerker et al. (1975) and Zaitoun et al. (2011) for HPAM solutions—that increasing ionic strength leads to more severe degradation of hydrolyzed polyacrylamides.

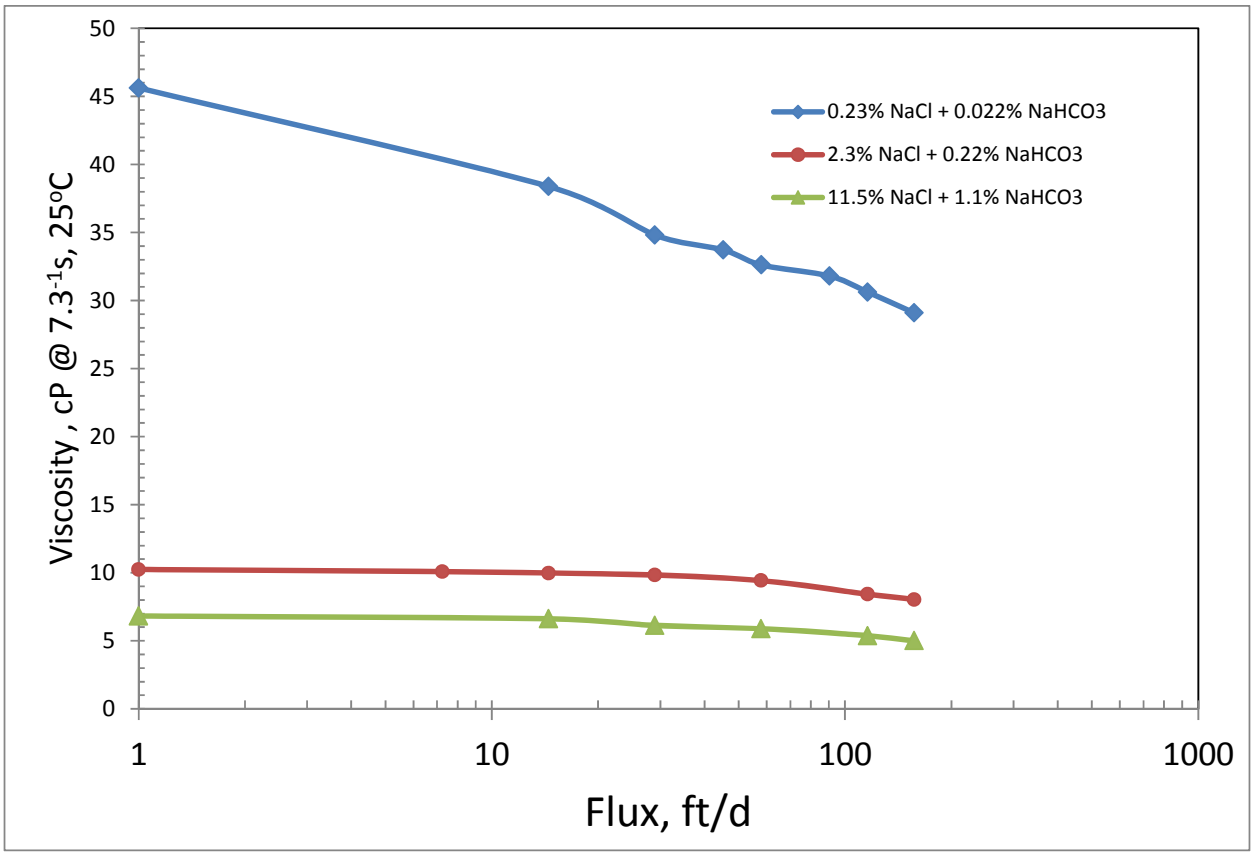

Fig. 50—Effluent viscosity versus flux and ionic strength. 1,000-ppm C1205.

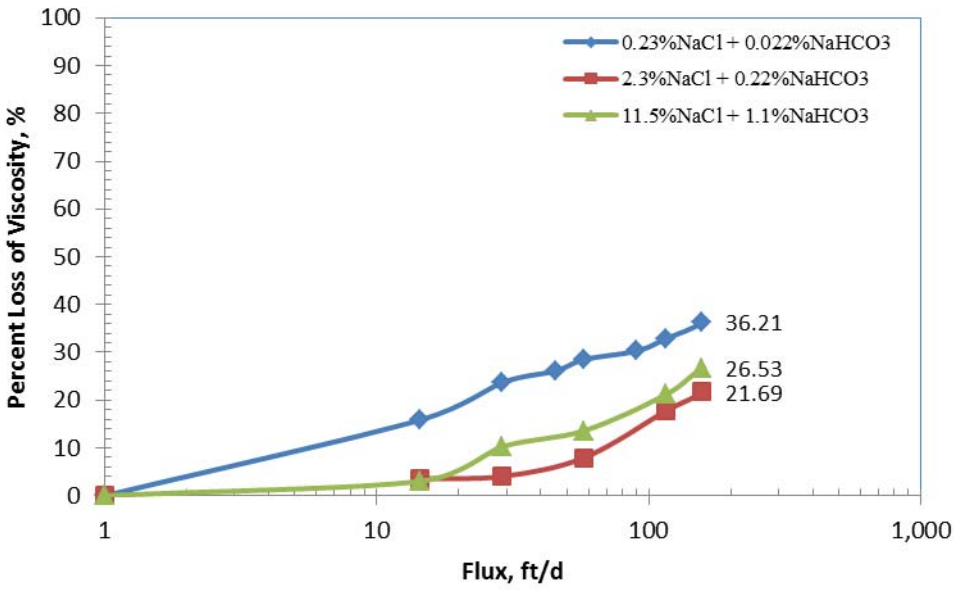

Fig. 51—Percent loss of viscosity versus flux. 1,000-ppm C1205.

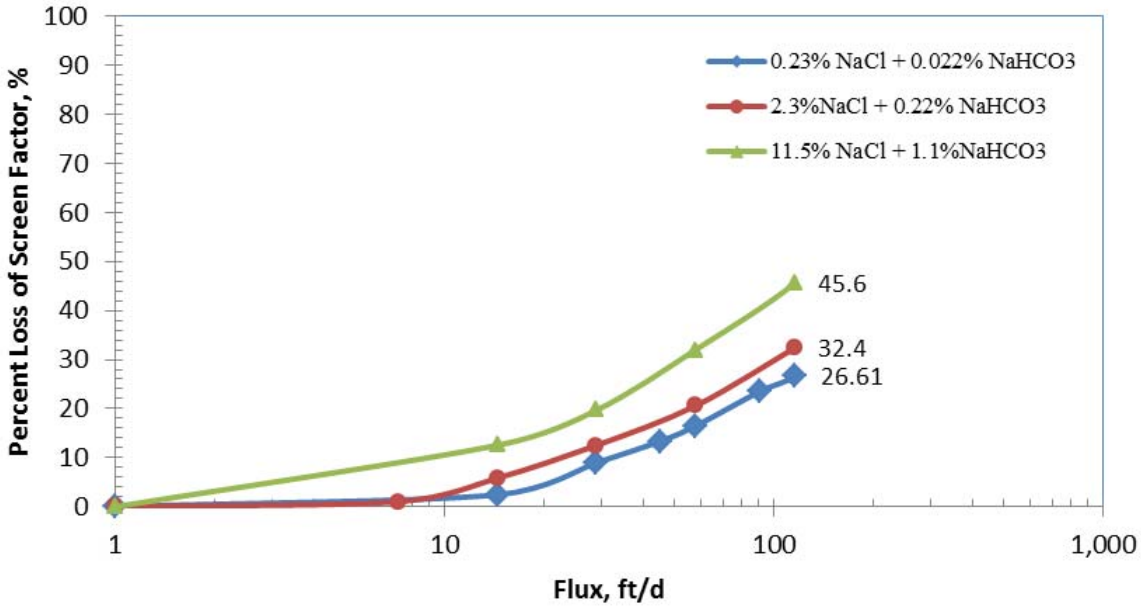

Fig. 52—Percent loss of screen factor versus flux. 1,000-ppm C1205.

Effect of Divalent Cations. Fig. 53 shows the effluent viscosity measured at 7.3 s^{-1}, 25°C, versus flux while injecting 1,000-ppm C1205 with 0.253%, 2.53% and 12.65% TDS through the 464-md polyethylene core, where the calcium chloride content was 1/10 the weight of sodium chloride. The associative polymer was more sensitive to calcium ions than sodium ions. The initial polymer solution viscosity with 0.23% NaCl and 0.022% $NaHCO_3$ was 45.6 cp, whereas, the initial viscosity of the solution with 0.23% NaCl and 0.023% $CaCl_2$ was 21.9 cp, which was a 52% viscosity loss for just a 0.001% TDS change. Also, as ionic content changed from 2.3% NaCl + 0.22% $NaHCO_3$ (2.52% TDS) to 2.3% NaCl + 0.23% $CaCl_2$ (2.53% TDS), the solution initial viscosity showed a 26% drop (from 10 cp to 7.4 cp). Therefore, the multivalent cations exert a stronger effect in reducing viscosities of associative polymer solutions.

Comparing the magnitudes of screen-factor and viscosity losses at constant flux for C1205 with similar ionic strength demonstrates that adding $CaCl_2$ leads to more severe mechanical degradation (Figs. 54 and 55). For example, at flux rate of 116 ft/d (192 cm^3/h), C1205 with 11.5% NaCl and 1.15% $CaCl_2$ showed 71.6% screen factor loss, whereas the C1205 with 11.5% NaCl and 1.1% $NaHCO_3$ experienced 45.6% screen factor loss.

The plot of percent loss of viscosity versus flux (Fig. 51) also demonstrated that mechanical degradation of C1205 polymer solutions does not always increase with ionic strength. This finding contrasts with some of previous reports for polyacrylamide based polymers (Maerker et al. 1975; Zaitoun et al. 2011). At low and moderate fluxes, C1205 solutions with the highest ionic content experienced the least degradation in the presence of Ca^{2+} (Figs. 54 and 55).

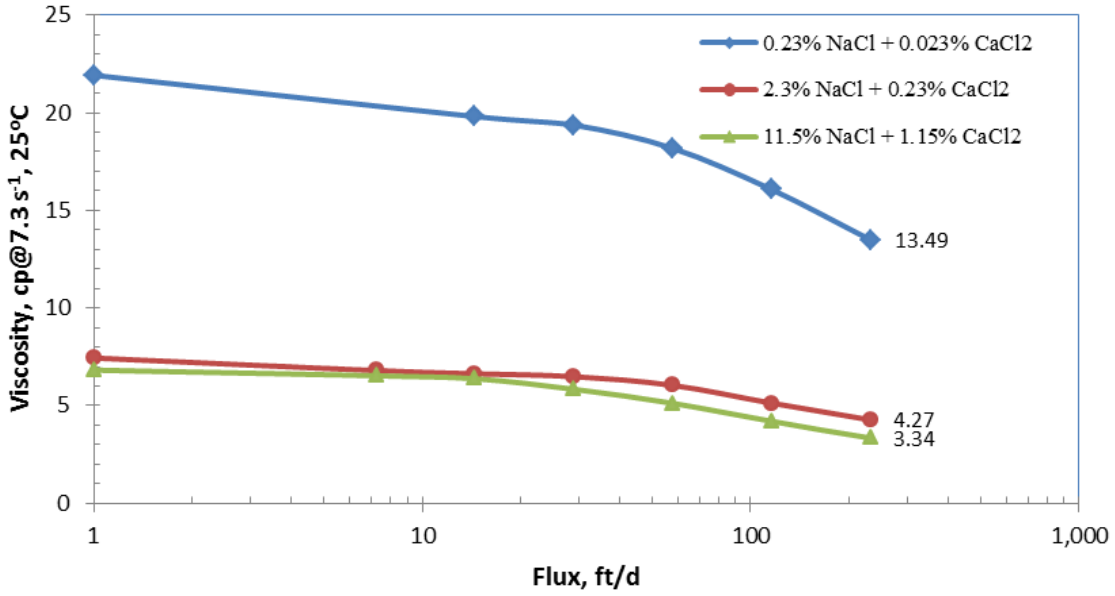

Fig. 53—Viscosity versus flux with Ca^{2+} present. 1,000-ppm C1205.

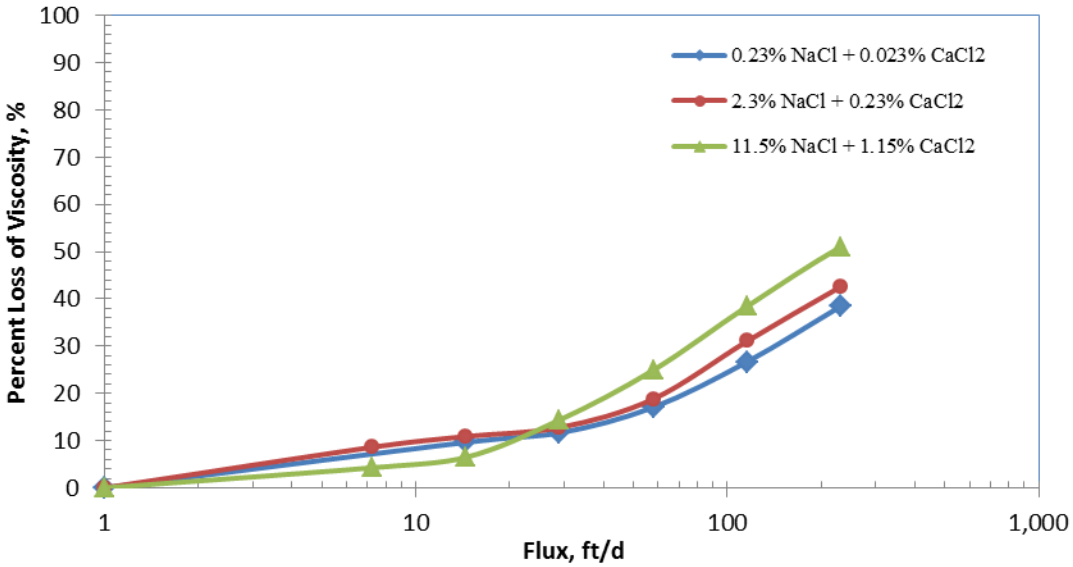

Fig. 54—Percent loss of viscosity versus flux with Ca^{2+} present. 1,000-ppm C1205.

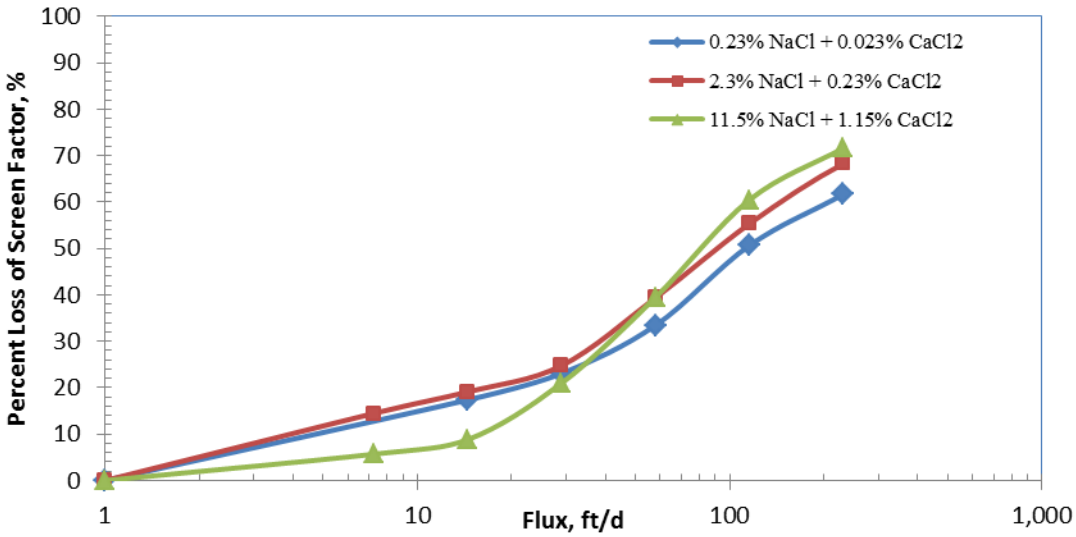

Fig. 55—Percent loss of screen factor versus flux with Ca^{2+} present. 1000-ppm C1205.

Comparison of C1205 and 3830S

Viscosity and Screen Factor. Comparisons were made of viscosity and screen factor for 1000-ppm C1205 and 3830S in 0.252 to 12.65% TDS brines, with or without calcium chloride (Figs. 56 to 62). The plots show that the associative polymer, C1205, consistently provided higher solution viscosities and screen factors than the conventional HPAM, 3830S. This finding is consistent with findings by Uhl et al. (1993).

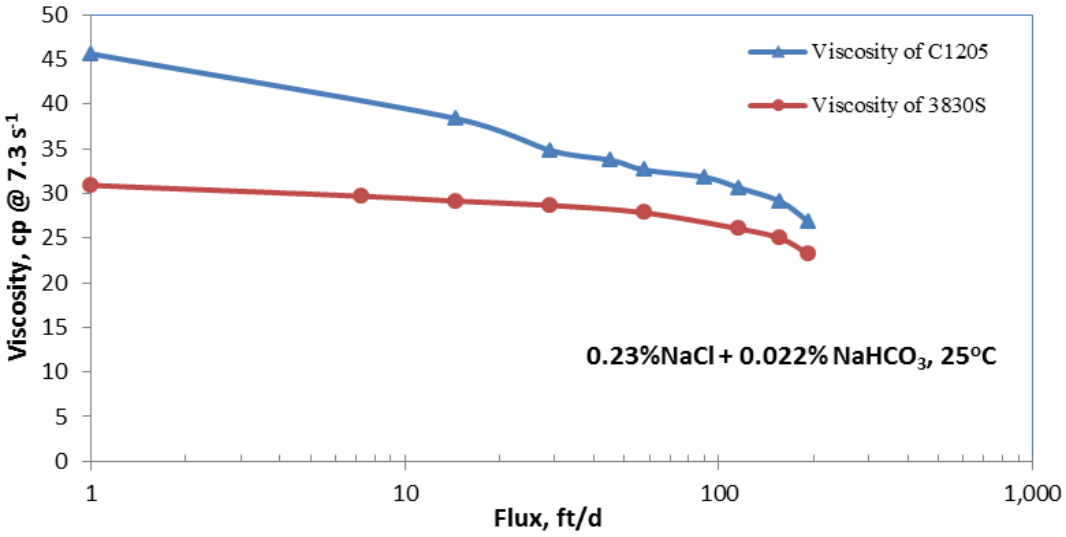

Fig. 56—Viscosity versus flux for 1,000-ppm C1205 and 3830S in 0.252% TDS brine.

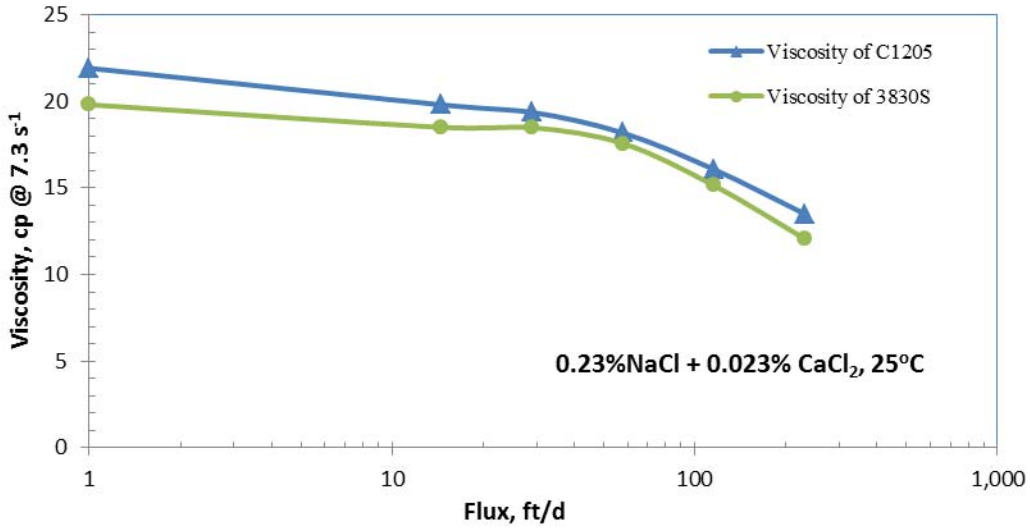

Fig. 57—Viscosity versus flux for 1,000-ppm C1205 and 3830S in 0.253% TDS brine.

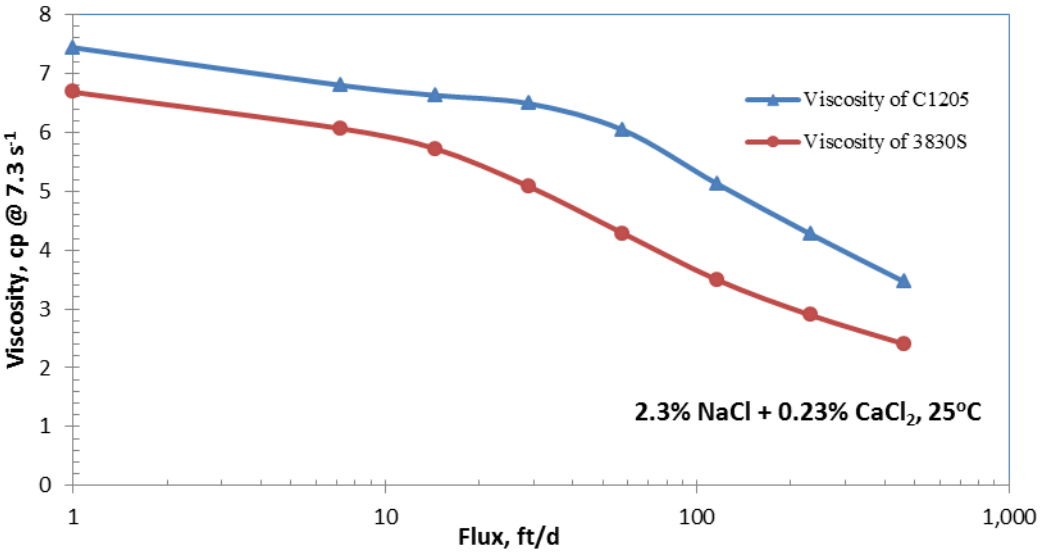

Fig. 58—Viscosity versus flux for 1,000-ppm C1205 and 3830S in 2.53% TDS brine.

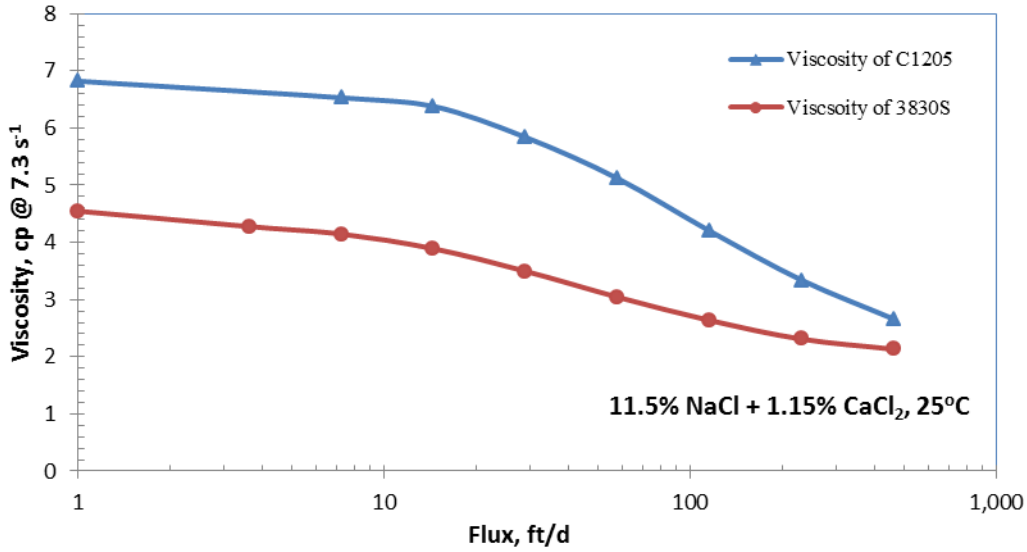

Fig. 59—Viscosity versus flux for 1,000-ppm C1205 and 3830S in 12.65% TDS brine.

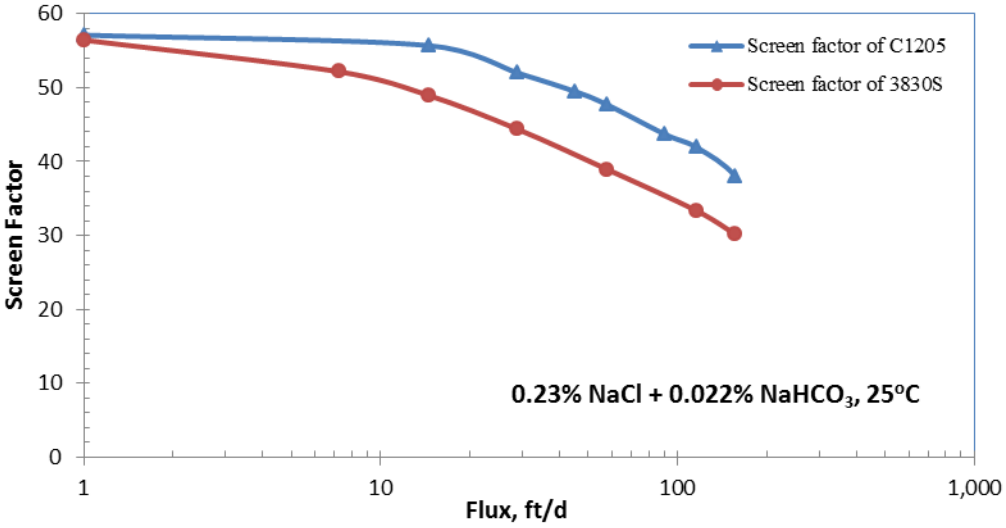

Fig. 60—Screen factor versus flux for 1,000-ppm C1205 and 3830S in 0.252% TDS brine.

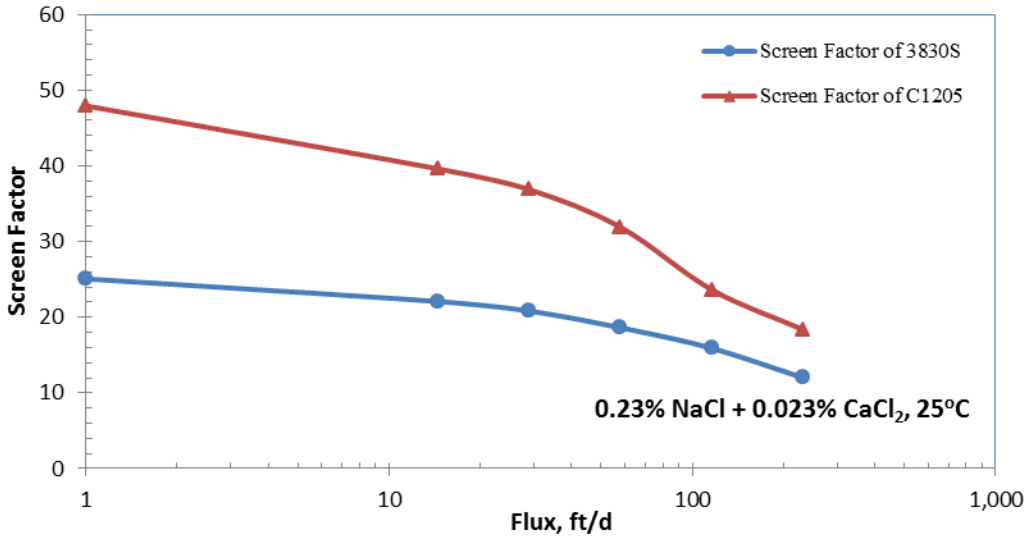

Fig. 61—Screen factor versus flux for 1,000-ppm C1205 and 3830S in 0.253% TDS brine.

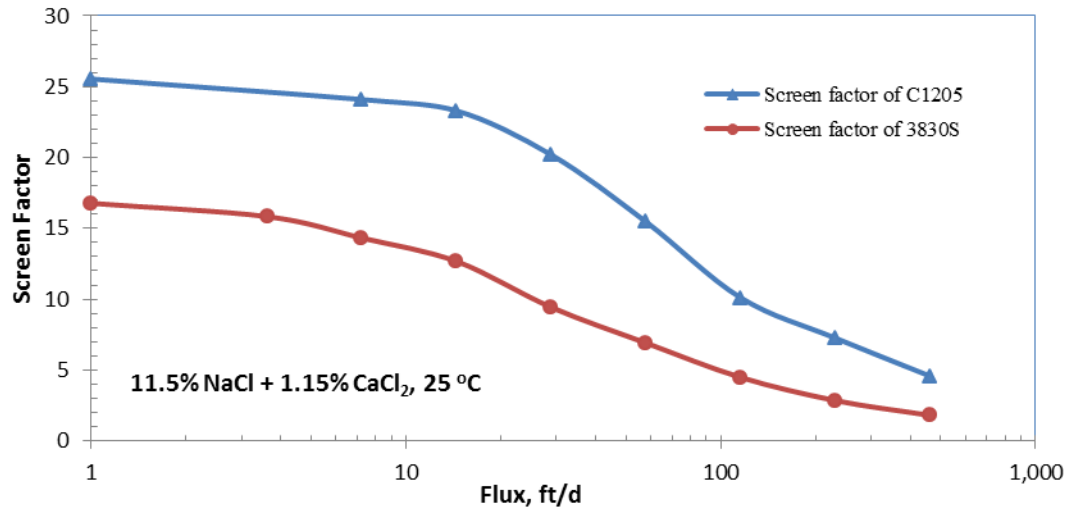

Fig. 62—Screen factor versus flux for 1,000-ppm C1205 and 3830S in 12.65% TDS brine.

Mechanical Stability. Several plots of percent loss of viscosity and screen factor versus flux (for 1,000-ppm C1205 and 3830S in 0.252% to 12.65% TDS brines) compare the mechanical stability of these two polymer solutions (Figs. 63 to 70). For the specific brines that we tested, C1205 generally exhibited better mechanical stability than 3830S—i.e., by providing lower percent loss of viscosity and screen factor (Figs. 64, 67, 68, 69, and 70). However, there were circumstances where 3830S showed better stability than C1205 (Figs. 63, 65, and 66). Although mechanical stability of the hydrophobic associative polyacrylamides was not always better than the conventional HPAM, C1205 always provided higher viscosity and screen factor. For example, in brine salinity of 0.252% TDS, C1205 polymer solution showed higher percent loss of viscosity than 3830S (Fig. 63). However, the viscosity of C1205 was much higher than that of 3830S. C1205 began with 45.6 cp and ended with 26.8 cp, whereas, 3830S began with 30.9 cp

and ended with 23.2 cp (Fig. 56). Similar results were found for polymer solutions in brines with 0.253% TDS and 12.65% TDS (Figs. 65, 66, 69, 70). Bock et al. (1988) examined 1,500-ppm terpolymers of acrylamide with the sulfonated monomer, AMPS, and N-octylacrylamide in brine with 3% NaCl and 0.3% $CaCl_2$. They concluded that the associating polymer had higher loss of viscosity than the conventional HPAM. Our results with C1205 and 3830S in 0.23% NaCl and 0.023% $CaCl_2$ were similar to those of Bock et al. (1988). However, their work did not examine polymer behavior in more saline brines. Even though the associative polymer may show more shear sensitivity than the conventional HPAM under some circumstances, the associative polymer (C1205) still provides higher viscosity and screen factor, and presumably, better mobility control, than the conventional HPAM (3830S) in porous media.

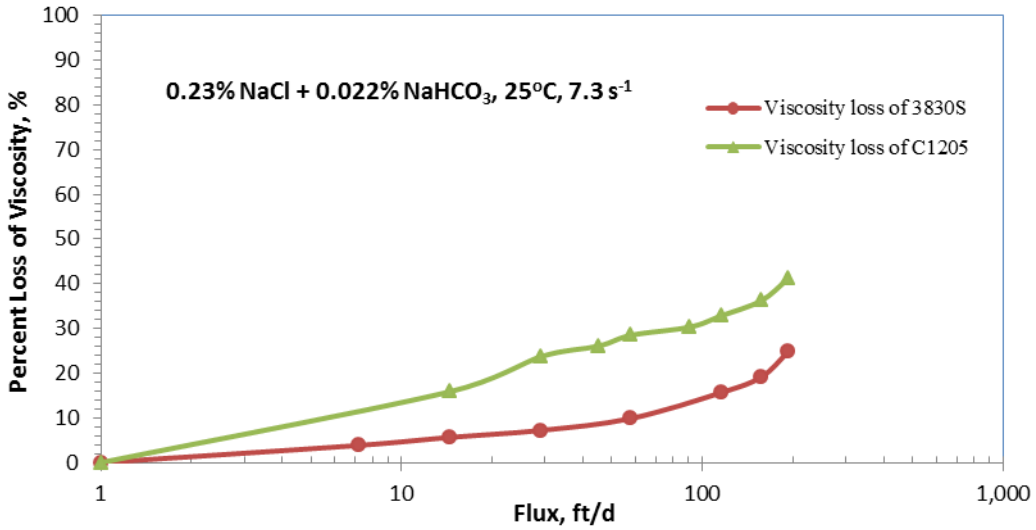

Fig. 63—Percent loss of viscosity versus flux in 0.252% TDS brine. 1,000-ppm C1205 and 3830S.

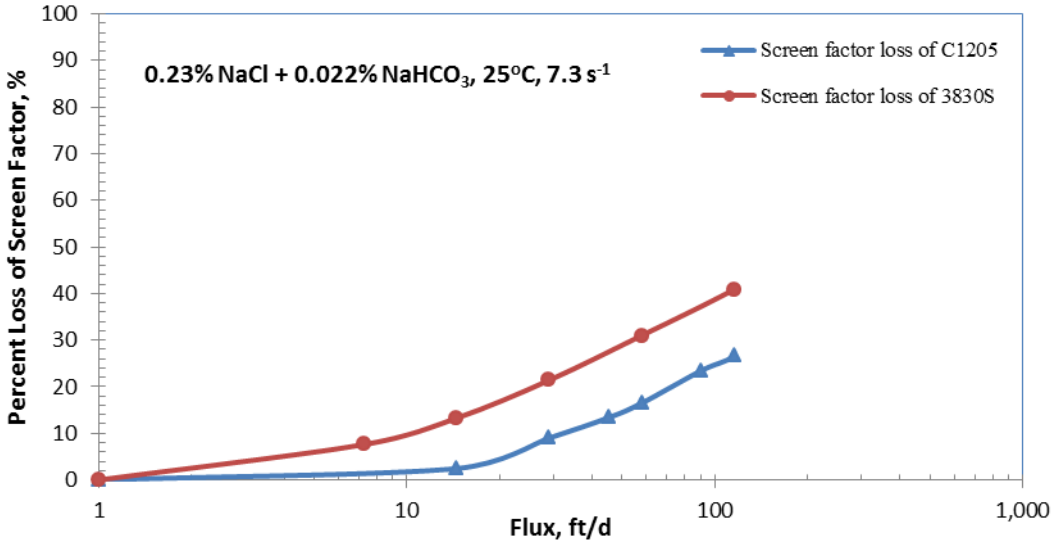

Fig. 64—Percent loss of screen factor versus flux in 0.252% TDS brine. 1,000-ppm C1205 and 3830S.

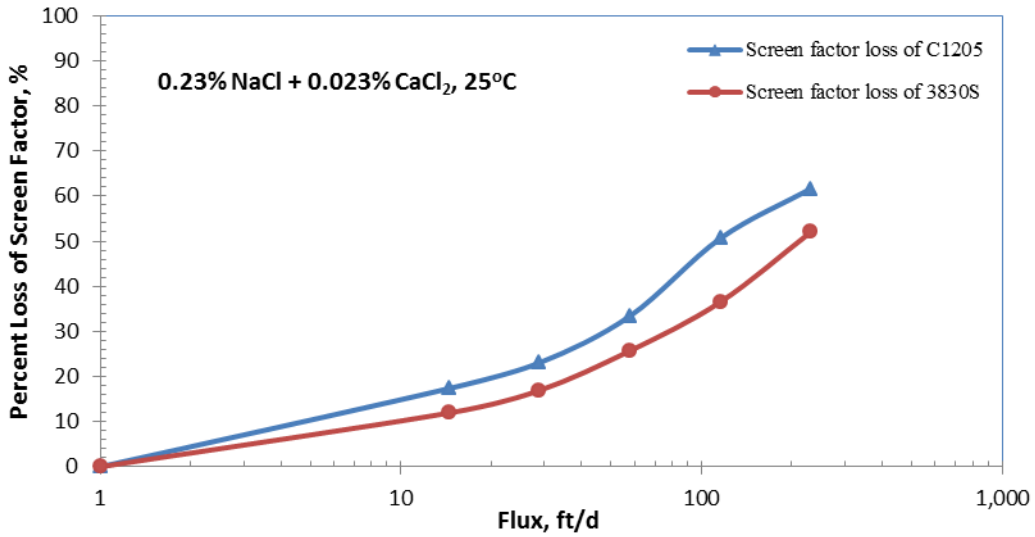

Fig. 65—Percent loss of screen factor versus flux in 0.253%TDS brine. 1,000-ppm C1205 and 3830S.

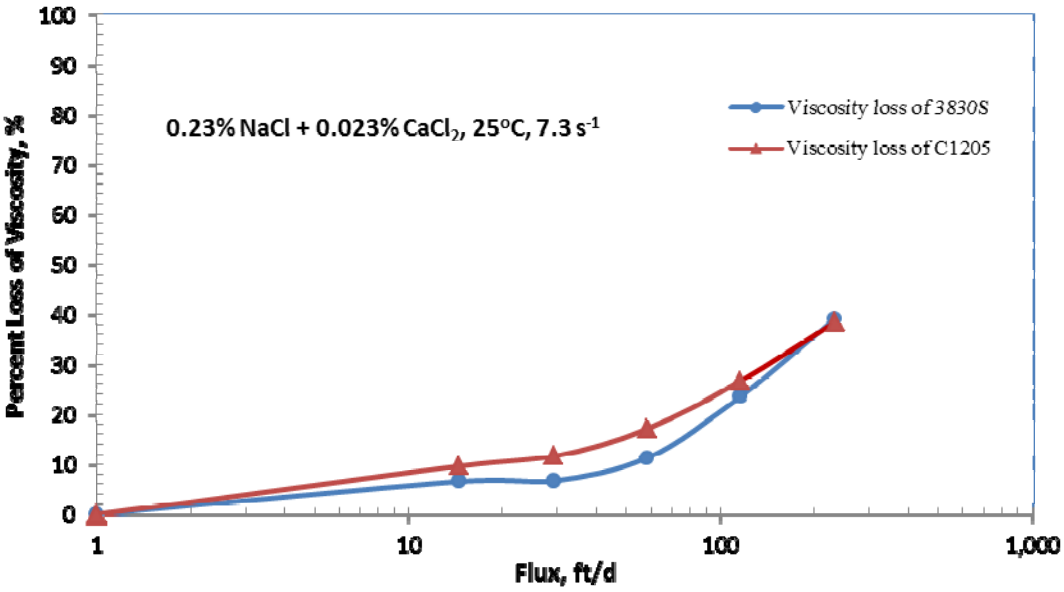

Fig. 66—Percent loss of viscosity versus flux in 0.253%TDS brine. 1,000-ppm C1205 and 3830S.

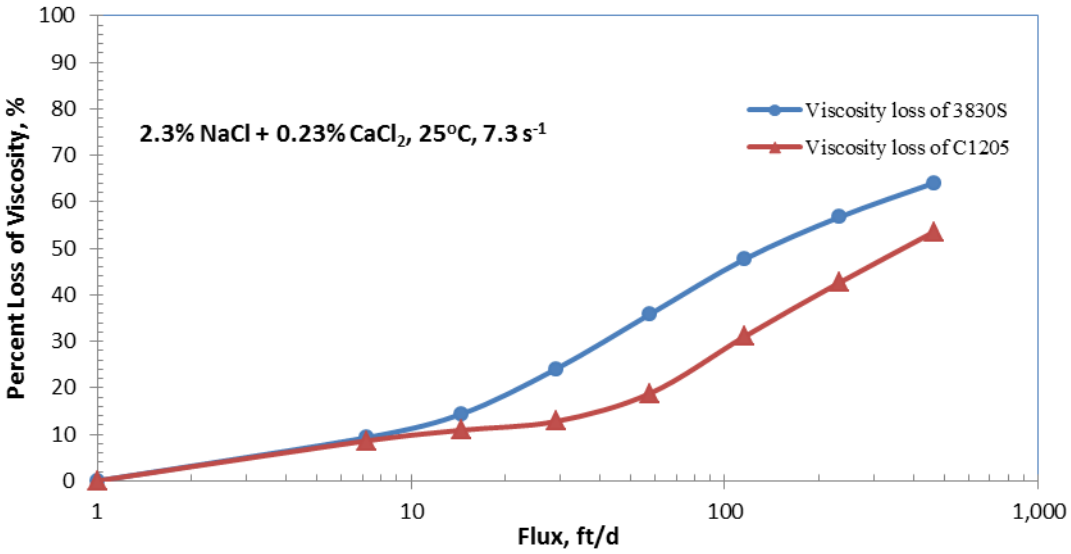

Fig. 67—Percent loss of viscosity versus flux in 2.53% TDS brine. 1,000-ppm C1205 and 3830S.

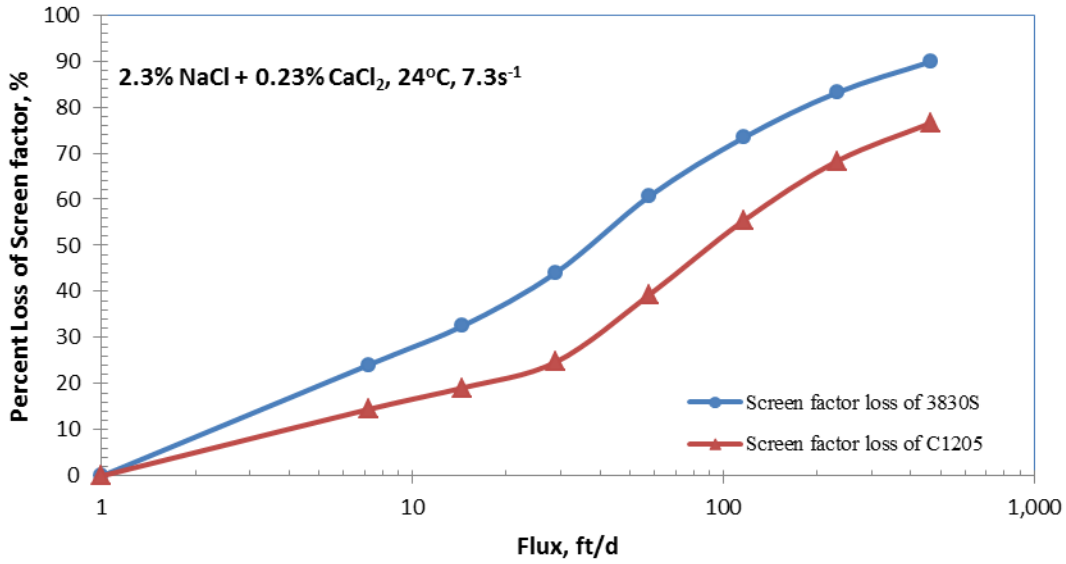

Fig. 68—Percent loss of screen factor versus flux in 2.53% TDS brine. 1,000-ppm C1205 and 3830S.

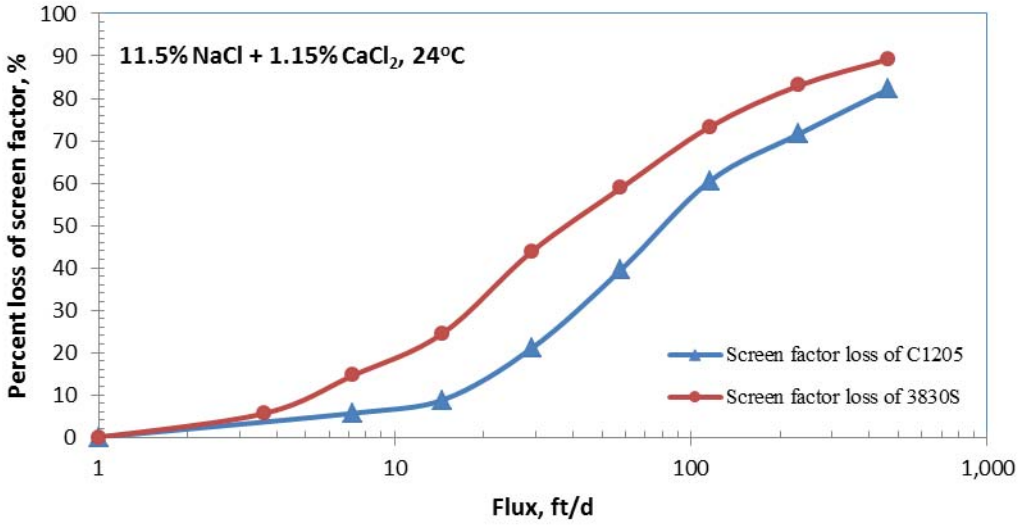

Fig. 69—Percent loss of screen factor versus flux in 12.65% TDS brine. 1,000-ppm C1205 and 3830S.

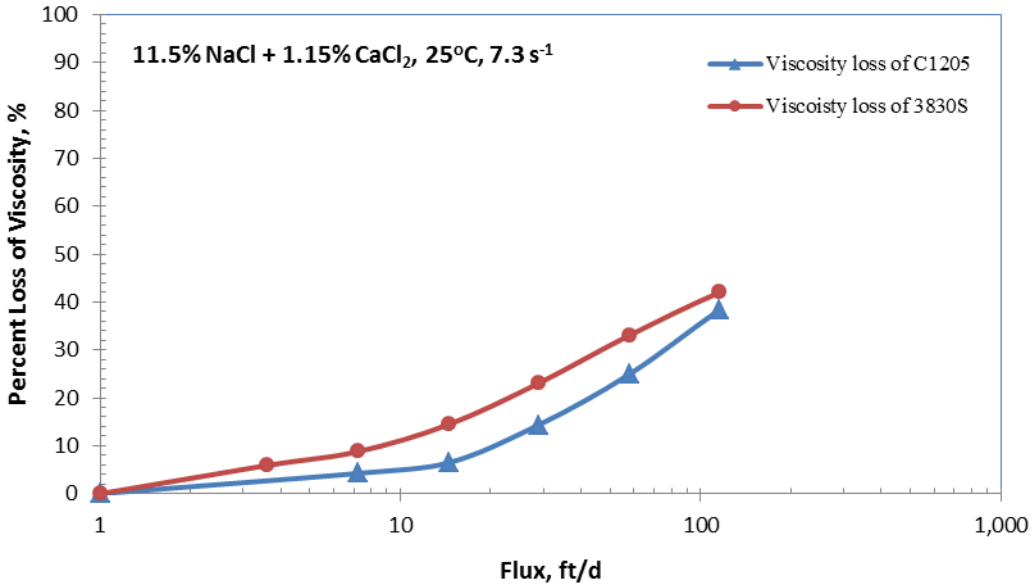

Fig. 70—Percent loss of viscosity versus flux in 12.65%TDS brine. 1,000-ppm C1205 and 3830S.

Conclusions

As expected, mechanical degradation of the associative polymer increased with velocity in porous media, and rheology of the associative polymer in the viscometer showed Newtonian behavior at low shear rates and shear thinning at higher shear rates. As with HPAM, calcium exerted a stronger influence than sodium in reducing solution viscosity. However, the degree of

mechanical degradation of associative polymer solutions does not always increase with ionic strength. This finding differs from previous reports for HPAM. When compared with the conventional HPAM, even though the associative polymer may show more shear sensitivity under some circumstances, it still provided higher viscosity and screen factor, and presumably, better mobility control, than the conventional HPAM.

NOMENCLATURE

c_{BW} = Bright Water material concentration, ppm
c_p = polymer concentration, ppm
E_v = formation sweep efficiency
F_r = resistance factor (water mobility/polymer solution mobility)
HPAM = partially hydrolyzed polyacrylamide
h = formation height, ft
h_1 = height of Layer 1, ft [m]
h_2 = height of Layer 2, ft [m]
k = permeability, darcys [μm^2]
k_1 = permeability of Layer 1, mD [μm^2]
k_2 = permeability of Layer 2, mD [μm^2]
k_{ro} = relative permeability to oil
k_{roo} = endpoint relative permeability to oil
k_{rw} = relative permeability to water
k_{rwo} = endpoint relative permeability to water
L = length of Bright Water bank in watered-out Layer, ft
L_{ws} = well spacing, ft
L_{T1} = the shortest distance water traverses through the oil bank, ft
L_{T2} = the farthest distance water traverses through the oil bank, ft
M = endpoint mobility ratio
Mw = molecular weight,
no = oil-saturation exponent
nw = water-saturation exponent
OOIP = original oil in place
PV = pore volumes of fluid injected
Δp = pressure difference, psi [Pa]
S_f = screen factor
S_{oi} = initial oil saturation
S_{or} = residual oil saturation
S_{orp} = residual oil saturation of polymer flood
S_{orw} = residual oil saturation of waterflood
S_w = water saturation
S_{wi} = initial water saturation
S_{wr} = residual-water saturation
TDS = total dissolved solids
V_p = pore volume of reservoir
t_d = flow time for polymer solution in a screen viscometer, s
t_{ds} = flow time for brine in a screen viscometer, s
u = flux, ft/d [m/d]
μ = viscosity, cp [mPa-s]
ϕ = porosity
ϕ_1 = porosity in Layer 1
ϕ_2 = porosity in Layer 2
μ = viscosity, cp [mPa-s]

μ_o = viscosity of oil, cp [mPa-s]
μ_p = viscosity of polymer, cp [mPa-s]
μ_w = viscosity of water, cp [mPa-s]

REFERENCES

Akanni, O.O. 2010. Analysis of In-Depth Profile Modification Reservoir Sweep Improvement and Comparison with Polymer Flooding for Improved Oil Recovery. MS thesis, New Mexico Institute of Mining and Technology, Socorro, New Mexico.

Argillier, J.F., Audibert, A., Lecourtier, J., Moan, M., and Rausseau, L. 1996. Solution and Adsorption Properties of Hydrophobically Associating Water-Soluble Polyacrylamides. *Colloids and Surfaces A: Physicochemical and Engineering Aspects* **113**, 247-257.

Bock, J., Valint, P.L., Pace, S.J., and Gardner, G. 1987. Enhanced Oil Recovery with Hydrophobic Associating Polymers Containing Sulfonate Functionality. USA Patent Number 4,702,319. 27 October.

Bock, J., Valint, P.L., Pace, S.J., Siano, D.B., Shulz, D.N., and Turner, S.R. 1988. Hydrophobically Associating Polymers. In *Water-Soluble Polymers for Petroleum Recovery*. Stahl, G.A. and Schulz, D.N., Eds. Plenum Press. NY. 147-160.

Buchgraber, M., Clements, T., Castanier, L.M., and Kovseck, A.R. 2009. The Displacement of Viscous Oil by Associative Polymer Solutions. Paper SPE 122400 presented at the SPE Annual Technical Conference and Exhibition, New Orleans, LA, 4-7 October.

Chang, H.., Sui, X., Guo, Z., et al. 2006. Successful Field Pilot of In-Depth Colloidal Dispersion Gel (CDG) Technology in Daqing Oil Field. *SPEREE* **9**(6)): 664-673.

Chang, K-T., Frampton, H., and Morgan, J.C. 2002. Composition and Method for Recovering Hydrocarbon Fluids from a Subterranean Reservoir. U.S. Patent No. 6,454,003 B1.

Choi, S.K., Sharma, M.M., Bryant, S.L., and Huh, C. 2010. pH-Sensitive Polymers for Novel Conformance-Control and Polymer-Flood Applications. *SPEREE* **13(**6): 926-939.

Coats, K.H., Dempsey, J.R., and Henderson, J.H. 1971. The Use of Vertical Equilibrium in Two-Dimensional Simulation of Three-Dimensional Reservoir Performance. *SPEJ*, **11**(1): 63–71.

Craig, F.F. 1971. *The Reservoir Engineering Aspects of Waterflooding*. Monograph Series, SPE, Richardson, Texas **3:** 45–75.

Dong, L. and Wang, B. 1995. Hydrophobically Associating Terpolymer and Its Complex with a Stabilizer in Brine for Enhanced Oil Recovery. Paper SPE 29007 presented at the International Symposium on Oilfield Chemistry, San Antonio, TX. 14-17 February.

Dupuis, G., Rousseau, D., Tabary, R., and Grassl, B. 2010. Flow of Hydrophobically Modified Water-Soluble Polymers in Porous Media: New Experimental Insights in the Dilute Regime. *SPE Journal Online* (March) 43-54. SPE 129884.

Eoff, L., Dalrymple, D., and Reddy, B.R. 2005. Development of Associative Polymer Technology for Acid Diversion in Sandstone and Carbonate Lithology. *SPEPF* (August) 250-256.

Evani, S. 1984. Water-Dispersible Hydrophobic Thickening Agent. USA Patent Number 4,432,881. 21 February.

Evani, S. 1989. Enhanced Oil Recovery Process Using a Hydrophobic Associative Composition Containing a Hydrophilic/Hydrophobic Polymer. USA Patent Number 4,814,096. 21 March.

Fletcher, A.,. Flew, S., Forsdyke, I., Morgan, J., Rogers, C., and Suttles, D. 1992. Deep Diverting Gels for Very Cost-Effective Waterflood Control. *J. Petr. Sci. Eng*. **7(**1-2**):** 33-43.

Frampton, H., Morgan, J.., Cheung, S.., and Chang, K. 2004. Development of a Novel Waterflood Conformance Control System. Paper SPE 89391 presented at the SPE/DOE Symposium on Improved Oil Recovery, Tulsa, OK, 17–21 April.

Gaillard, N. and Favero, C. 2010. High Molecular Weight Associative Amphoteric Polymers and Uses Thereof. USA Patent Number 7,700,702. 20 April.

Ghaddab, F., Kaddour, K., Tesconi, M., Brancolini, A., Carniani, C., and Galli, G. 2010. EI Borma-In-Depth Profile Modification: A Tertiary Method for Enhanced Oil Recovery for a Mature Field. Paper SPE 136140 presented at the SPE Production and Operations Conference and Exhibition, Tunis, Tunisia, 8–10 June.

Green, D.W., and Willite, G.P. 1998. *Enhanced Oil Recovery*. Textbook Series, SPE, Richardson, Texas **6**: 100–185.

Huh, C., and Pope, G.A. 2008. Residual Oil Saturation from Polymer Floods: Laboratory Measurements and Theoretical Interpretation. Paper SPE 113417 presented at the SPE/DOE Improved Oil Recovery Symposium, Tulsa, OK, 19–23 April.

Husband, M., Ohms, D., Frampton, H., et al. 2010. Results of a Three-Well Waterflood Sweep Improvement Trial in the Prudhoe Bay Field Using a Thermally Activated Particle System. Paper SPE 129967 presented at the SPE Improved Oil Recovery Symposium. Tulsa, OK, 24–28 April.

Khodaverdian, M., Sorop, T. Postif, S. and Van den Hoek, P. 2009. Polymer Flooding in Unconsolidated Sand Formations: Fracturing and Geomechnanical Considerations. Paper SPE 121840 presented at the SPE EUROPEC/EAGE Annual Conference and Exhibition, Amsterdam, The Netherlands, 8–11 June.

Kujawa, P., Audibert-Hayet, A., Selb, J., and Candau, F. 2004. Rheological Properties of Multisticker Associative Polyelectrolytes in Semidilute Aqueous Solutions. *J. of Polymer Science. Part B: Polymer Physics* **42**, 1640-1655.

Lake, L.W. 1989. *Enhanced Oil Recovery*. 268-273, 314–353, Englewood Cliffs, New Jersey: Prentice Hall, Inc.

Lu, H., Feng, Y., and Huang, Z. 2008. Association and Effective Hydrodynamic Thickness of Hydrophobically Associating Polyacrylamide through Porous Media. *J. of Applied Polymer Science* **110**, 1837-1843.

Maia, A.M.S., Borsali, R., and Balaban, R.C. 2009. Comparison between a Polyacrylamide and a Hydrophobically Modified Polyacrylamide Flood in a Sandstone Core. *Materials Science and Engineering C* **29**, 505-509.

Maerker, J.M. 1975. Shear Degradation of Partially Hydrolyzed Polyacrylamide solutions. SPE J.15(4): 311-322; Trans., AIME, 259. SPE-5101-PA. doi: 10.2118/5101-PA.

McCormick, C.L. and Johnson, C.B. 1988. Structurally Tailored Macromolecules for Mobility Control in Enhanced Oil Recovery. In *Water-Soluble Polymers for Petroleum Recovery*. Stahl, G.A. and Schulz, D.N., Eds. Plenum Press. NY. 161-180.

McCormick, C.L., Nonaka, T., Johnson, C.B., 1988. Water-Soluble Copolymers. 27. Synthesis and Aqueous Solution Behaviour of Associative Acrylamide/ n- alkylacrylamide copolymers. Polymer **29** (4), 731-739.

Needham, R.B., and Doe, P.H. 1987. Polymer Flooding Review. *JPT* **39** (12): 1503–1507.

Ohms, D., McLeod, J., Graff, C.J., et al. 2009. Incremental Oil Success from Waterflood Sweep Improvement in Alaska. Paper SPE 121761 presented at the SPE International Symposium on Oilfield Chemistry, The Woodlands, TX, 20–22 April.

Pope, G.A. 1979. The Application of Fractional Flow Theory to Enhanced Oil Recovery, SPE paper 7660, April 6.

Pritchett, J., Frampton, H., Brinkman, J., et al. 2003. Field Application of a New In-Depth Waterflood Conformance Improvement Tool. Paper SPE 84897 presented at the SPE International Improved Oil Recovery Conference, Kuala Lumpur, Malaysia, 20–21 October.

Pusch, G., Lotsch, T., and Muller, T. 1987. Investigation of the Oil Displacing Efficiency of Suitable Polymer Products in Porous Media, Aspects of Recovery Mechanisms During Polymer Flooding. DGMK-Report, 295-6. *German Soc. Petrol. Sci. Coal Chem*. Hamburg, Germany.

Seright, R.S. 1988 Placement of Gels to Modify Injection Profiles. Paper SPE/DOE 17332 presented at the 1988 SPE/DOE Enhanced Oil Recovery Symposium, Tulsa, OK, 17-20 April.

Seright, R.S, Liang J., Lindquist, W.B., and Dunsmuir, J.H. 2002: "Characterizing Disproportionate Permeability Reduction Using Synchrotron X-Ray Computed Microtomography," *SPE Reservoir Evaluation & Engineering*, **5**(5), (Oct. 2002) 355-364.

Seright, R.S., Lane, R.H., and Sydansk, R.D. 2003. A Strategy for Attacking Excess Water Production. *SPEPF* **18** (3): 158–169.

Seright, R.S., Prodanovic, M., and Lindquist, W.B. 2006: "X-Ray Computed Microtomography Studies of Fluid Partitioning in Drainage and Imbibition Before and After Gel Placement: Disproportionate Permeability Reduction," *SPE Journal* (June) 159-170.

Seright, R.S., Seheult, J.M., and Talashek, T.A. 2009. Injectivity Characteristics of EOR Polymers. *SPE Reservoir Evaluation and Engineering* **12** (5): 783–792.

Seright, R.S. 2009. Use of Polymers to Recover Viscous Oil from Unconventional Reservoirs. First Annual Report. Contract No.: DE-NT0006555, US DOE, Washington DC (October 2009). http://baervan.nmt.edu/randy/.

Seright, R.S. 2010a. Potential for Polymer Flooding Reservoirs with Viscous Oils., *SPE Reservoir Evaluation and Engineering* **13**(4), August, 730-740.

Seright, R.S.2010b.Use of Polymers to Recover Viscous Oil from Unconventional Reservoirs. Second Annual Report, U.S. Department of Energy, DOE Contract No.: DE-NT0006555, US DOE, Washington, DC, October 2010.

Seright, R.S. 2010c. http://baervan.nmt.edu/randy/.

Seright, R.S., Fan, T., Wavrik, K., and Balaban, R.C. 2011. New Insights into Polymer Rheology in Porous Media. *SPE Journal* (March) 35-42. SPE 129200.

Seyidov, M. and Lane, R.H. 2010. Deep Placement Gel Bank as an Improved Oil Recovery: Modeling, Economic Analysis and Comparison to Polymer Flooding. Paper SPE 133414 presented at the SPE Western North America Regional Meeting, Anaheim, CA 26–30 May.

Schneider, F.N., and Owens, W.W. 1982. Steady State Measurements of Relative Permeability for Polymer/Oil Systems. *SPE Journal* (Feb. 1982) 79-86.

Sorbie, K.S. 1991. *Polymer-Improved Oil Recovery*. 115. Glasgow, Scotland: Blackie and Son, Ltd.

Sorbie, K.S. and Seright, R.S. 1992. Gel Placement in Heterogeneous Systems with Crossflow. Paper SPE 24192 presented at the SPE/DOE Symposium on Enhanced Oil Recovery, Tulsa, OK, 22–24 April.

Stryker, A.R., Watkins, R., Olsen, D.K., et al. 1995. Feasibility Study of Heavy Oil Recovery in the United States. Final Report, Contract No. DE-AC2294PC91008, US DOE, Washington, DC (September 1995).

Sydansk, R.D., and Romero-Zeron, L. 2011. *Reservoir Conformance Improvement*. Society of Petroleum Engineers, Richardson, TX.

Taber, J.J. 1969. Dynamic and Static Forces Required to Remove Discontinuous Oil Phase from Porous Media Containing Both Oil and Water. *SPE Journal* (March 1969) 3-12.

Taylor, K.C. and Nasr-El-Din, H.A. 1998. Water-Soluble Hydrophobically Associating Polymers for Oil Recovery: A Literature Review. *Petroleum Sci & Engineering* **19**. 265-280.

Taylor, K.C. and Nasr-El-Din, H.A. 2007. Hydrophobically Associating Polymers for Oil Field Applications. CIMMP Paper 2007-016 presented at the Canadian International Petroleum Conference, Calgary, Alberta, 12-14 June.

Thomas, C.P., Faulder, D.D., Doughty, T.C., Hite, D.M., and White, G.J. 2007. Alaska North Slope Oil and Gas, a Promising Future or an Area in Decline? Summary Report DOE/NETL-2007/1279, US DOE, Washington, DC (August 2007)

Trantham, J.C., Threlkeld, C.B., and Patterson, H.L. 1980. Reservoir Description for a Surfactant/Polymer Pilot in a Fractured, Oil-Wet Reservoir—North Burbank Unit Tract 97. *JPT* **32** (9): 1647–1656.

Uhl, J.T., Ching, T. Y., Bae, J.H., 1993. A Laboratory Study of New, Surfactant-Containing Polymers for High-Salinity Reservoirs. SPE 26400, Proc. 68th Ann. Tech. Conf. and Exhib. Of Soc. Pet. Eng., Houston, TX, USA.

Van den Hoek, P.J., Al-Masfry, R., Zwarts, D., Jansen, J.D., Hustedt, B., and van Schijndel, L. 2009. Optimizing Recovery for Waterflooding under Dynamic Induced Fracturing Conditions. *SPEREE* **12** (5): 671–682.

Volpert, E., Selb, J., Candau, F., Green, N, Argillier, J.F., and Audibert, A. 1998. Adsorption of Hydrophobically Associating Polyacrylamides on Clay. *Langmuir* **14**, 1870-1879.

Wang, D., Huifen, X., Zhongchun, L., Qingyan, Y., Chen. F. 2000. Visco-Elastic Polymer Can Increase Microscale Displacement Efficiency in Cores. Paper SPE 63227 presented at the 2000 SPE Annual Technical Conference and Exhibition, Dallas, TX. 1–4 October.

Wang, D., Huifen, X., Zhongchun, L., and Qingyan, Y. 2001a. Study of the Mechanism of Polymer Solution with Visco-Elastic Behavior Increasing Microscopic Oil Displacement Efficiency and the Forming of Steady "Oil Thread" Flow Channels. Paper SPE 68723 presented at the 2001 SPE Asia Pacific Oil and Gas Conference and Exhibition, Jakarta, Indonesia. 17–19 April.

Wang, D., Cheng, J., and Xia, H. 2001b. Viscous-Elastic Fluids Can Mobilize Oil Remaining after Water-Flood by Force Parallel to the Oil-Water Interface. Paper SPE 72123 presented at the 2001 SPE Asia Pacific Improved Oil Recovery Conference, Kuala Lumpur, Malaysia. 8-9 October.

Wang, D.M., Han, P., Shao, Z., Weihong, H., and Seright, R.S. 2008a. Sweep Improvement Options for the Daqing Oil Field. *SPEREE* **11** (1):18–26. doi: 10.2118/9944-PA.

Wang, D.M., Seright, R.S., Shao, Z., and Wang, J. 2008b. Key Aspects of Project Design for Polymer Flooding at the Daqing Oil Field. *SPEREE* (December) 1117-1124.

Wang, D., Wang, G., Xia, H., Yang, S., Wu, W. 2011. Incremental Recoveries in the Field of Large Scale High Viscous-Elastic Fluid Flooding are Double that of Conventional Polymer Flooding. Paper SPE 146473 presented at the SPE Annual Technical Conference and Exhibition, Denver, CO. 30 Oct.–2 Nov.

Willhite, G.P. and Seright, R.S. eds., 2011. *Polymer Flooding*, Society of Petroleum Engineers, Richardson, TX.

Wreath, D.G. 1989. A Study of Polymer Flooding and Residual Oil Saturation, MS Thesis, University of Texas at Austin.

Wu, W., Wang, D., and Jiang, H. 2007. Effect of the Visco-Elasiticity of Displacing Fluids on the Relationship of Capillary Number and Displacement Efficiency in Weak Oil-Wet Cores. Paper SPE 109228 presented at the SPE Asia Pacific Oil and Gas Conference and Exhibition, Jakarta, Indonesia, 30 October–1 November.

Xia, H., Wang, D., Wu, J., and Kong, F. 2004. Elasticity of HPAM Solutions Increases Displacement Efficiency under Mixed Wettability Conditions. Paper SPE 88456 presented at the 2004 Asia Pacific Oil and Gas Conference and Exhibition. Perth, Australia. 18-20 October.

Yanez, P.A.P., Mustoni, J.L., Relling, M.F., Chang, K.T., Hopkinson, P., and Frampton, H. 2007. New Attempt in Improving Sweep Efficiency at the Mature Koleul Kaike and Piedra Clavada Waterflooding Projects in the S. Jorge Basin in Argentina. Paper SPE 107923 presented at the SPE Latin American and Carribbean Petroleum Engineering Conference, Buenos Aires, Argentina, 15–18 April.

Zaitoun, A., Makakou, P., Blin, B., Al-Maamari, R.S., Abdel-Goad, M., Al-Sharji, H.H. 2011. Shear Stability of EOR Polymers. SPE 141113. Proc. Int. Symp. Oilfield Chem., Woodlands, TX.

Zapata, V.J. and Lake, L.W. 1981. A Theoretical Analysis of Viscous Crossflow. Paper SPE 10111 presented at the SPE Annual Technical Conference and Exhibition, San Antonio, TX, 5–7 October.

Zhang, G. 2010. Comparison of In-Depth Profile Modification and Polymer to Recover Viscous Oils. PRRC Report 10-05. December 2010.

Zhao, H., Zhao, P, Bai, B., Xiao, L., and Liu, X. 2006. Using Associated Polymer Gels to Control Conformance for High Temperature and High Salinity Reservoirs. *J. Canadian Petroleum Technology* **45**(5) 49-54.

Zitha, P.L.J., Chauveteau, G., and Leger, L. 2001. Unsteady-State Flow of Flexible Polymers in Porous Media. *J. Colloid and Interface Science* **234**, 269-283.

APPENDIX A

Analytical Examination of Bright Water (by Guoyin Zhang)

Summary

In this report, fractional flow calculations were used to analyze the potential of Bright Water and polymer flooding to recover viscous oils where conventional methods (e.g., thermal recovery) may not be applicable. For the application of Bright Water, the calculations show that oil viscosity and reservoir heterogeneity strongly affect the selection of the Bright Water process. A small bank of Bright Water is preferred when dealing with less viscous oils. For more viscous oils, it is more cost-effective to choose a larger bank. This observation is more evident with increase in permeability contrast (k_1/k_2). The effect of reservoir heterogeneity (k_1/k_2) and formation height ratio (h_1/h_2) were examined followed by a simple benefit comparison between Bright Water and polymer flooding. The results indicate the following: (1) For slightly or moderately heterogeneous reservoirs ($k_1/k_2 \leq 10$), polymer flooding with a proper ($M<0.5$) mobility ratio has much more potential than most Bright Water treatments. (2) With an increase of permeability contrast (k_1/k_2), the potential of Bright Water treatments becomes evident. (3) When severe heterogeneity ($k_1/k_2 \geq 50$) is present, Bright Water with a large bank shows more potential than polymer flooding with a mobility ratio > 0.1. (4) Both Bright Water and polymer flooding benefit from a decrease in formation height ratio (h_1/h_2). This benefit is slightly greater for Bright Water than polymer flooding. Our study also recognizes that, for viscous oil displacement, a Bright Water bank in the watered-out layer (Layer 1) determines the main oil target, and the formation shape factor (L/h) affects the reservoir sweep efficiency (E_v) for the subsequent waterflood.

Introduction

The previous study recognized that polymer flooding has great potential to recover viscous oils from the North Slope of Alaska, where thermal methods may not be applied because the target formations are relatively close to permafrost (Seright 2010). The performance of polymer flooding when dealing with such cases as one homogenous layer, two layers without crossflow and with crossflow has been discussed extensively. In this research, a two-layer reservoir was considered with the watered-out layer (Layer 1) initially at residual oil saturation (S_{or}) and the oil bearing layer (Layer 2) at residual water saturation (S_{wr}). Free crossflow occurs between the two layers. Both polymer flooding and Bright Water were examined for this case and a simple benefit analysis was performed to assess the potential of both processes to recover viscous oils.

Bright Water

The concept of Bright Water was developed by a joint research project conducted by several companies (BP, Chevron, Texaco, and Nalco) (Frampton et al. 2004). Bright Water consists of certain polymeric "kernel" particles which are capable of "popping" under the influence of temperature and time. The expanded particles can block the pore throats of the thief zone (high-permeability layer) and then provide resistance to fluid flow in porous media. Therefore, Bright Water is usually considered as a water-blocking process to improve the sweep efficiency of a waterflood. The process usually uses very high concentrations of polymers and surfactants which are added to aid the dispersion of those polymer particles, resulting in a cost typically several times higher than for conventional polymer flooding. Table A-1 shows the formulation of Bright

Water used in a field project where 10,000-ppm polymer together with 4,500-ppm surfactant were injected (Ghaddab, et al. 2010).

Table A-1- Real data from a Bright Water pilot project		
Water injection rate (m^3/h)	15	
Polymer injection (liters/min)	2.4	
Polymer concentration (%)	1	10,000 ppm
Dispersant injection (lt/min)	1.09	
Dispersant concentration (%)	0.45	4,500 ppm
Initial wellhead pressure (bar)	49	

Table A-2-Default parameters						
Bright Water		Polymer			Reservoir	
c_{BW}, (ppm)	Price, ($/lb)	c_p, (ppm)	μ_p, (cp)	Price, ($/lb)	Layer 1	Layer 2
10,000	1.5	900	10	1.5	V_p=500 bbl	V_p=500 bbl
	7.5	3,000	100		$S_{oi}=S_{or}$=0.12	S_{oi}=0.88
		5,000	200		S_{wi}=0.88	$S_{wi}=S_{wr}$=0.12
		10,000	1,000		k_1=1 Darcy	k_2=0.1 Darcy
					ϕ_1=0.3	ϕ_2=0.3
					h_1=10 ft	h_2=10 ft
Water treatment and injection cost, ($/bbl)=0.25						
Note: 1. Two costs of Bright Water are considered. 2. Permeability contrast (k_1/k_2) of 10 and formation height ratio (h_1/h_2) of 1 are mostly used in the calculations. It will be specified when other values are used. 3. Relation between viscosity and polymer concentration derives from 19 million Mw HPAM (Seright 2010).						

Assumptions

Fractional flow analysis (Pope 1979, Zapata and Lake 1981; Green and Willhite 1998) was applied to both Bright Water and polymer flooding to deal with the problem specified in Fig. A-1. Assumptions were that the oil-bearing layer (Layer 2) was at residual water saturation (S_{wr}) and free crossflow occurs between the two layers.

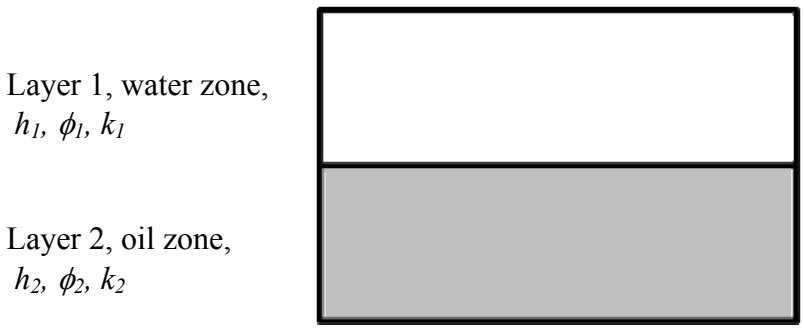

Fig. A-1—Two-layer system.

Only viscous forces are considered and other assumptions are:

1. Gravitational effects are negligible. Capillary pressure effects are negligible, except for their influence on the relative permeability curves.
2. Polymer rheology is Newtonian, and all fluids are incompressible.
3. Polymer retention balances inaccessible pore volume.
4. The residual oil saturation for polymer flooding is the same as that for waterflood.
5. Only linear flow (fractured well or horizontal well) was considered.
6. The Bright Water bank is instantaneously placed at the proper location with no dispersion.
7. After placement, permeability within the Bright Water bank is permanently reduced to zero.

The relative permeability characteristics of Alaska's North Slope reservoirs were given by Eqs. 1 and 2.

$$k_{rw}=k_{rwo}[(S_w-S_{wr})/(1-S_{or}-S_{wr})]^{nw}, \quad \text{.....(A-1)}$$

$$k_{ro}=k_{roo}[(1-S_{or}-S_w)/(1-S_{or}-S_{wr})]^{no}, \quad \text{.....(A-2)}$$

where, k_{rwo}=0.1, k_{roo}=1, S_{or}=0.12, S_{wr}=0.12, nw=4, no=2.5.

Most of the figures plot oil recovery on the y-axis for a given cost of water, polymer or Bright Water that was injected. In this paper, all oil recovery was expressed in terms of mobile oil recovered (percentage). Mobile oil saturation is given by $(1-S_{wr}-S_{or})$. Since Layer 1 is at residual oil saturation, our calculation assumes no oil is displaced from Layer 1 and all produced oil originates from Layer 2. For cases of Bright Water application, 100%, 60%, or 20% Bright Water indicates the percentage of the watered-out zone (Layer 1) covered by Bright Water. Other default parameters are shown in Table A-2. Notice that the total pore volume of our model is 1,000 bbls and mobile oil saturation is $1-S_{wr}-S_{or}$=0.76, which means the total mobile oil is 500*0.76=380 bbls. Based on different oil prices, the total value of the mobile oil may be 7,600, 19,000, and 30,400 USD at the oil price of 20, 50, and 80 USD per barrel, respectively.

Parameters Affecting Performance of Bright Water

Before we start the calculation, two significant parameters which affect the effectiveness of Bright Water should be discussed. The first one is the size of the Bright Water bank formed in the watered-out zone. Basically, after the establishment of the Bright Water bank in this zone, the oil bank underlying the Bright Water bank (shown in Fig. A-2 as Part 2) is the main target for further waterflooding. When water injection is initialized, water will first enter Layer 1 and then will be forced to traverse through the oil bank in Layer 2 underneath the Bright Water bank,

displacing oil from this area. Most of the oil in Parts 1 and 3 (Fig. A-2) is bypassed and does not contribute much to the oil recovery during waterflood. This statement is true especially when the oil viscosity is relatively high and the reservoir is severely heterogeneous (this will be discussed in the following section). Therefore, the oil recovery depends directly on the size of the Part-2 oil bank in Layer 2, or the size of Bright Water bank formed in Layer 1.

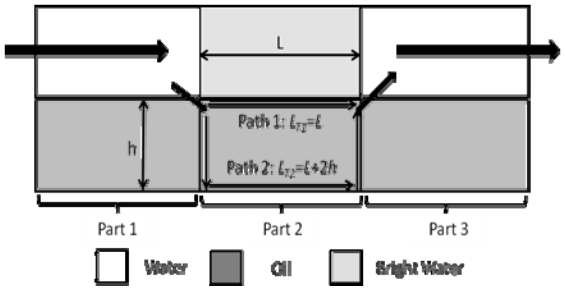

Fig. A-2—Schematic of fluid flow of Bright Water

Table A-3-Assumptions for sweep efficiency of Bright Water							
L, ft	h, ft	L/h	$L_{T1}=L$, ft	$L_{T2}=L+2h$, ft	L_{T1}/L_{T2}	E_v, %	Assumption
100	10	10	100	120	0.8333	100	$L/h\geq10$ or $L_{T1}/L_{T2}\geq0.8333$, E_v=100%
100	1000	0.1	100	2100	0.0476	5	$L/h\leq10$ or $L_{T1}/L_{T2}\leq0.0467$, E_v=5

E_v = formation sweep efficiency

Table A-4-Sweep efficiency of Bright Water under various conditions.							
BW, %	L, ft	h, ft	L/h	$L_{T1}=L$, ft	$L_{T2}=L+2h$, ft	L_{T1}/L_{T2}	E_v, %
20	100	20	5	100	140	0.71429	87
		40	2.5		180	0.55556	68
		60	1.667		220	0.45455	56
		80	1.25		260	0.38462	47
		100	1		300	0.33333	41
60	300	20	15	300	340	0.88235	100
		40	7.5		380	0.78947	96
		60	5		420	0.71429	87
		80	3.75		460	0.65217	80
		100	3		500	0.60000	73
		100	4		600	0.66667	81
100	500	20	25	500	540	0.92593	100
		40	12.5		580	0.86207	100
		60	8.333		620	0.80645	98
		80	6.25		660	0.75758	92
		100	5		700	0.71429	87
L_{ws}, ft		500					

The other factor is the formation sweep efficiency (E_v) achieved in the Part-2 oil bank. When water traverses through this area, as shown in Fig. A-2, the shortest distance (Path 1) and the farthest distance (Path 2) covered by the injected water is L and $L+2h$ where L and h are the length of Bright Water bank and thickness of Layer 2, respectively. When length is much greater than height, the ratio of $L/(L+2h)$ is close to one, and Path 1 and Path 2 will be almost the same as for a waterflood. Therefore, very high sweep efficiency could be achieved. Otherwise, when L/h is small, poor sweep efficiency could result. E_v might be almost 100% when $L/h \geq 10$ (or $L/(L+2h) \geq 0.8333$) and Ev=5% when $L/h \leq 10$ (or $L/(L+2h) \leq 0.0476$), see Table A-3. Taking a linear relation between the sweep efficiency (E_v) and the ratio of $L/(L+2h)$, any sweep efficiency could be calculated given the formation shape factor (L/h). Length (L) can be calculated from the product of Bright Water bank size (in percentage) and well spacing (L_{ws}), see Table A-4. For example, a 20% Bright Water bank in Layer 1 corresponds to 100-ft (0.2*500 ft=100 ft) target oil bank in Layer 2, and the sweep efficiency (E_v) is about 87% if the formation height of Layer 2 is 20 feet. While, if the formation height is 100 ft, the sweep efficiency will decline from 87% to 41%. Note in Table A-3 that a given shape factor (L/h) always results in the same sweep efficiency.

Based on the above analysis, the performance of Bright Water is affected by both the size of the Bright Water bank in Layer 1 (which determines the main oil target) and the formation shape factor (L/h) (which determines the reservoir sweep efficiency).

In our calculations, we optimistically assume 100% reservoir sweep efficiency for Bright Water applications. We also assume all the Bright Water remains in the watered-out zone with no spillage into the low-permeability zone and the permeability of the area covered by Bright Water is zero. Of course, these assumptions may be overly optimistic for Bright Water.

Results: Performance of Bright Water

Fractional flow calculations (http://baervan.nmt.edu/randy/home.html) were applied to examine the potential of Bright Water to recover viscous oils. First, Fig. A-3 considers reservoirs with 1-cp water displacing 1,000-cp viscous oil. Three cases were considered. Case A: Two layers (k_1/k_2=10, h_1/h_2=1) with crossflow, no Bright Water; Case B: Two layers (k_1/k_2=10, h_1/h_2=1) with crossflow, 40% Bright Water in Layer 1; and Case C: One homogeneous layer. Fig. A-3 indicates that at a cost of $2,000 (arbitrarily chosen), for Case A, oil recovery is only about 4% (of the total mobile oil volume). For Case B, where 40% Bright Water was applied, the oil recovery is about 32%, which is 8 times higher than for Case A. In contrast, for Case C (one homogeneous layer), oil recovery is 62% at the same cost (see the dashed line in Fig. A-3). The existence of a Bright Water bank in the high-permeability layer improves the performance of waterflood by blocking the watered-out zone and improving sweep in the two-layer reservoir.

Selection of Bright Water Bank Size

The performance of Bright Water to improve a waterflood was discussed above. Next, the proper bank size of Bright Water in the watered-out zone needs to be established, because this relates closely to the cost of Bright Water process. To address this issue for different oil viscosities, we calculated the oil recovery from the oil layer underneath the Bright Water bank, relative to the total oil recovery. The results are provided in Fig. A-4 at 1 pore volume water injection. Some ideas are demonstrated here. When displacing low viscosity oil (see the 1-cp oil curve), if 20% Bright Water is used, the percentage of oil recovery is only about 20%. In other words, Bright Water process should not be needed if oil viscosity is 1 cp. In contrast, for 10-, 100- and 1,000-cp oils, the corresponding percentages rise dramatically with the increase of the oil viscosity. For

instance, with a 20% Bright Water bank, this percentage for 1,000-cp oil goes up to 82%, i.e., only 18% oil is displaced from areas other than that underneath Bright Water bank. The same phenomenon is observed for other Bright Water bank sizes. In short, Bright Water seems to be more effective when dealing with viscous oils and larger banks show more potential than smaller banks.

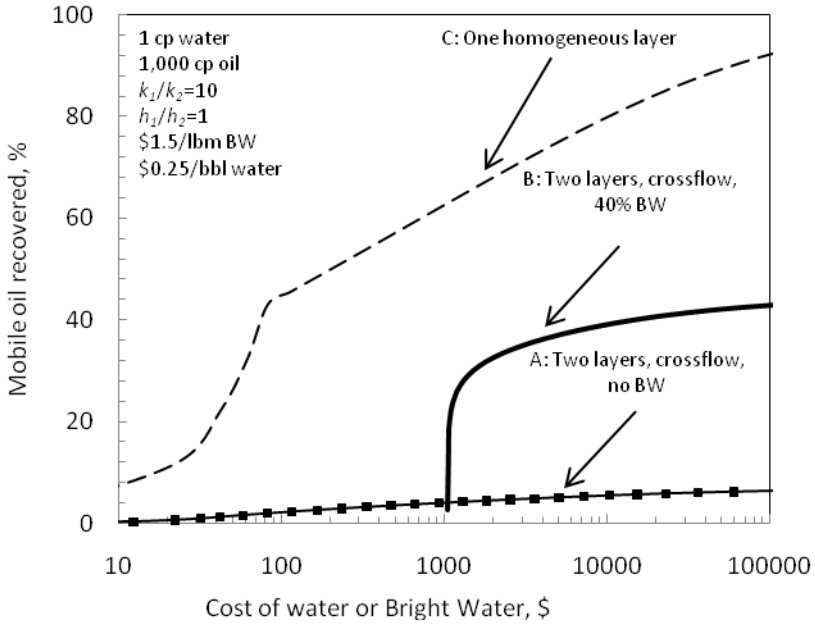

Fig. A-3—1-cp water displacing 1,000-cp oil for different cases.

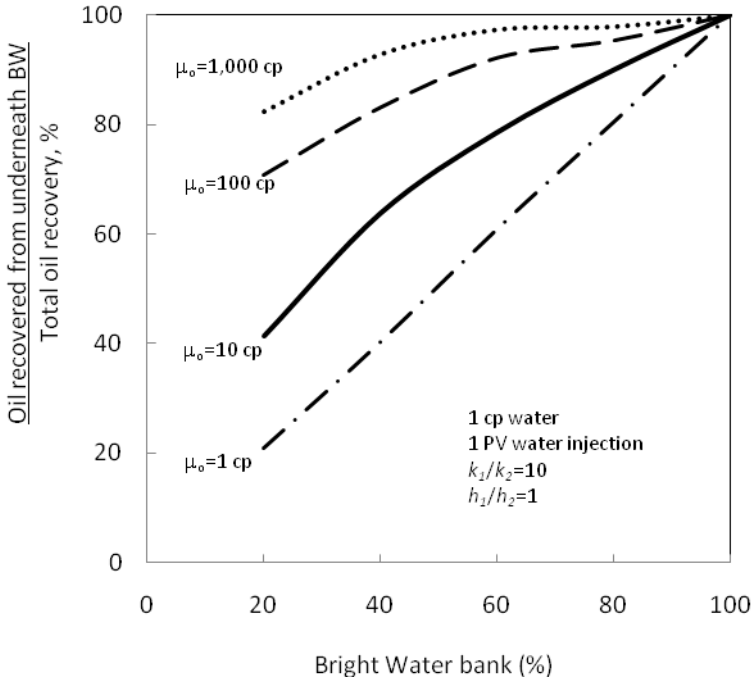

Fig. A-4—Effect of oil viscosity and BW size on recovery from oil bank underneath BW bank.

This observation was further analyzed and confirmed from Figs. A-5, A-6, and A-7. Only oil viscosity changes in these figures and all the other conditions are the same (such as k_1/k_2=2, h_1/h_2=1). For each curve, 20%, 60%, and 100% Bright Water banks were considered. When displacing 10-cp oil (as shown in Fig. A-5), at the cost of about $600, 20% Bright Water is able to achieve over 80% oil recovery. By contrast, the same oil recovery can cost about $2,000 and $3,000 for 60% and 100% Bright Water, respectively. Therefore, a smaller bank of Bright Water shows more economical benefit than a larger bank when displacing low viscosity oils. Actually, when oil viscosity is as low as 10 cp (for k_1/k_2=2), 1-cp water is the best option (see the solid squares in Fig. A-5). When oil viscosity increases to 100 cp (see Fig. A-6), for oil recovery below 70% (see the recovery at the intersection point of 20% and 60% Bright Water), a small bank of Bright Water (20% BW) shows more potential. If oil recovery between 70% and 80% is pursued, 60% Bright Water is better than 20% and 100% Bright Water. For oil recovery over 80%, 100% Bright Water begins to show more potential. If the oil viscosity is 1,000 cp, see Fig. A-7, the benefit of 100% Bright Water is more pronounced (see the oil recovery gap between 100% and 60% Bright Water) if over 52% (recovery at the intersection point of 60% and 100% Bright Water) oil needs to be recovered. Therefore, oil viscosity plays a significant role in the selection of the size of the Bright Water bank. The higher the oil viscosity, the larger the Bright Water bank required (assuming cost of the Bright Water bank is not considered).

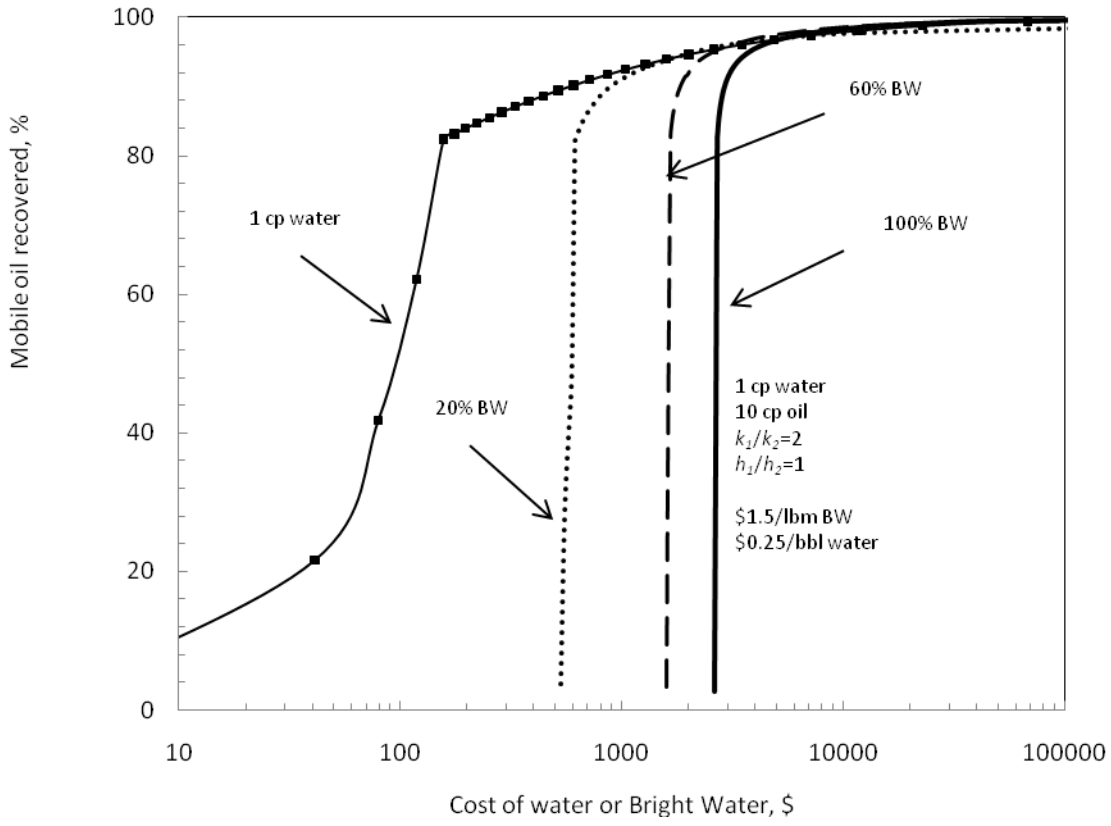

Fig. A-5—Effect of oil viscosity on the selection of Bright Water bank. 10-cp oil, k_1/k_2=2.

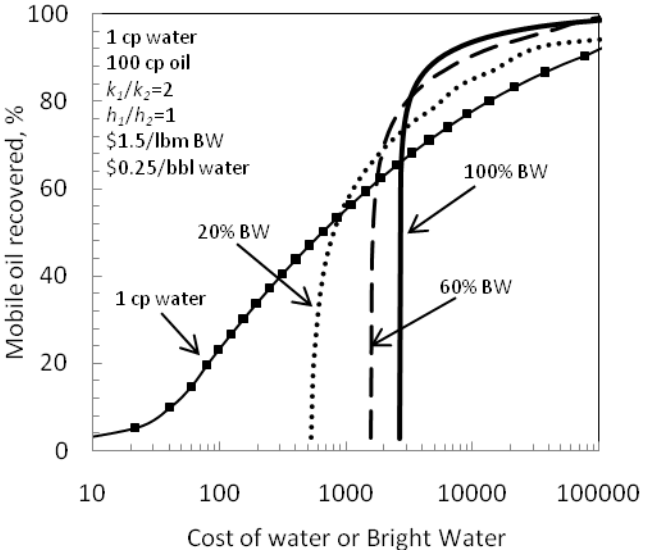

Fig. A-6—Effect of oil viscosity on the selection of Bright Water bank. 100-cp oil, k_1/k_2=2.

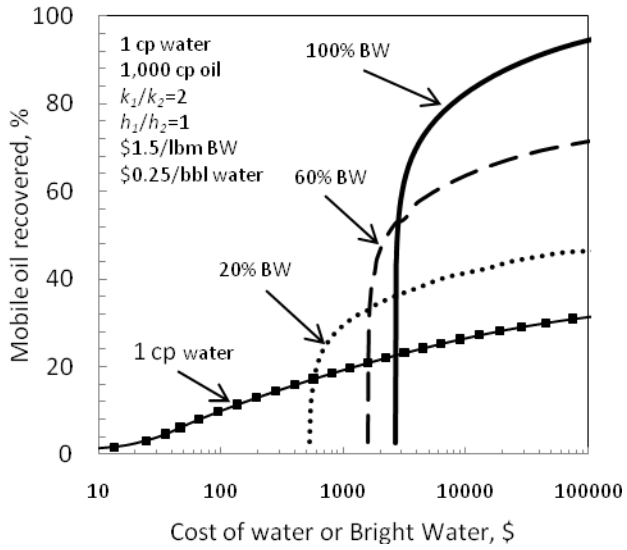

Fig. A-7—Effect of oil viscosity on the selection of Bright Water bank. 1,000-cp oil, k_1/k_2=2.

We also investigated the effect of permeability contrast (k_1/k_2) on the selection of the Bright Water bank size. The calculation shows that with increasing reservoir heterogeneity, the pore volume of Bright Water needed in the high-permeability layer should also be increased. This is demonstrated in Fig. A-8 where the permeability ratio was changed from 2 to 10, and all the other conditions are the same as mentioned in Fig. A-6. Comparing Figs. A-6 and A-8 reveals that when the permeability contrast (k_1/k_2) increases to 10, the oil recovery (at the intersection of 60% and 100% Bright Water) drops from 80% to 58%. In other words, a large bank of Bright Water is preferred over a small bank when the permeability contrast increases (k_1/k_2).

From the above analysis, we conclude that a small bank of Bright Water is preferred when dealing with less viscous oils. For more viscous oils, it is more cost-effective to choose a large Bright Water bank. This observation is more pronounced with an increase of the permeability contrast (k_1/k_2) from 2 to 10.

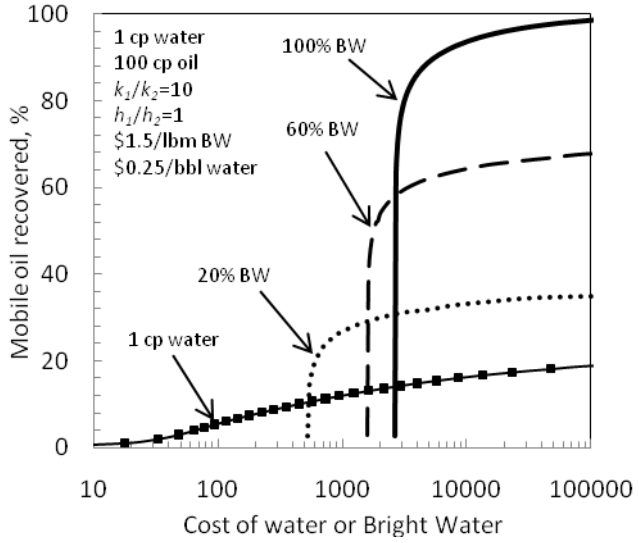

Fig. A-8—Effect of permeability contrast on the selection of Bright Water bank. 100-cp oil, k_1/k_2=10.

Effect of Reservoir Heterogeneity on Bright Water and Polymer Flooding

In this section, the effect of reservoir heterogeneity was examined. Then, a simple benefit comparison was completed between Bright Water and polymer flooding. Two prices of Bright Water were used. One is the optimistic case where Bright Water is assumed to cost the same as normal polymer (BW=$1.5/lbm). The other case assumes that Bright Water costs five times as much as normal polymer (BW=$7.5/lbm).

Bright Water. Figs. A-9 and A-10 plot the effect of permeability contrast (k_1/k_2=2, 5, 10, and 50) on 60% and 100% Bright Water applications. First, consider Fig. A-9 (60% Bright Water case). When k_1/k_2 increases from 2 to 5, oil recovery reduces from 54% to 48% (compared at a cost of $3,000). With the further increase in permeability contrast, for example, from 5 to 50, the oil recovery declines from 48% to 44%, decreasing only by 8%. Fig. A-10 shows that if 100% Bright Water is assumed to remain in the watered-out zone the performance of Bright Water is independent of the permeability contrast. Actually, this is unrealistic because 100% Bright Water cannot be achieved technically.

Polymer Flooding. The effect of reservoir heterogeneity on polymer flooding was also examined at the same permeability contrasts of 2, 5, 10, and 50 (see Figs. A-11 and A-12). Fig. A-11 demonstrates the result of polymer flooding with a mobility ratio (M) equal to 0.1. For this case, if $k_1/k_2 \leq 1/M$, the reservoir heterogeneity has little effect on the polymer flood. For $k_1/k_2 > 1/M$, as shown by the dashed line in Fig. A-11 where k_1/k_2=50, the performance of polymer flooding begins to decrease. By contrast, for unfavorable polymer flooding, i.e., mobility ratio (M) ≥ 1, as shown in Fig. A-12, at the cost of $2,000, the oil recovery decreases from 95% to 52%, 28% and 7% when the permeability ratio increases from 2 to 5, 10, and 50, respectively. Therefore, for polymer flooding with unfavorable mobility ratios, increased reservoir heterogeneity yields lower sweep efficiency. This finding is consistent with results observed by others (Sorbie and Seright 1992).

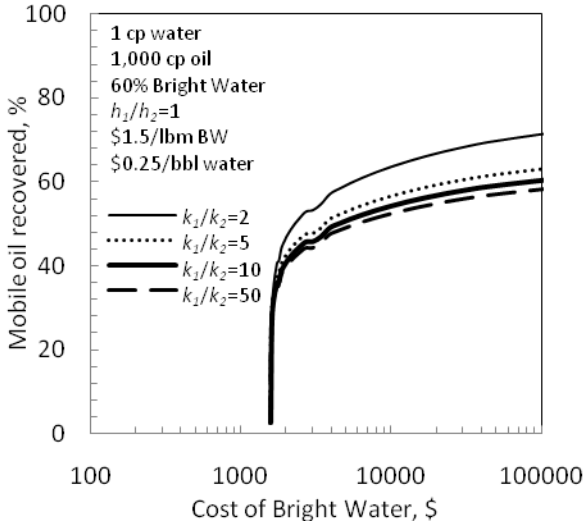

Fig. A-9—Effect of heterogeneity on Bright Water. 60% BW.

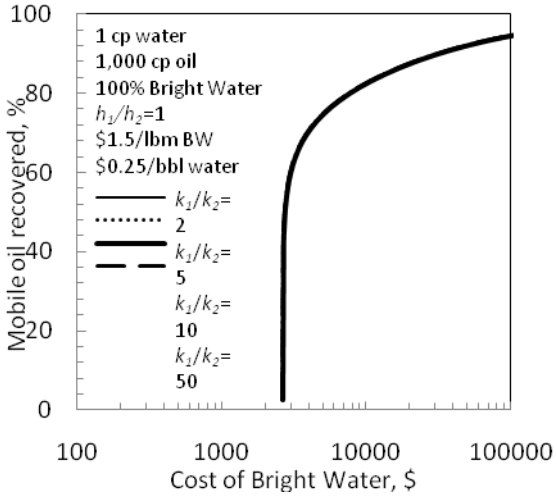

Fig. A-10—Effect of heterogeneity on Bright Water. 100% BW.

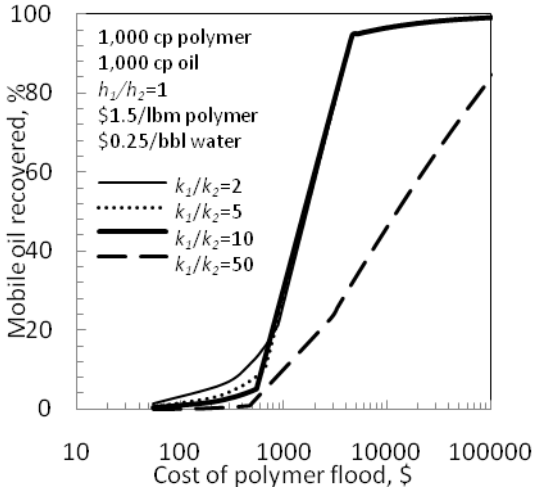

Fig. A-11—Effect of heterogeneity on polymer flooding. 1,000-cp polymer (M=0.1).

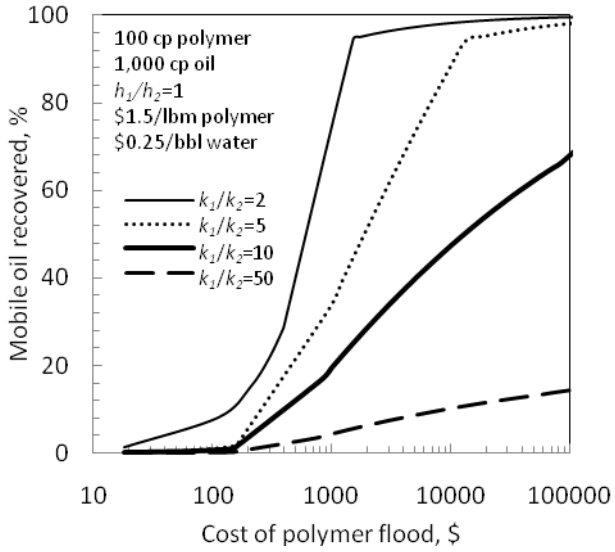

Fig. A-12—Effect of heterogeneity on polymer flooding. 1,000-cp polymer (M=1).

Comparison of Bright Water and Polymer Flooding

Bright Water ($1.5/lbm BW) Costs the Same as Normal Polymer ($1.5/lbm Polymer). Figs. A-13 through A-16 plot the results of Bright Water and polymer flooding for 1,000-cp oil at permeability ratios of 2, 5, 10, and 50. In these calculations, 1-cp water, 10-cp, 100-cp, and 1,000-cp polymer were considered for each permeability ratio (200-cp polymer was plotted only for $k_1/k_2 \geq 10$). As discussed previously, for Bright Water applied to viscous oils, large banks are preferred. Therefore, 100% Bright Water is used here to compare with polymer flooding (again, this is an unrealistic goal for Bright Water). Recall that the increase of permeability ratio has no effect on 100% Bright Water. Therefore, all Bright Water recovery curves (for different permeability ratios) remain the same. The comparison and discussion were made based on three permeability contrasts (k_1/k_2).

Slightly Heterogeneous Reservoir, k_1/k_2=2. As shown in Fig. A-13, 100-cp and 1,000-cp polymer floods perform much better than Bright Water. For example, at the cost of about $2,000, 100-cp polymer achieves approximately 86% oil recovery. For Bright Water (see thick solid line), only 70% recovery is achieved at the higher cost of $4,000. Notice that in a slightly heterogeneous reservoir, an unfavorable 10-cp polymer flood with a mobility ratio (M) equal to 10 also shows more potential than Bright Water at oil recovery below 48%.

Moderately Heterogeneous Reservoir, $k_1/k_2 \leq 10$. Two permeability ratios, k_1/k_2=5 and 10 were considered. First, when the permeability ratio (k_1/k_2) increases to 5, as demonstrated in Fig. A-14, oil recovery by 10-cp polymer declines to a much lower value than that possible by Bright Water. 100-and 1,000-cp polymer floods still provide better performance than Bright Water at the same cost.

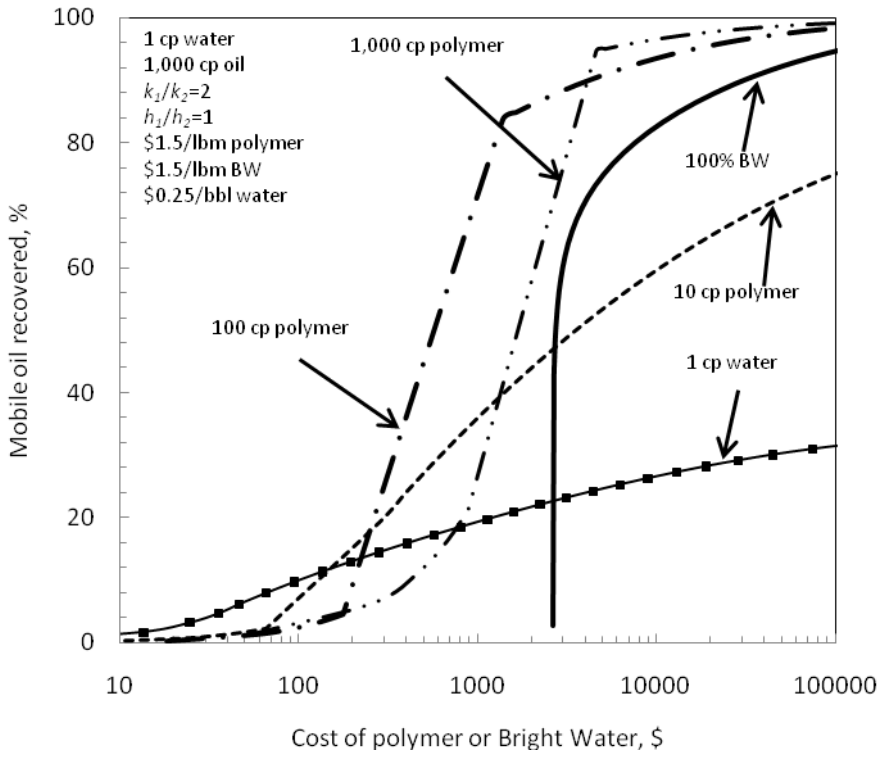

Fig. A-13—Comparison of Bright Water and polymer flooding. 1,000-cp oil, k_1/k_2=2.

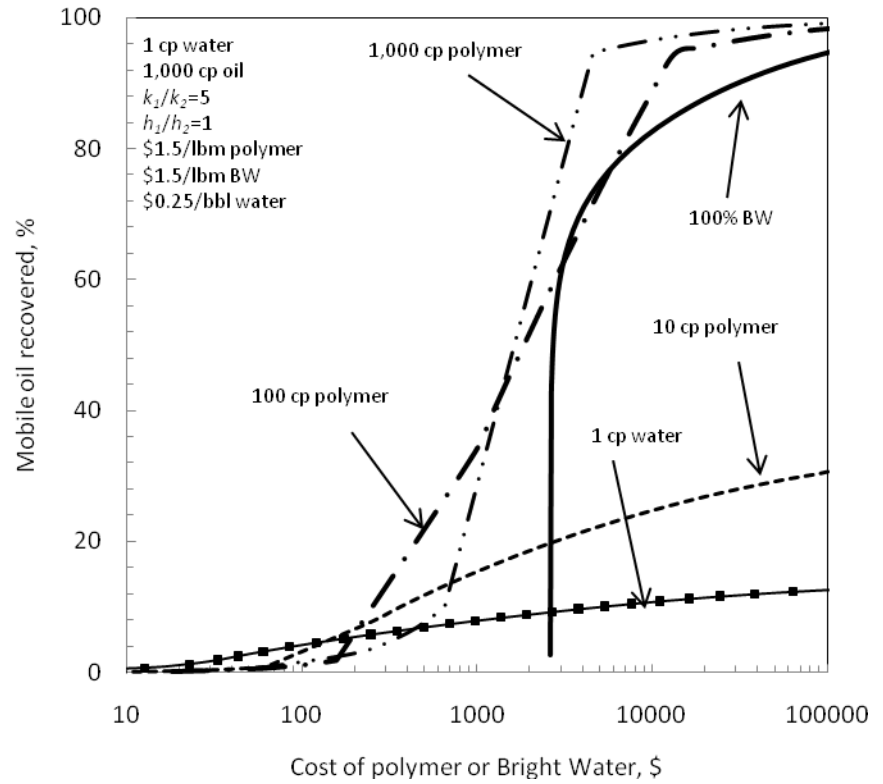

Fig. A-14—Comparison of Bright Water and polymer flooding. 1,000-cp oil, k_1/k_2=5.

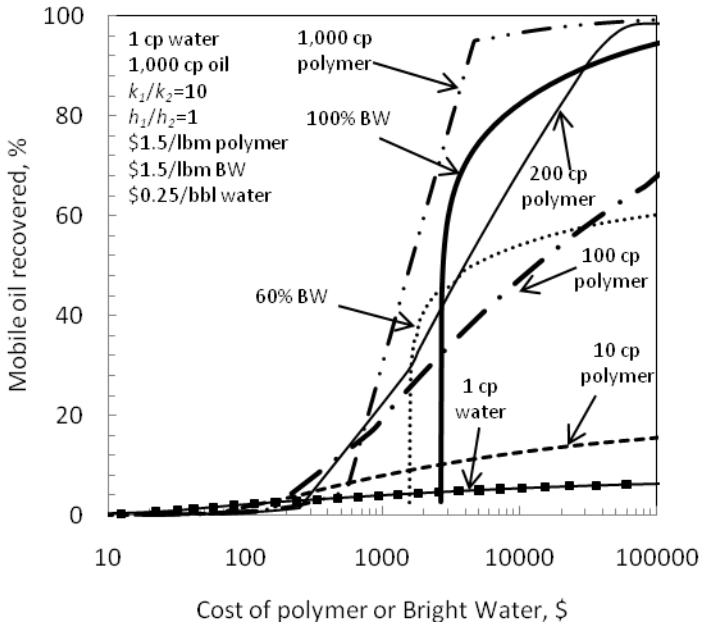

Fig. A-15—Comparison of Bright Water and polymer flooding. 1,000--cp oil, k_1/k_2=10.

If permeability ratio (k_1/k_2) increases to 10, as shown in Fig. A-15, the potential for Bright Water increases. For instance, at a cost of $3,000, Bright Water achieves higher oil recovery than 100-cp polymer. At costs between $3,000 and $30,000, Bright Water is even better than 200-cp polymer flooding, which has a mobility ratio of 0.5. However, if 60% Bright Water is used for this case (see the dotted line in Fig. A-15), 200-cp polymer is much better than Bright Water.

Severely Heterogeneous Reservoir, k_1/k_2=50. For this case, as shown in Fig. A-16, Bright Water is better than polymer flooding with a mobility ratio of 0.1. The potential of a large Bright Water bank to recover viscous oils from highly heterogeneous reservoir begins to be evident.

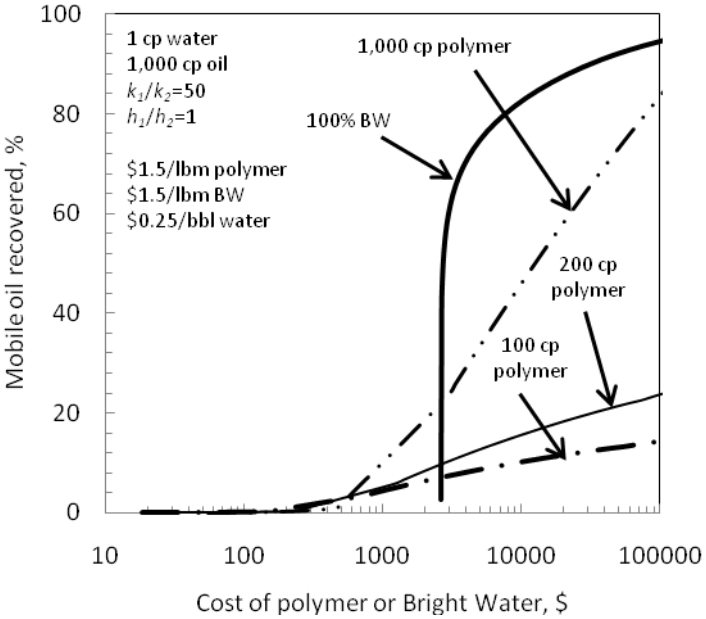

Fig. A-16—Comparison of Bright Water and polymer flooding. 1,000-cp oil, k_1/k_2=50.

In summary, polymer flooding with a proper mobility ratio can always achieve higher oil recovery than Bright Water in slightly and moderately heterogeneous reservoirs ($k_1/k_2 \leq 10$). In severely heterogeneous reservoirs ($k_1/k_2=50$), the potential of Bright Water with a large bank becomes evident. All the above analysis is based on the assumption that Bright Water costs as much as normal polymers.

Bright Water ($7.5/lbm BW) Costs Five Times as Much as Normal Polymer ($1.5/lbm Polymer). In the previous discussion, Bright Water is assumed to cost the same as normal polymer. If the real cost of Bright Water is much higher than polymer, the analysis that we performed may be too optimistic for Bright Water. On the other hand, if a reasonable injectivity for a viscous polymer solution cannot be maintained, the application of Bright Water may be favored. For instance, at a permeability ratio (k_1/k_2) of 10 as shown in Fig. A-15, Bright Water is better than 200-cp polymer flooding at costs between $3,000 and $30,000. If we re-plotted the recovery vs. cost curve using $7.5/lbm BW (see Fig. A-17), 200-cp polymer shows more potential than 100% Bright Water. This recognizes that, if neither 100-cp polymer (due to low oil recovery) nor 1,000-cp polymer (due to poor injectivity) is appropriate for this case, 200-cp polymer may be a better option.

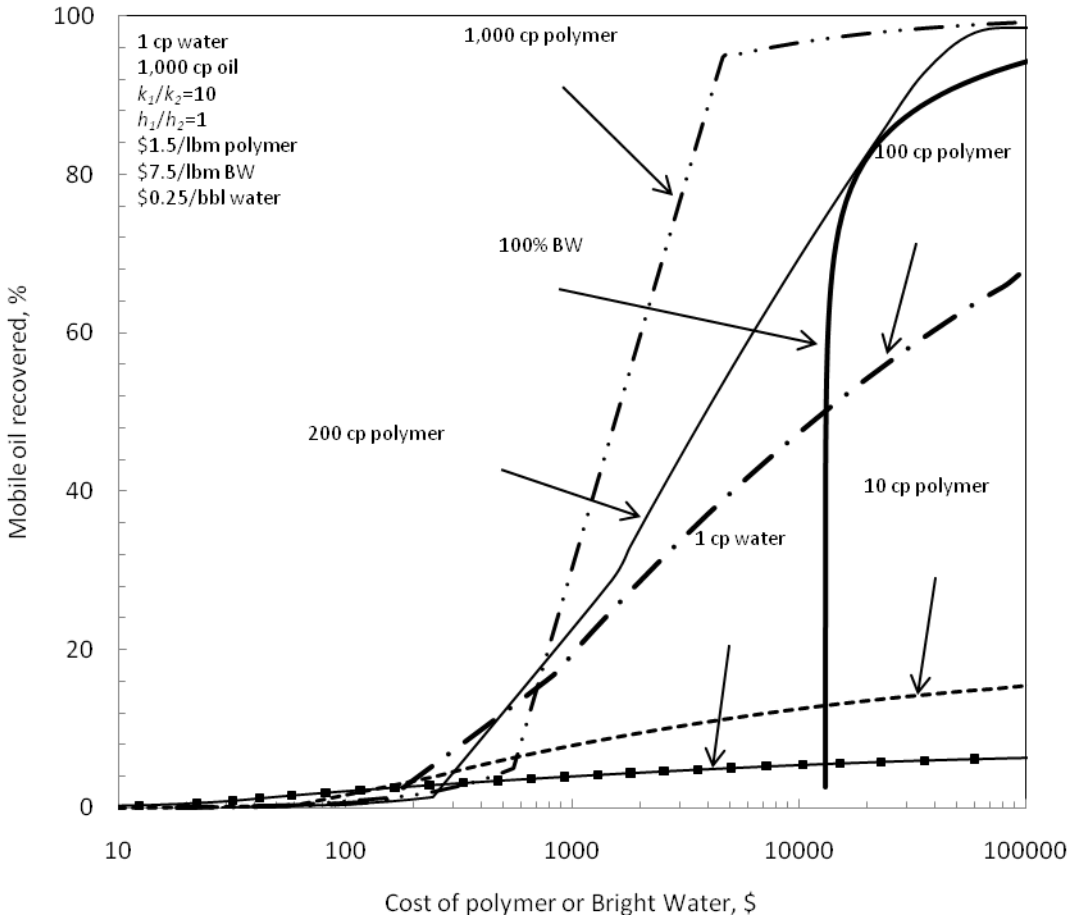

Fig. A-17—Comparison of Bright Water and polymer flooding. 1,000-cp oil, k_1/k_2=10. BW=$7.5/lbm.

Effect of Formation Height Ratio on Bright Water and Polymer Flooding

The previous calculation considered the same formation height for the two layers, i.e., $h_1=h_2$. By intuition, if the thickness of the watered-out layer is smaller compared with that of the oil layer, a smaller amount of Bright Water will be needed to block the high-permeability layer (Layer 1). This will be advantageous to the application of Bright Water. For polymer flooding, the loss of polymer solution to the high-permeability layer will be reduced also. To compare which process gets more benefit from the formation height ratio decrease, the calculation was performed by only changing the thickness of the watered-out layer and assuming that all the features of the oil layer remain unchanged (still 500 bbls pore volume with initial oil saturation, S_{oi}=0.88 and residual water saturation, S_{wr}=0.12). Therefore, if formation height ratio, h_1/h_2=0.1, the high-permeability layer has a pore volume of 50 bbls and the total pore volume is 550 bbls (recall that the total pore volume is 1,000 bbls at h_1/h_2=1). In this section, formation height ratios (h_1/h_2) of 0.05, 0.1, 0.5 and 1 were considered. Other parameters used were: the permeability ratio (k_1/k_2) is 10, 1,000-cp oil, and 100% Bright Water.

Bright Water. Fig. A-18 shows the effect of reducing the formation height ratio (h_1/h_2) on Bright Water. Generally, for oil recovery below 80%, the benefit is evident. For example, the cost for h_1/h_2=0.05 is only about $500 to achieve 60% oil recovery. While, the same oil recovery can cost $3,000 for the case of h_1/h_2=1, which is 6 times more costly. Nevertheless, when the oil recovery is above 80%, the benefit gap decreases because large pore volumes of water dominate the cost.

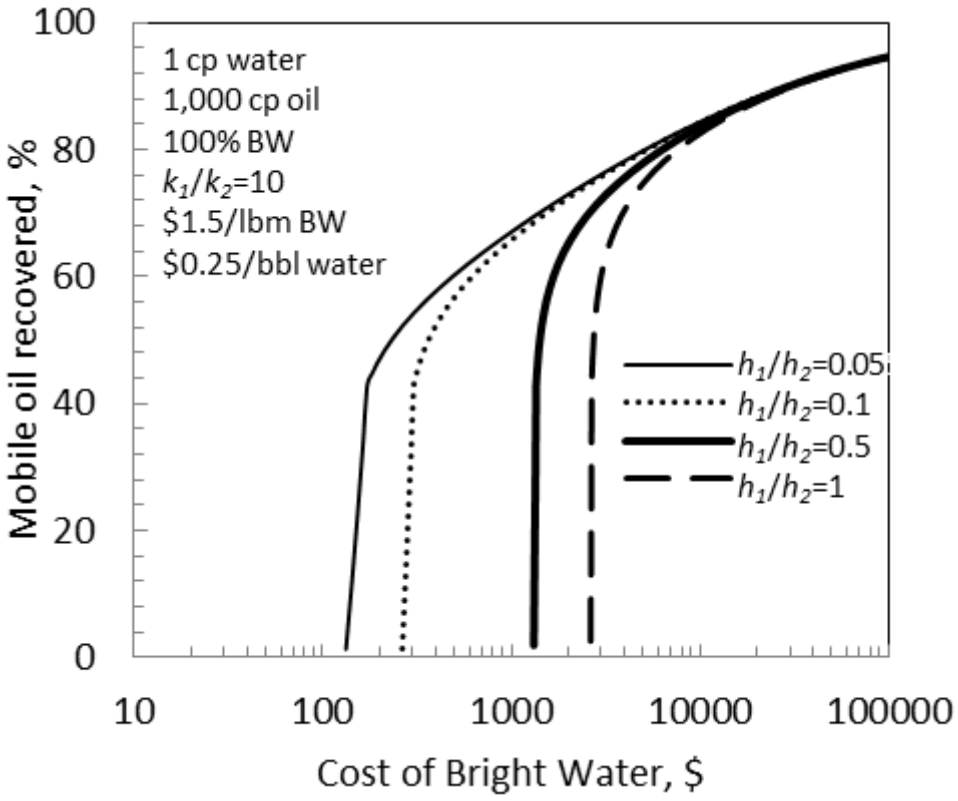

Fig. A-18—Effect of formation height ratio on Bright Water. 100% BW.

Polymer Flooding. The same analysis was completed for polymer flooding with mobility ratios (M) of 0.1 and 1 (as shown in Figs. A-19 and A-20). A decrease of formation height ratio (h_1/h_2) also benefits polymer flooding. For instance, for a highly favorable polymer displacement (see Fig. A-19), the cost for h_1/h_2=0.05 is about $1,500 to achieve 80% oil recovery. This cost could be $3,100 for h_1/h_2=1. Similar to Bright Water application, when over 95% oil recovery is desired for polymer flooding, the cost of different formation height ratios approaches the same value. For more favorable polymer flooding (Fig. A-19), the oil production rate decreases rapidly after polymer breaks through from the oil layer (actually, a very high oil recovery is already achieved at polymer breakthrough). When a less favorable polymer flood is performed, as shown in Fig. A-20, it always benefits from a smaller formation height ratio (h_1/h_2). A comparison of Figs. A-19 and A-20 reveals that a favorable polymer flood achieves much higher recovery than an unfavorable flood at the same cost.

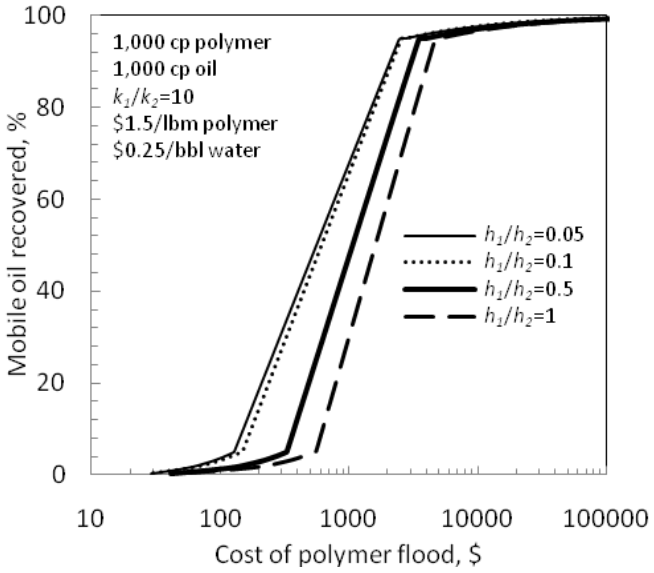

Fig. A-19—Effect of formation height ratio on polymer flooding. 1,000-cp polymer.

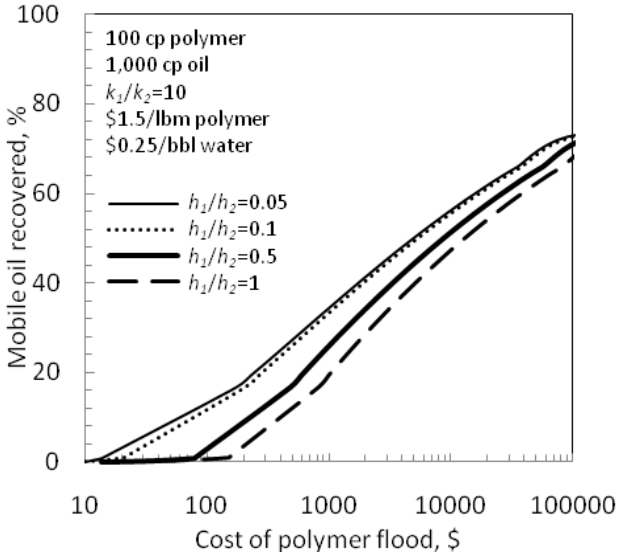

Fig. A-20—Effect of formation height ratio on polymer flooding. 100-cp polymer.

Comparison of Bright Water and Polymer Flooding at Different Formation Height Ratios (h_1/h_2)

A comparison of the two processes is made in Figs. A-21 and A-22 where h_1/h_2=0.1, k_1/k_2=10 and 1,000-cp oil were used. When Bright Water has the same cost as polymer, polymer flooding recovers more oil than Bright Water except at costs between \$300 and\$1,000, where Bright Water shows slightly more potential than 1,000-cp polymer flooding (see Fig. A-21). Accordingly, when Bright Water costs 5 times more than polymer, 200-cp polymer flooding is better than Bright Water, with the exception of costs between \$1,500 and \$12,000. Comparing Figs. A-15 and A-21 (where BW=\$1.5/lbm, different h_1/h_2) and Figs. A-17 and A-22 (where BW=\$7.5/lbm, different h_1/h_2) indicates that both Bright Water and polymer flooding gain benefit from a decrease of formation height ratio (h_1/h_2). This benefit is a little more noticeable for Bright Water than polymer flooding.

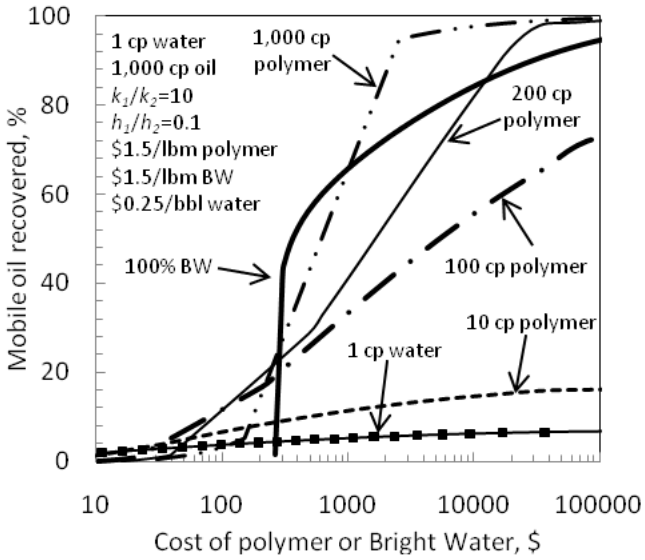

Fig. A-21—Comparison of Bright Water and polymer flooding at h_1/h_2=0.1. BW=\$1.5/lbm.

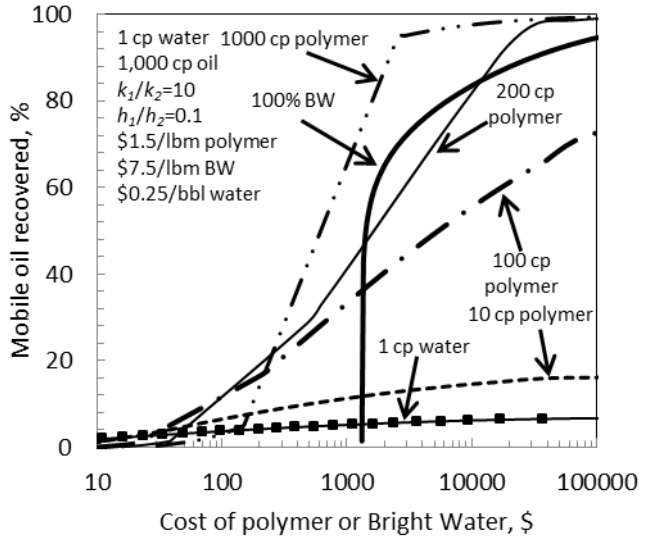

Fig. A-22—Comparison of Bright Water and polymer flooding at h_1/h_2=0.1. BW=\$7.5/lbm.

Conclusions

1. A small bank of Bright Water is preferred when dealing with less viscous oils. For more viscous oils, it is more cost-effective to choose a large Bright Water bank. This observation is more evident with an increase of permeability contrast (k_1/k_2).
2. For a favorable polymer displacement, i.e., mobility ratio (M) below 1, when permeability ratio $k_1/k_2 \leq 1/M$, the heterogeneity of reservoir has little effect on the performance of polymer flooding. If $k_1/k_2 > 1/M$ or an unfavorable polymer displacement (mobility ratio, $M \geq 1$) is performed, polymer flooding suffers a substantial loss of effectiveness with increasing permeability contrast.
3. Assuming Bright Water costs the same as normal polymers (on a per weight of chemical basis), a comparison between Bright Water and polymer flooding of viscous oils shows that:
   (1) For slightly and moderately heterogeneous reservoirs ($k_1/k_2 \leq 10$), polymer flooding with a favorable mobility ratio ($M \leq 0.5$) is much better than most Bright Water treatments.
   (2) With increasing permeability contrast (k_1/k_2), the potential of Bright Water treatments becomes more pronounced.
   (3) For severely heterogeneous reservoirs ($k_1/k_2 \geq 50$), Bright Water with a large bank shows more potential than polymer flooding with a low mobility ratio.
4. Both Bright Water and polymer flooding benefit from a decrease of formation height ratio (h_1/h_2). This benefit is slightly more noticeable for Bright Water than polymer flooding.
5. For viscous oil displacement, a Bright Water bank in the watered-out layer (Layer 1) determines the main oil target and the formation shape factor (L/h) affects the reservoir sweep efficiency (E_v) for the subsequent waterflood.